

AD-A041 662

ARMY ELECTRONICS COMMAND WHITE SANDS MISSILE RANGE N--ETC F/G 4/2
CALIBRATION TECHNOLOGY FOR METEOROLOGICAL SATELLITES. (U)

JUN 77 L E WILLIAMSON

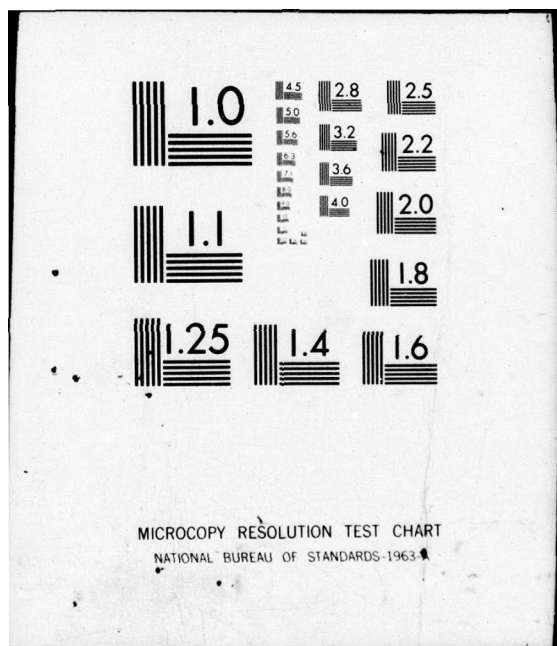
MONOGRAPH SER-3

UNCLASSIFIED

NL

1 OF 2
AD A041 662





MICROCOPY RESOLUTION TEST CHART
NATIONAL BUREAU OF STANDARDS-1963

WILLIAMSON - CALIBRATION TECHNOLOGY

No. 3

AU NU. _____
DDC FILE COPY.

DISTRIBUTION STATEMENT A
Approved for Public Release
Distribution Unlimited



No. 3

AD A 041662

CALIBRATION TECHNOLOGY
FOR
METEOROLOGICAL
SATELLITES



(1)
B.S.

L. Edwin Williamson

ATMOSPHERIC SCIENCES LABORATORY

MONOGRAPH SERIES

No. 1: EARTH'S ELECTRICAL STRUCTURE - June 1975
Willis L. Webb

No. 2: METEOROLOGICAL SATELLITE APPLICATIONS - October 1975
Willis L. Webb, Editor

No. 3: CALIBRATION TECHNOLOGY FOR METEOROLOGICAL SATELLITES
April 1977, L. Edwin Williamson, Editor

Released an internal technical report by:

'Atmospheric Sciences Laboratory
Col. William C. Petty, CO & Director
U. S. Army Electronics Command
White Sands Missile Range, New Mexico 88002

Disclaimers

The findings in this report are not to be construed as an official Department of the Army position, unless so designated by other authorized documents.

The citation of trade names and names of manufacturers in this report is not to be construed as Official Government indorsement or approval of commercial products or services referenced herein.

CALIBRATION TECHNOLOGY FOR METEOROLOGICAL SATELLITES.

14 Manograph + Set - 3

10
Edited by
L. EDWIN WILLIAMSON

(12) 150 p.

11 Jun 1977

First Edition.

D D C

JULY 18 1977

A

DISTRIBUTION STATEMENT A

**Approved for public release;
Distribution Unlimited**

400844

CONTENTS

	Page
Foreward	v
Authorship and Acknowledgements	vi
Chapter 1 Introduction	1
A. Background and Calibration Objectives	1
B. The Meteorological Products of Satellite Technology	3
Chapter 2 Classification of Error Sources	13
A. Target	13
1. Random Noise	13
2. Polarization Effects	15
3. Unknown Source Characteristics	15
4. Other Target Related Errors	15
B. Atmosphere	16
C. Instrument Optics	16
1. Angular Response	16
2. Contamination	16
3. Degradation	17
4. Geometry	17
5. Spectral Response	17
6. Stray Light	18
7. Thermal Effects	18
D. Sensor	18
1. Angular Base	18
2. "Bias or Zero"	19
3. Degradation or Contamination	19
4. Erroneous Gain	19
5. Geometry	20
6. Microphonics	20
7. Pointing Errors	20
8. Pressure Effects	20
9. Air Convection or Ventilation	21
10. Saturation Effects	21
11. Spectral Response	21
12. Thermal Effects	21
13. Time Constant	22
E. Data Processing	22
1. Erroneous Data Transmission	22
2. Random Noise	22
3. Computation Errors	23

Letter on file

A1 | |

	Page
4. Capacity of the System	23
F. Timing or Calibration Frequency	23
Chapter 3 Sensor Systems and Radiation Sources	24
A. Instrument Types	24
1. Scanning Radiometers	24
2. Fixed Radiometers	25
3. Restricted Scan Radiometers	25
4. Sounders	26
5. Active Microwave	27
B. Types of Radiation Sources	27
1. Ultraviolet	27
a. High Temperature Black Bodies	27
b. Lamps	28
c. Discharge Tubes and Plasmas	28
d. Synchrotron Radiation	28
e. Luminescent or Fluorescent Materials	28
f. Solar	29
2. Shortwave (Visible)	29
a. Diffusion Plates	29
b. Lamps, Lasers and Light Emitting Diodes	29
c. Plasmas	33
d. Solar	33
e. Spectrometer/Monochromator	33
f. Solar Simulator	34
3. Longwave (IR)	34
a. "2π" Cylinder	34
b. Cavities	35
c. Flat Plates	35
d. Honeycombs	35
e. Water	35
4. Microwave	37
C. Other Optical Elements	38
Chapter 4 Error Mechanisms for Selected Sensor Types	39
A. Solar Measurements and Blackbody Cavity Detectors	39
1. Circumsolar Radiation	39
2. Loss of Radiation Through Aperture	39
3. Effects of Diffraction	39
4. Effects of Time Constant	40
5. Time Rate of Change of Radiometer Temperature	40

6. Unwanted Thermal Resistance by Coating	40
7. Uncertainty in Area Aperture	41
B. Sources of Error for a Scanning Radiometer in Space	41
1. Change in Calibration Lamp Irradiance	41
2. Excitation of Calibration Lamp	41
3. Photo-Multiplier Tube (PMT) High Voltage Excitation	41
4. Van Allen Radiation	41
5. Partial Blockage of the Sun Calibration Mirror or Aperture	42
6. Spectrally Selective Contaminant	42
C. Examples	43
1. Hypothetical	43
a. Non-linearity of Instrument Response	43
b. Incorrect Spectral Response	45
2. NIMBUS 6 - ERB	48
3. SMS 2	49
Chapter 5 Calibration Systems - Standards, Detectors, Scales	50
A. Standards	50
1. NBS (USA) Radiometric Reference	50
2. NRC (Canada) Radiometric Reference	51
3. NPL (U.K.) Radiometric Reference	51
B. Detectors	52
1. Angstrom Electrical Compensation	52
2. Abbott Silver Disc Pyrheliometer	52
3. Cavity Radiometers	53
C. International Radiometric Scales	54
1. International Pyrheliometric Scale	54
2. Solar Constant Reference Scale	54
3. Intercomparison of Scales	54
D. Precision and Accuracy of Radiometric Devices . .	56
Chapter 6 Calibration Processes	58
A. General	58
B. On-board Systems	60
1. System Checks - Go/No Go	60
2. Electronics	60
a. Precision Voltage Staircase	60
b. Noise Check	60
3. Sensor	61
a. Space Look	61

	Page
b. Internal Targets	61
(1) Normally Shuttered Channels	61
(2) Diffuse Plates	62
(3) Standard Lamps	62
(4) Thermal (IR) Blackbodies	63
4. Intercomparison Between Instruments	63
C. Use of Natural Targets	64
1. Earth Surface	65
a. Dark Objects	65
b. Manmade Objects	65
c. Water Bodies	65
d. Reflection Discontinuities	66
e. Bright Surfaces	66
f. Uniform Surfaces of Known Characteristics and Constancy	67
2. Clouds and the Atmosphere	67
3. Extraterrestrial	68
a. Lunar	68
b. Solar	68
Chapter 7 Calibration of Specific Instruments	71
A. Scanners	71
1. Operational Linescan System (OLS)-DMSP	71
2. Visible Infrared Spin Scan Radiometer (VISSR) SMS/GOES	74
3. Scanning Radiometers (SR) NOAA	77
4. Electrically Scanning Microwave Radiometer (ESMR) NIMBUS 6	79
B. Fixed - SKYLAB S-194	80
C. Restricted Scan - Earth Radiation Budget (ERB) . .	82
D. Sounders	85
1. Vertical Temperature Profile Radiometer (VTPR)	85
2. Limb Radiance Inversion Radiometer (LRIR) . .	87
3. Pressure Modulated Radiometer (PMR)	88
E. Active Microwave - SKYLAB S-193	89
Review and Commentary	91
Appendix I	95
Appendix II	103
Appendix III	109
Acronyms and Definitions	115
References and Bibliography	121
Author - Subject Index	136

FOREWORD

The Department of Defense (DOD) has conducted, as part of its research and development base, a program identified as New Initiatives - the purpose of which is to encourage investigative effort into new technical avenues which offer promise of results that may be applied to the defense posture. One such new initiative program was begun in 1972 to deal with the application of meteorological satellite technology to tactical Army problems. The effort produced, in its first few months, the definition of programs that can offer substantial savings of money and manpower. To date, one of these concepts titled SATFAL (Duncan, 1976) has been approved for exploratory development and another titled SATTEL (Alexander, Thomas, Dubbin, 1976) is nearing this stage. The broad application of meteorological satellite technology to DOD interests is discussed by Webb, 1975. The early necessity for satellite-acquired data of known quality for the purpose of quality assurance, and emphasis on the necessity for satellite correlated air-and-ground truth data by such investigators as Coulson and Jacobowitz (1972) and of significant space programs such as Skylab Concentrated Atmospheric Project (SCARP), (Whitehead, 1974) and others led to the production of a facility dedicated to this purpose.

The pursuit of this program and its integration into the broad field of remote sensing technology brought a distinct awareness of the absence of documentation on concepts that could be used to define the state-of-the-art of environmental satellite sensor calibration. Several authors have dealt with calibration problems of specific systems, and the works of Coulson (1975), Drummond et al (1970), and Reeves et al (1975) together, adequately describe the science of remote sensing. Combined, these works total nearly 3000 pages, of which barely one percent directly addresses the subject of calibration. Many important aspects of the overall calibration process remain in very narrow distribution channels or are otherwise obscurely situated, and no consolidated work aimed at summarizing the overall problem is available. The following effort is directed at focussing attention on that void, in hopes of directing more systematic and intensive attention into this area in the future.

AUTHORSHIP AND ACKNOWLEDGEMENTS

This report was prepared at the initiative and under the aegis of the US Army Electronics Command, Atmospheric Sciences Laboratory, White Sands Missile Range, New Mexico. The work was accomplished in three principal phases. The first was the use of a Steering Committee, the membership of which represented the highest levels of competence and expertise and which encompassed all aspects of the calibration of satellite acquired data. This committee was used to develop the scope and objectives of the report. The second phase was the assignment of an individual of equivalent competency to collect, review and select appropriate technical material for inclusion in the report. The third phase was the assembly, editing, compiling and publication of the report.

The first of these phases was performed through the appointment to the Steering Committee of six individuals of outstanding capabilities in the areas of sensor concept, design, fabrication, laboratory and flight performance, data processing and data interpretation. Of equal importance, they represented users of environmental satellite data and recognized the apparent deficiency of and necessity for adequate calibration processes and documentation thereof. The Steering Committee was tasked to perform three specific functions, specifically, to define the general scope and format of the study, to contribute toward the content of the report (material pertinent to the members' own area of independent expertise), and to guide the preparation of the report throughout to insure its continuing suitability to the user community. The Steering Committee consisted of the following individuals:

Dr. Thomas Barnett
Earth Observations Division
Johnson Space Center - NASA
Houston, Texas

Dr. Kinsell Coulson
Department of Meteorology
University of California
Davis, California

Dr. Fred House
Aeronautical Engineering Dept.
Drexel University
Philadelphia, Pennsylvania

Dr. Herbert Jacobowitz
Radiation Branch
NOAA/NESS
Suitland, Maryland

Dr. Thomas Vonder Haar
Atmospheric Sciences Dept.
Colorado State University
Fort Collins, Colorado

Dr. Victor Whitehead
Earth Observations Division
Johnson Space Center - NASA
Houston, Texas

The second phase of the preparation was to engage the services of an individual for the singular task of collecting and reviewing all available literature on the subject, and reducing the critical technical information into coherent conciseness. This individual was

Dr. James Cogan
Consulting Meteorologist
Lexington, Massachusetts

I, while serving as Team Leader, Satellite Facilities Team and as Principal Investigator for the Meteorological Satellite Evaluation System Work Unit for the Atmospheric Sciences Laboratory, have been privileged to Chair the Steering Committee and to compile, revise, edit and coordinate the publication of the final report. In so doing I have earned credit for any errors, mis-statements or expressions of subjectivity.

The work by Dr. Cogan and each member of the Steering Committee has been outstanding and complete in all aspects. The opportunity to work with such a group of dedicated scientists, bound by a common awareness of a technical challenge and a dedication to professional ideals has been to me, a special reward.

I also extend my appreciation to Mrs. Donna Hyatt and Miss Susen Phipps for their diligence and perserverence in the numerous typings. Ms. (SP5, USA-WAC) Ceri Philipp is especially thanked for her assistance in preparation of the Appendix on Acronyms and Definitions.

Lastly to my friend and mentor, Dr. Willis L. Webb, Chief of the Meteorological Satellite Technical Area, Atmospheric Sciences Laboratory, under whose direction and leadership the need and purpose of this work arose. Under his example I have found both inspiration and aspiration.

L. EDWIN WILLIAMSON
April 1977

CHAPTER I

INTRODUCTION

A. BACKGROUND AND CALIBRATION OBJECTIVES

It is characteristic of any area of investigation that a user of data or information must understand the quality of his data before he attempts to derive conclusions from an analysis thereof. The degree of confidence in the quality determines the commitment to the analysis. Few technological areas have produced in their entire histories, masses of data comparable to the technology of environmental satellites. The mere volume of this type of data has helped to create a whole new sub-technology dedicated solely to the retention, extraction and distribution of these data. The interpretation of such data is currently the focus of thousands of researchers who are trying to unravel some of the mysteries of the earth planet and its thermal engine. The challenge inherent in the utilization of these data are significant.

A proper perspective may be gained by the reader if he recognizes the magnitude of the technical area being addressed, in that he may not be fully aware of the substantial numbers that are being inferred. As of 1 January 1976 there had been a minimum of thirty-nine geosynchronous satellites launched, with twenty or so more scheduled for imminent launching (COMSAT Technical Review, 1976). There are presently a total of 3910 man made objects* in orbit (NASA, 1976). Each of these satellites represents hundreds and sometimes thousands of man-years of effort in both pre-launch and post-launch activities. While only a few of the instrument systems aboard these satellites can be classed as environmental sensors, most of them collect information through an environment that is not a part of the system

* This is the number of objects, including space junk. The operating definition of 'object' is that it is radiating in the rf or has a predicted orbital life in excess of six months.

design. Consequently, factors pertinent to calibration of environmental sensing devices may apply to a large segment of technology not specifically dedicated to environmental assessment. However, the focus of this study is the meteorological satellite and the data derived therefrom. It is recognized that there are basically three current satellite systems that can be said to encompass the general category of meteorological satellites. They are the Synchronous Meteorological Satellites which are operated by the NOAA/NESS and/or NASA, the NOAA/NASA polar orbiters of the NOAA-Nimbus-ITOS class, and the DMSP polar orbiters operated by the DOD.

The assurance of data quality acquired by sensors which are located hundreds (or even thousands) of miles away, and accessible only after radio transmission and various other electronic or other manipulations, should not readily be taken for granted. The integration of information from multiple sources, some citing accuracies of thermal properties, say, to a few tenths of degrees, and others citing accuracies to a few whole degrees, can produce confusion. This report addresses the problem of determination of the quality of the data provided by these systems, in the hope that it can stimulate the user interest required to arrive at a solution.

It should be noted that some of the most obvious and important uses of meteorological satellite data do not require calibration of any sort. The location of clouds and the patterns formed by clouds provide valuable direct information to a wide variety of users. However, if the user wishes to know specific values such as what is the temperature, the temperature profile, the albedo, the radiant heat loss over the northern hemisphere this year compared to the mean of the last five years, etc., it is necessary that he be able to determine the spectral aperture radiance with a measure of the degree of confidence that can be placed on the determined value. Ideally the user should be able to compare the observation from instrument a to instrument b; from satellite A to satellite Z; and from the first day in the operational life of the system to its last day. It is only by having such a capability can the optimum use of complex systems such as atmospheric sounders be achieved. A measure of the long term change in heat budget would be sure to fail without sufficient attention paid to calibration procedures. While the emphasis here is on meteorological satellite systems, this ability to compare the

cont on p 3

(cont'd p. 2)

output of different systems over a period of time is just as important to users of Landsat and other satellites.

This report describes the steps involved in providing this total system calibration and a description of the multitude of effects that can interfere with it. The report emphasizes that total system calibration must include full-life-cycle application of calibration techniques as most factors affecting equipment performance contain or produce time-dependent responses and surface radiation characteristics.

This report is not intended to represent a handbook or instructional guideline to calibration. Rather its purpose is to familiarize the reader - the users and managers of satellite acquired environmental data or data systems - with the basic technology, terminology and documented status of the somewhat neglected technology of total system calibration.

B. METEOROLOGICAL PRODUCTS OF SATELLITE TECHNOLOGY

The science of meteorology finds expression in the collection, and subsequent manipulation, or data depicting perhaps a dozen parameters which, together, describe the physical, chemical and thermodynamic state of the atmosphere. Myriad instruments, techniques, and processes have painted an illustrious history over the past 200 years. However, all the fascinations of the past two centuries have been eclipsed by those of the last two decades. Specifically, the meteorological satellite has given a new dimension to observation and measurement capabilities of both temporal and spatial arenas. Access to orbit has put the meteorologists "eyes" at a place where he can see where he needs to, when he needs to. His basic response to this new capability is twofold. First, he must determine the adequacy of the new way of looking at old things, and secondly, he must determine if there are things heretofore unobserved that might provide a new or better insight than the older perspectives. Most notable among the latter is the imagery that is available from satellites, and which permits the meteorologist to view the dynamic processes on a hemispheric scale, and while the processes are underway. Limiting the usefulness of this vantage point is the restricted capability to see or measure through clouds or moisture-laden atmospheric columns. The role of moisture in nearly all atmospheric thermodynamic processes requires that whatever new processes come about, they must, at least for the present, be coupled with the old

processes that have provided the meteorologist some way of handling the atmospheric data. Restated, imagery from satellites is, so to speak, here to stay. It has made outstanding contributions, and will no doubt make others. However, it will not survive alone. Attention must now be given to the first and primary response to the new technology, that of determining the adequacy of new ways of determining quantitative aspects of historically observed parameters. The process can be started by comparing the results of the two.

The following synopsis is a condensation of works by Professor James Scoggins and associates at Texas A&M University (see Scoggins, 1976, 1977).

Quantitative satellite data are typically acquired from the NOAA/NESS or NASA by users, for specific satellites, instruments, dates and places, in accordance with expressed user interest. Studies associated with the following factors were based on data obtained from NOAA/NESS, acquired by the ITPR, NEMS & SCR instruments on the NIMBUS V satellite, and from the NOAA network of radiosonde stations.

The basic premise of the process is to determine how closely a given parameter (represented on a gridded field) derived from satellite data resembles that derived from radiosonde data. Several parameters, including geopotential height, geostrophic wind, temperature, dew point temperature, Showalter index, and some vertical cross-sections, have been selected to illustrate the resemblances.

Geopotential Height

Geopotential height fields were prepared for nine constant pressure surfaces. Average and standard deviations of difference between satellite and rawinsonde were derived, and are represented in Figure 1.1. Significant features of this comparison are that the heights derived from satellite data are higher than those derived from rawinsonde data, and these differences in height are generally less than 20 meters below 150 mb, and as much as 55 meters at 100 mb.

Geostrophic Wind

Profiles of average differences and standard deviation of differences between geostrophic wind speed (m/s) and direction (deg) computed from rawinsonde (RW) and satellite (sat) geopotential heights. Figure 1.2. Noteworthy among the implications of these comparisons are that the average velocity differences, both in the u and v components and in the scalar vector are generally less than 5 m/sec and the average direction differences are generally less than 25 degrees.

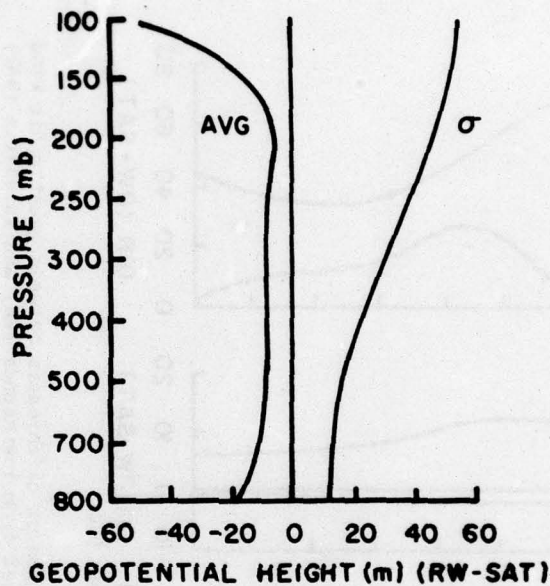


FIGURE 1.1: Profiles of average and standard deviations of differences between geopotential heights (m) measured by rawinsonde (RW) and satellite (SAT). (After Scoggins, 1976.)

Temperature

Figure 1.3 a and b represent the temperature field at 700 mb from rawinsonde and satellite data, respectively. In general, the orientation, gradient, and configuration of the isotherms of the satellite data approximate those of the rawinsonde data, but the values of the satellite isotherms appear to be lower by one to four degrees.

Dew Point Temperature

Profiles of the average and standard deviation of the differences between rawinsonde and satellite dew points are shown in Figure 1.4. Examination of the figure reveals that the average satellite derived dew points are higher than rawinsonde dew points by 2-4 degrees C, at all levels below 300 mb.

Showalter Index

A comparison of satellite (NIMBUS 5) derived with rawin-

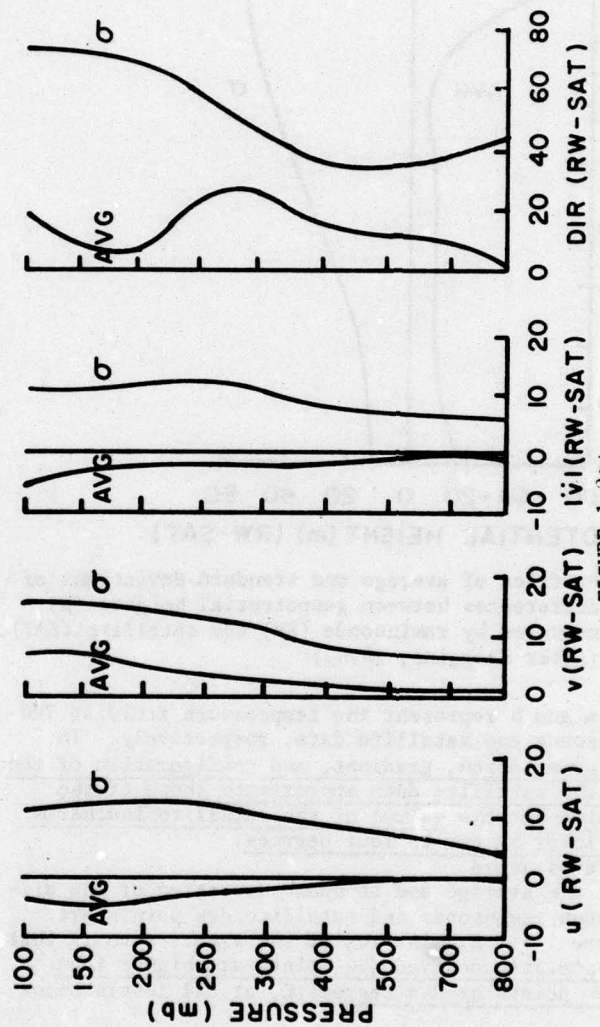


FIGURE 1.2:

Profiles of average and standard deviation of differences between geostrophic wind speed (ms^{-1}) and direction (deg) computed from rawinsonde (RW) and satellite (SAT) geopotential heights. (After Scoggins, 1976.)

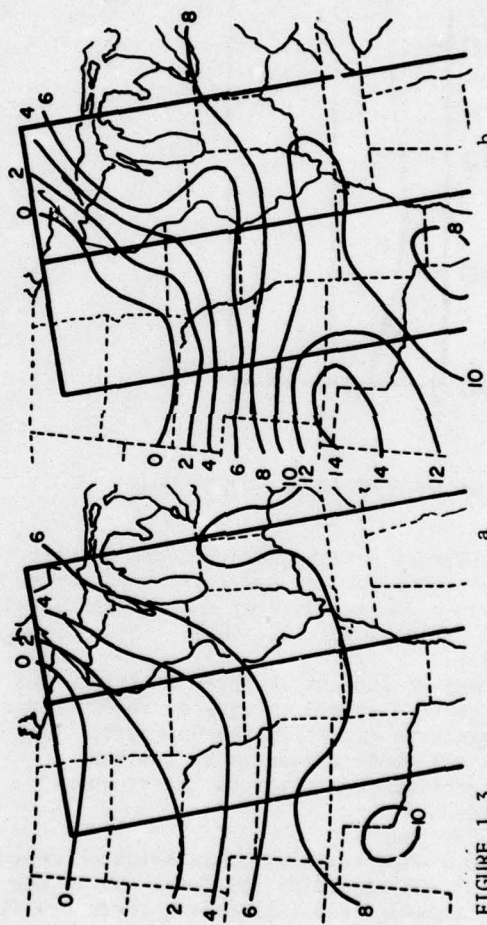
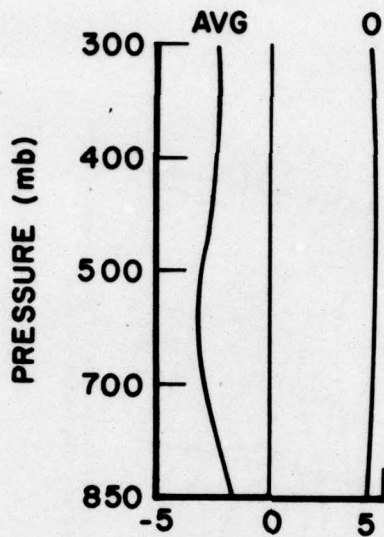


FIGURE 1.3
Temperature fields at 700 mb prepared from rawinsonde and satellite data. (After Scoggins, 1976)
a. Temperature field prepared from average of 1200 and 0000 GMT rawinsonde data.
b. Temperature field prepared from satellite data.



DEW POINT (RW-SAT) (deg)

FIGURE 1.4: Profiles of average and standard deviation of differences between dew point temperature measured by rawinsonde (RW) and satellite (SAT) at 1700 GMT on August 25, 1975. (After Scoggins, 1976.)

sonde derived Showalter Indices is shown in Figure 1.5. While the use of current satellite indices for specific severe weather forecasts (in which the Showalter index is strongly influential) would appear to be limited, their utility as general indicators of "first-guess" approaches is evident.

Vertical Cross Sections

Figure 1.6 a and b show vertical cross sections derived from rawinsonde (a) and satellite (b) data. While the overall similarity is apparent and impressive, there are differences which suggest that substitution of satellite profiles for rawinsonde profiles into a forecasting scheme, at present, might be premature, e.g., there are horizontal differences of approximately 50 km in frontal locations, and ver-

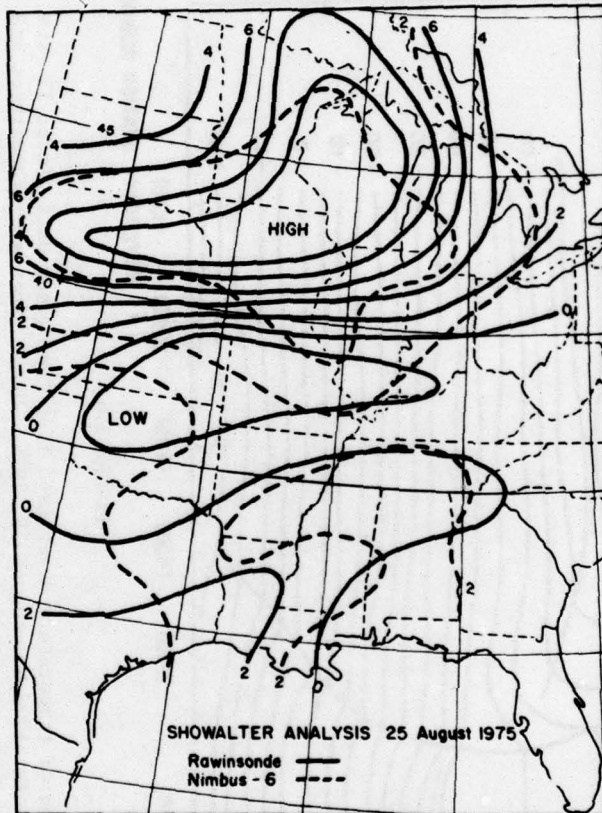


FIGURE 1.5: Analysis of Showalter Index prepared from rawinsonde (solid lines) and satellite (dashed lines) data. (After Scoggins, 1976.)

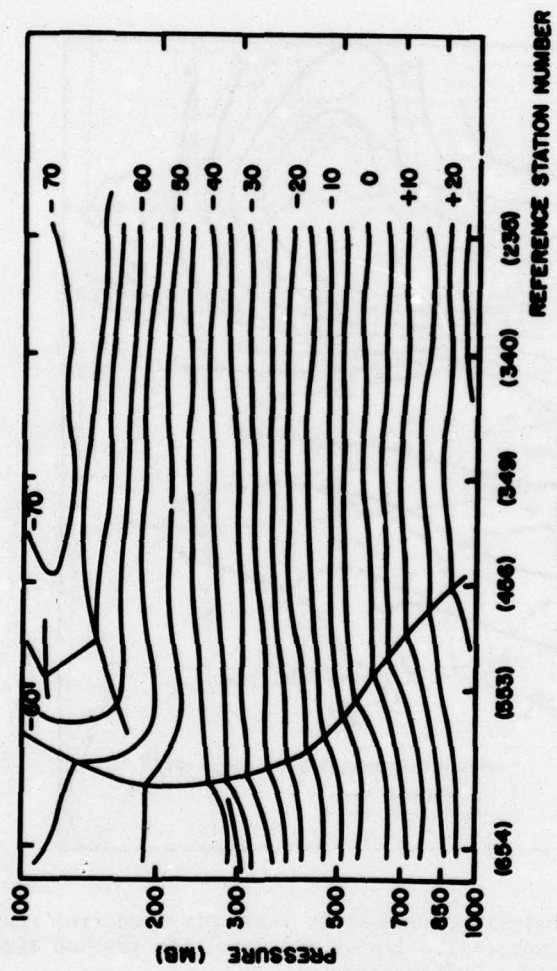


FIGURE 1.6a

Cross section of temperature determined from rawinsonde data, Sect. II (sta. 654 to sta. 235) for 1700 GMT August 25, 1975. Heavy lines are tropopause and the front; light lines are Celsius temperature. (After Scoggins, 1976.)

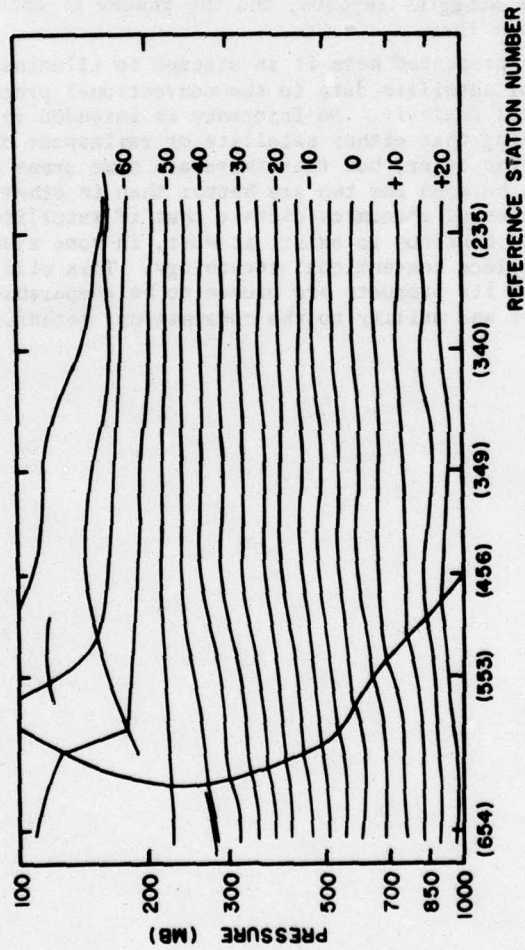


FIGURE 1.6b

Cross section of temperature determined from satellite data, Sect. II (sta. 654 to sta. 235) for 1700 GMT August 25, 1975. Lines are the same as for Figure 1.6a (After Scoggins, 1976).

tical differences of .5-1 km in certain isotherms and in tropopauses. Much other thorough detailed analysis is contained in the Scoggins reports, and the reader is encouraged to scrutinize them.

What has been presented here is an attempt to illuminate the relevance of satellite data to the conventional process of meteorological analysis. No inference is intended relative to concluding that either satellite or rawinsonde data is better than the other, but that there are some areas in which agreement between the two are better than in other areas. Basic laws of economics dictate that if satellite technology is to continue to exist, it must, in some areas, displace and replace conventional technology. This will happen only when its products are proven to be comparable in quality, cost and utility to the conventional techniques.

CHAPTER II

CLASSIFICATION OF ERROR SOURCES

In this section a number of potential causes of error in satellite measurements are discussed in several categories. Within each category, possible causes of error are described briefly, especially with regard to basic causes and effects, if known. The aim of this section is to acquaint the reader with possible sources of error so that he may take precautions to limit or account for their effects, insofar as possible. In addition, the section contains brief descriptions (or references thereto) of potential errors for some typical instruments. It is beyond the scope of this report to present detailed methods of eliminating or accounting for every potential error, especially since the instruments and requirements of individual investigators differ significantly. The purpose is to identify the nature of as many classes of error sources as possible, and to bring the reader to a familiarity with that nature and with some processes that are being used to account for its effects. In a very simplified sense, these error sources (depicted in Figure 2.1) are grouped for discussion as follows:

A. TARGET

The target can be interpreted to be the source of the radiation being collected. It may be a cavity, a plate, a cloud, the earth's land or sea surface, or even an emitting layer of the atmosphere surrounding the sensor. Several areas of potential error factors can be delineated, as follows.

1. Random Noise

Possible causes include variations in voltage, variations in source output with time, ventilation rate, and statistics of photon emission. If the frequency of the noise is high with respect to the time constant of the sensor, then the effect of the noise is generally minimized. Random noise is usually more significant in the sensor than in the source during calibration, although this may not be the case if the source is a plasma or an arc lamp.

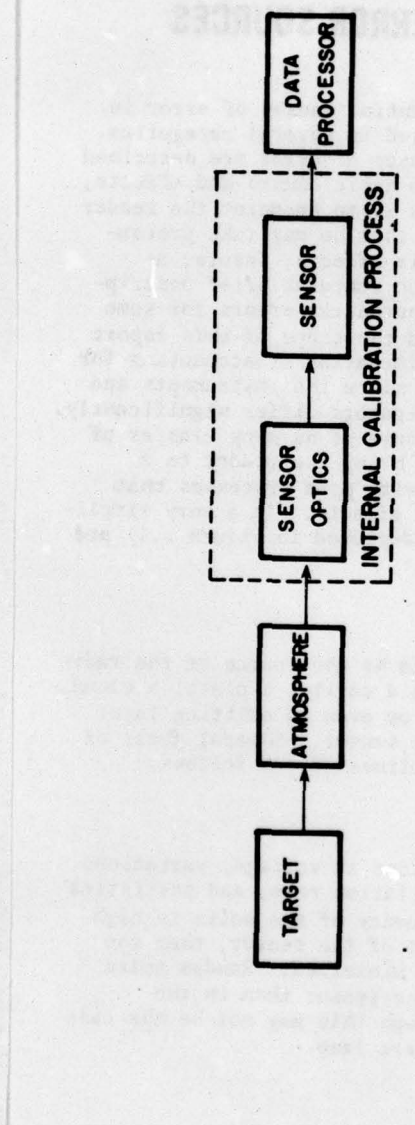


FIGURE 2.1: Error Sources Affecting System Calibration

Five basic types of system errors. Internal Calibration process may affect other areas or may act as an independent error source.

2. Polarization Effects

Some instruments are sensitive to polarization, especially those operating in the microwave region, and a complete lack of polarization is difficult to achieve in natural and artificial sources of shorter wavelength radiation. The most unpolarized natural source is the sun; light directly from the disk of the sun is virtually unpolarized. However, scattering and reflection are efficient polarization processes, and consequently diffuse radiation from the sun is normally partially polarized. Other polarization processes are transmission and emission from surfaces not normal to the incident beam.

3. Unknown Source Characteristics

Seldom are all characteristics of a source such as emissivity (ϵ), temperature (T), or transmissivity (τ) of the window (if appropriate), known exactly, and most change with time. To decrease their effects, frequent calibration is needed under conditions as close as possible to those in which the source will be used. Some characteristics that may cause errors are source instability, source degradation, angular differences, non-uniformity across surface, variation of source emission, and sharp absorption lines in spectral interval of the sensor.

4. Other Target Related Errors

A number of errors may arise in procedures and equipment used in relation to the target. Although not strictly a part of the target, these procedures and equipment, e.g., a radiation thermometer being used to determine the target temperature, affect its precision and accuracy. Some of these potential sources of error are listed below.

- (a) absolute accuracy and precision of calibration or target against laboratory standards,
- (b) different procedures for calibration of target against standard than for sensor against target,
- (c) background effects (e.g., reflection off target or surroundings or radiation emitted by the sensor),
- (d) method of determining the spectral characteristics of the target,
- (e) characteristics of other optical elements used in conjunction with the target, and (f) contamination of target material.

B. ATMOSPHERE

The intervening gas between target and detection system may induce variations in polarization, intensity and spectral distribution. Changes in atmospheric composition with time and/or space can cause variations in the signal of a satellite instrument viewing the surface of the earth or a ground based radiometer looking upwards. Signal changes induced by the atmosphere are sometimes accounted for by observational data or by computation of atmospheric attenuation. For example, a downward looking radiometer near the earth's surface used in conjunction with one of the same type on a satellite can provide measurements for elimination of the contribution of the atmosphere to received signals, provided of course, that each radiometer has been properly calibrated against the other. Careful documentation of the differences in response along with concurrent measurements of atmospheric variables such as temperature, humidity, composition, and aerosol content, at times may permit the resultant correction to be extrapolated to other locations where these same variables are measured.

C. INSTRUMENT OPTICS

Numerous error sources can be ascribed to the optical system associated with a particular sensor, as follows.

1. Angular Response

Most real instruments are sensitive to the angular distribution of radiation, e.g., cosine effect in pyranometers. Instruments with a restricted FOV are subject to vignetting of sensor surface by entrance optics, and to angular variation of reflection or absorption by filters, mirrors, lenses, and other optical elements. Each detector has a characteristic off-axis sensitivity pattern that may or may not be known.

2. Contamination

Dust, lint, other particles deposited in the atmosphere, and even fingerprints, may contaminate one or more optical elements. In space, outgassed materials from the spacecraft may adhere to optical and detector surfaces. Contamination is more serious for the elements most difficult to calibrate,

namely the foreoptics. These problems often remain even after careful design and operational procedures.

3. Degradation

Degradation, like contamination, is most serious for elements such as the foreoptics and the source, and is difficult to calibrate. It arises in spite of care in design and practice. Causes of degradation include natural aging of materials, weathering of surface based instruments, and high energy ultraviolet and particle radiation in space where high energy radiation may degrade both optics and electronics. A further cause of degradation may arise from changes in crystal structure of filters, often shifting the spectral response or changing the transmission. Change in crystal structure may arise, in turn, from aging or high energy radiation.

4. Geometry Errors

Misalignment of the optics is very common and often causes spurious effects that are difficult to detect. Simple reflection from misaligned filters or prisms may produce errors that propagate throughout the system. Errors in angular orientation of prisms or gratings in spectrometers result in erroneous spectral responses. In addition, the proper location and shape of the FOV on the surface of the earth depends entirely on geometry.

A type of geometry error may occur as a consequence of the computation of "configuration" or "shape factors", which are often estimated from rather simple assumptions.

5. Spectral Response

Insufficient accuracy in the determination of spectral response can lead to significant errors. As noted in the discussion on geometry errors (4 above) orientation of filters, prisms, or gratings may lead to erroneous data on spectral response. Other reasons for incorrect spectral response include unknown or changing transmission characteristics of filters, reflecting surfaces being spectrally selective, or improperly determined dispersion characteristics of optical components. Polarization is generally spectrally dependent, and therefore spectral response depends on polarization for instruments sensitive to it.

Furthermore, often only a relative spectral response is known, whereas an absolute spectral response is required for many applications.

6. Stray Light

Proper compensation for stray light is especially important for precise measurements. Its causes include internal reflection, scattering by glass or other materials, contamination of surfaces, diffraction of light at edges of field stops and thermal effects. Although the ideal of an exact match of the amount of stray light during both calibration and operation is generally not realized, the calibration procedure should involve the quantification of stray light if at all possible. Stray light cannot always be entirely eliminated, but it can be minimized by proper design and meticulous operational practice.

7. Thermal Effects

These effects are most important for measurements in the thermal infrared and measurements of solar radiation by thermopiles. A method of accounting for such effects is by frequent calibration against a black body of known temperature. Another is by chopping the incoming radiation and comparing readings when the detector is blocked and exposed. Heating of the filter or glass envelope by absorbed sunlight can cause infrared exchange to the sensor surface, which leads to a false measurement of solar flux. Also certain optical elements such as filters may change with temperature and expansion and contraction of mounting hardware may cause misalignment of components, resulting in measurement errors.

The temperature of optical elements used in conjunction with the source should be monitored and accounted for. Explicit compensation should be made for thermal self radiation of elements ahead of the chopper or calibration source. Thus there is a need for a sufficient number of temperature sensors to estimate all thermal effects that might be experienced.

D. SENSOR

1. Angular Response

The combined effects of optics and detector may cause non-uniformity across the FOV or a response varying with angle (of course, they also could tend to compensate each other). This angular dependence is especially important if the calibration source does not fill the FOV or is not uniform. Because the reflectivity of all paints depends on the angle of incidence, the response of a sensor covered with paint may also be angularly dependent. Other sensors such as photomultiplier tubes or light sensitive diodes have an angular dependence because of the characteristics of the surface itself. Angular effects are minimized for instruments with a small FOV since incident radiation is nearly normal at the surface of the detector. The geometry of cavity radiometers also minimizes such effects.

2. "Bias or Zero"

Determination of bias is extremely important for the measurement of absolute values. Bias frequently occurs, but it can be corrected or compensated for during data reduction. For example, the dark current of a photomultiplier can be measured when there is no illumination, and the result subtracted from the measurements. Proper calibration can often handle the effect of bias, but bias must be monitored regularly since it may be a function of time, temperature, or other factors.

3. Degradation or Contamination

Weathering of ground based sensors and contamination by particles are difficult to avoid. Degradation also may occur as a result of large doses of ultraviolet or high energy particle radiation, material breakdown arising from high temperature and excessive electrical current that may cause fatigue in the sensor. Degradation or contamination may change both bias and gain. Proper calibration can manage these problems, but since the processes are slow, regular monitoring is necessary.

4. Erroneous Gain

Common causes of this type of error are variations in bias voltage or operating temperature. Usually it is a problem in the electronics, an exception being photo-multiplier tubes. However, erroneous gain settings may be caused by

using standard sources that do not simulate reality sufficiently well, and consequently gain settings are incorrect. The best means of detecting and compensating for erroneous gain is frequent calibration.

5. Geometry Errors

Errors due to geometry of the sensor are probably not as serious as other types, although inhomogeneities over the face of the sensor or misalignment of components often cause problems which are difficult to detect. Of course, proper definition of the FOV depends on geometry.

6. Microphonics

Generally this problem is not serious for space or surface radiometers because of the usual lack of strong vibration, but it can be serious on aircraft or spacecraft in which other electrical or mechanical systems are operating. The use of solid state components, many encapsulated, helps to minimize the problem, but it is still significant in some instruments. For instance, microphonic noise was experienced in the scanning channels of the ERB instrument of the NIMBUS 6 satellite.

7. Pointing Errors

These errors involve the geometry of the system. The primary problem is likely to be an improperly defined FOV, possibly leading to registration errors and incorrect calibration values if using a natural source such as the sun, moon, or a calibration target on the earth's surface. A pointing error in a satellite instrument may only be corrected by re-orienting the sensor (usually the entire satellite), or by introducing a correction during data processing, if the error value is known.

8. Pressure Effects

Radiometers are usually not sensitive to pressure, although the response may change when transferred from the laboratory to the vacuum of space. Such a change may arise from convection currents near the detector or by bombardment of the sensor by molecules in the atmosphere, resulting in different heat transfer characteristics.

9. Air Convection or Ventilation

As mentioned above, a change in response of a radiometer on being transferred from the laboratory to space may be a consequence of convection currents near the detector. Similarly, the response of certain types of pyradiometers (e.g., those of the Gier and Dunile design) is strongly affected by wind effects on the sensor unless some method of compensation is utilized, and convection problems inside some pyranometers cause significant measurement errors. The operation of the Gunn-Bellani pyranometer, on the other hand, depends on gas transport by convection currents. Convection effects can sometimes be minimized by baffles or other air control devices.

10. Saturation Effects

If a signal saturates the instrument, information is lost. Therefore, calibration signals should bracket all possible meaningful observations. Photomultiplier tubes, ionization chambers, and other high gain devices may be saturated by moderate flux densities in space. Partial saturation may cause subtle errors which are difficult to detect in the output signal. It may be possible to change the saturation level by changing bias voltage or other operating parameters, but the most logical and efficient way is to keep incident light levels within operating specifications. This latter goal may be achieved by the proper use of filters, restriction of the FOV, or other methods of flux control.

11. Spectral Response

The causes of errors in spectral distribution include imperfect window transmission, spectral dependence of paint absorptivity, or a spectrally sensitive work function of cathode material. These errors are minimized by calibrating the instrument with radiation of a spectral distribution as close as possible to that of the radiation to be measured.

12. Thermal Effects

Almost all radiation instruments are sensitive to temperature. Electrical resistance varies with temperature, alignment of components is effected by temperature, and random electron emission is proportional to temperature.

The best way to eliminate the problem is by thermal control of the sensor, but such is not always possible. In the absence of thermal control, a complete thermal response calibration is necessary and the calibration must be performed under various levels of sensor irradiance for each of a number of likely operating temperatures. Once in use, the instrument temperature must be monitored.

13. Time Constant

The time constant is an important factor for a sensor that scans spatially or spectrally, especially on an aircraft or spacecraft, because of rapid change of the incident radiation. If the time constant is comparable to the scan time of a radiometer, the signals may be badly distorted. The speed of response is generally slower for an instrument responding to temperature than for one responding to individual photons. Under certain circumstances the time constant can be adjusted to provide convenient integration, but usually a rapid response is desired. If the time constant is known, correction factors may be developed.

E. DATA PROCESSING

1. Erroneous Data Transmission

The transmission of erroneous data may arise from many of the possible sources of error already discussed in this section, or from random or systematic discrepancies in the electronics of a recorder or transmitter. Possible means of detection and correction include comparison of output from two similar instruments such as the THIR and SR, and a knowledge of what range of measurements is likely to occur. However, the occurrence of one or more measured values that are outside the normal range does not necessarily mean the data are in error, but that they should be handled with caution.

2. Random Noise

In any recording, transmitting, receiving, or processing system, random noise can and probably always does occur. These short period, uncorrelated fluctuations may be a consequence of variations in voltage input, the electronics, recorder speed, atmospheric effects between transmitter and receiver and a number of other causes. For any single

measurement, noise may result in a significant error, but in many cases it can be minimized when the data are averaged or smoothed.

3. Computation Errors

Truncation and round-off errors can be significant if high accuracy is desired. Their importance may become even greater if the required output involves a complicated procedure of processing, since such errors tend to increase as they propagate through the system, possibly leading to a large error in the final output.

4. Capacity of the System

The processing system may become saturated if all possible data are transmitted; if some data are dropped the accuracy may degrade, or certain features within the data may be lost. Most contemporary satellites can acquire more data than the recording, transmission and/or processing system can handle. This problem is usually handled by sectorizing, with its concurrent loss or "throw-away" of data from much of the earth. Archiving of vast amounts of data presents its own peculiar set of quality considerations. While most of these factors cannot readily be addressed as calibration, rare indeed is the researcher who has not abandoned at least some well made plan because the desired data could not be recovered from archive in a usable format.

F. TIMING OR CALIBRATION FREQUENCY

Accuracy and frequency in calibration are essential, but usually at odds with each other and with acquisition of data. One must calibrate frequently enough so that signal changes from unwanted effects are as close to zero as possible, or at worst linear. Accuracy usually requires a sufficiently long "look" at the calibration source. Notwithstanding the requirement for these data in the sensing cycle, there must be sufficient time to acquire data.

The above classification simply groups some rather extensive and elaborate calibration subjects. Generally it expands and emphasizes part of the "long and complicated chain" described by Hanel (in Drummond, 1975).

CHAPTER III

SENSOR SYSTEMS AND RADIATION SOURCES

A. INSTRUMENT TYPES

Several categories of instruments will be described briefly. Details for various individual sensors may be found in Chapter 7 and the various User's Guides, papers, and reports more or less available to the public. Some of the written material is referenced at the end of the description for each type of radiometer. It is worth noting here that the detailed descriptions of specific instruments usually published by the builders are often difficult to obtain, since these reports generally have a very limited distribution. The types discussed below include the most common radiometers used in meteorology, but it is not intended that a complete listing be made of all past, present and planned radiometers.

1. Scanning Radiometers

Scanning radiometers operate in the visible, infrared and microwave regions. Several notable instruments including the SR, VHRR, THIR, VISSR, ESMR, and SCAMS are in this classification. These instruments perform a horizontal scan perpendicular to the sub-satellite track, acquiring one or more lines of data during each scan. Scan line to scan line movement is provided by the forward motion of the spacecraft, except in geosynchronous satellites, where a stepping mirror performs this function. There are two basic types of scanning systems.

(a) Spin scan systems are those in which the scanning motion is provided by the rotation of the entire spacecraft. Line to line movement is generated by stepped movement of a scanning mirror on geosynchronous satellites and by spacecraft motion in the non-stationary orbiters.

(b) Mechanical and electronic scan systems, where a mirror or an antenna provides the scanning motion. An antenna may be moved mechanically like a mirror, or a "false" scan may be set up by the use of electronic phase shifting. The ERB has a different mechanical scanning system in which the entire telescope assembly moves.

Most scanners that operate in the visible, near infrared or thermal infrared use one set of scanning optics for all spectral regions, while those operating in the microwave often utilize separate antennas for different frequencies. Along each scan a chopper, or some other sort of "limiting" device determines the period of each look, thereby restricting cross-track smearing of the input (i.e., the signal representing more than one FOV).

Typical FOV's for current scanning radiometers range from about 80 m to >100 km near nadir. Generally, visible and near infrared sensors provide the best FOV (0.08 to 4 km), thermal infrared the second best (0.24 to 9 km), and microwave the largest (~12 to >100 km). Some factors that affect FOV are angular aperture (i.e., the solid angle the source subtends at the input aperture) for visible through thermal infrared instruments. Beam width is the equivalent term for microwave systems. Orbital geometry is obviously a FOV factor for any viewing system. (See Sissala, 1975; Lansing and Cline, 1975; Dickenson et al, 1974; Hickey and Karoli, 1974; McMillin et al, 1973; Sabatini, 1972; NASA, 1972a, 1972b; Pipkin, 1971.)

2. Fixed Radiometers

These sensors view the surface at a fixed angle, usually nadir, and generally have a large FOV. An example is the S194 with a FOV of 110 km at half-power beam width (half-power beam width refers to the width of the beam that encompasses 50 percent of total received energy). This class of radiometer includes those with an "unlimited" FOV that may view the whole disk of the earth. They may consist of a flat plate, a sphere, or a hemisphere, and are used for tasks such as monitoring total hemispheric global radiation. These sensors are sensitive to visible, infrared, or total solar radiation. Examples are the fixed sensors on the ERB and the older white plates and spheres of the TIROS and ESSA series. Fixed radiometers may be used to orient the satellite or adjust the gain of another radiometer as on the DMSP (Dickenson et al, 1974). (See Sissala, 1975; Hickey and Karoli, 1974; NASA, 1972a.)

3. Restricted Scan

This category of radiometers lies between those already

discussed. Instruments in this group may scan manually (e.g., the S191) or scan in discrete steps on command, or be caused to scan automatically. The eight scanning channels on the ERB operate on command or automatically. These radiometers are useful for observing a particular target for a predetermined period continuously at varying angles, for complicated and changing scan patterns, or for monitoring the radiation budget on a synoptic or lesser scale. Instruments in this category operate in the visible, infrared and microwave. FOV's range from 0.45 km (S191) to about 100 km (long dimension of ERB scanning channels). (See Sissala, 1975; Hickey and Karoli, 1974; NASA, 1972a.)

4. Sounders

Atmospheric soundings are inferred from measurements of radiances in the infrared spectrum, the microwave, or a combination of both and the data may apply to altitudes from the surface up to 85 km. The basic arrangement of most sounders is similar to that of scanning or fixed radiometers. A primary distinction is the near-simultaneous sensing in several wavelength intervals. For example the SSH carried on the DMSP satellite has 16 channels, 8 in the water vapor rotation bands between 18 and 30 μm , 6 in the 15 μm carbon dioxide band, one at 9.8 μm in the ozone band, and one at the 12.0 μm window. Most sounders have a window channel to infer the surface temperature. The FOV's of most infrared sounders range from about 25 to 70 km near nadir, and for microwave sounders from about 100 to 150 km at half-power beam width.

Two distinct types are the PMR/SCR and the LRIR. The former group uses intervening cells of carbon dioxide for the detection of radiation emitted by various layers of atmosphere. The SCR alternately views the atmosphere through a cell of varying pressure and through a clear column without the cell. The PMR has two channels each of which "looks" through a pressure modulated cell. In both instruments the higher the pressure or greater the optical depth of carbon dioxide in the cell the further down in the atmosphere the sensor "sees". The range of altitude of the resultant temperature profile is from the surface to 50 km for the SCR and 40 to 85 km for the PMR. These radiometers are fixed towards nadir with a FOV of about 30 km and 50 km for the SCR and 500 km along the sub-satellite track for the PMR.

The LRIR views the atmosphere at the limb (the edge of the

earth's "disc"). Scanning occurs vertically over a range of $\pm 1^\circ$, from about 50 km down to about 10 or 15 km (roughly the line of sight from the satellite tangent to the earth's surface). There are two temperature channels in the $15\mu\text{m}$ band of carbon dioxide, one in the ozone band at $9.6\mu\text{m}$, and one in the water vapor band at $25\mu\text{m}$. The first three channels have a FOV of $2 \times 20 \text{ km}$ (vertical x horizontal) and the latter $2.5 \times 25 \text{ km}$. A third temperature "channel" is derived from the difference of the other two. (See Nichols et al, 1975; Sissala, 1975; Dickenson et al, 1974; McMillen et al, 1973.)

5. Active Microwave

The previously noted microwave radiometers operate passively, while an active one operates as a radar transmitting at low power (if compared with ground based installations). An example of an active system is the S193 which operated aboard the SKYLAB. In the active mode it acts as a scatterometer to measure radar backscatter and an altimeter to measure terrain and ocean heights to a great accuracy (about 1 m). The planned Seasat satellite scheduled for launch in the late 1970's will carry an even more accurate instrument to measure, for example, wave heights. (See NASA, 1972a.)

B. TYPES OF RADIATION SOURCES

Sources of radiation which have been used or proposed for pre-launch calibration of radiometers are discussed in groups according to applicable spectral regions, e.g., the ultraviolet, visible, infrared, or microwave.

1. Ultraviolet

a. High Temperature Black Bodies

These may be considered as furnaces radiating as black bodies with a brightness or radiance temperature of several thousand degrees or more. Samson (1967) briefly describes a black body radiator that operates at a temperature of $11,900^\circ\text{K}$ at the axis of its cascade arc. Drummond et al (1970) describe several black bodies that operate at temperatures closer to 2000 or 3000°K . These latter black body devices produce useful amounts of radiation in the near ultraviolet (about 380 to 200 nm), but not in the vacuum

ultraviolet (200 to 120 nm) or extreme ultraviolet (120 to 10 nm). (The wavelength boundaries in the ultraviolet (uv) vary slightly between different authors, but the relative position of the three spectral regions is not disputed.)

b. Lamps

A variety of high intensity filament lamps and arc lamps are described by Samson (1967), Green (1966), Canfield et al (1973), and Ott et al (1973). Typical lamps are the tungsten strip and carbon arc lamps. The former has a characteristic temperature of about 2600°K and the latter about 3800°K . Lamps are used most often for calibration of sensors in the near uv, although some special lamps have been developed that radiate significantly in the vacuum uv (see Canfield et al, 1973).

c. Discharge Tubes and Plasmas

High intensity discharge sources convert gases, such as hydrogen or helium, into plasmas at temperatures of 10,000 to $20,000^{\circ}\text{K}$, producing radiation in the near, vacuum, and extreme uv. A variety of these tubes are described by Samson (1967), Green (1966), Ott et al (1973), Fastie and Kerr (1975), and Paresce et al (1971). Deviations in output of ± 10 percent are not uncommon.

d. Synchrotron Radiation

Synchrotron radiation is a highly stable absolute source for vacuum and extreme uv systems, especially the latter. The energy from this source may be measured to about 0.5 percent and the radiated power to about 3.5 percent according to Samson (1967), who discusses synchrotron radiation in some detail. Two disadvantages of a synchrotron source for some detectors are the high degree of polarization and the very small angular extent of the "beam" (D. Bede, private communication, 1976).

e. Luminescent or Fluorescent Materials

Green (1966) describes several materials that emit a low level of continuous radiation when stimulated by shortwave or particle radiation. These materials radiate primarily in the near uv, but also in the vacuum uv. Some phosphors

are kept at the NBS; emission spectra of two of them are illustrated in Green (1966).

f. Solar

The sun is the only natural source of uv for use on or near the earth's surface. It is a good, reasonably stable source in the near uv, but the solar output appears highly variable below about 200 nm. For the interval from 120 to 200 nm solar flux measurements differ by a factor of two or three (D. Bede, private communication, 1976). On earth the effective lower limit is about 295 nm because of atmospheric ozone (Green, 1966).

2. Shortwave (Visible)

a. Diffusion Plates

Diffusion plates are not strictly sources, but may be treated as such in the context of this section. These optical elements are specially ground or coated plates used to diffuse the direct beam from the sun or a lamp to provide a uniform and not too intense source of light. The plates may transmit or reflect the incident light. Jones et al. (1965) describe a light source that utilizes flashed opal glass as a diffusing surface, whereby light from two lamps in an enclosure is transmitted through the glass to the detector.

b. Lamps, Lasers, and Light Emitting Diodes

A variety of lamps are commonly used as standard sources. Some examples are 1000 W quartz-iodine lamps and carbon, tungsten, or carbon or tungsten in quartz lamps of 100 to 1000 W. Drummond et al (1970) describe a number of lamps in some detail. Tables 3.1, 3.2, and Figure 3.1 show some characteristics of typical lamps. Uniform light may be provided by the use of integrating spheres or diffusion plates. Solar simulators are often calibrated against standard lamps at various wavelengths (e.g., Neuder, 1970).

A laser can provide a precise light source at a specific wavelength, i.e., virtually monochromatic. A laser may be useful for the calibration of instruments with a very narrow spectral response or provide a specific reference point for the determination of spectral response over a

LAMP No.	(V)	IRRADIANCE
		at 1m $(\mu\text{W cm}^{-2})$
100-W lamp standards operated at 0.75A		
7741	97.57	570.2
7745	96.56	583.9
7746	94.94	549.5
7749	94.04	542.8
500-W lamp standards operated at 3.60A		
1	90.18	2963
3	90.00	3007
4	89.51	3072
5	89.24	2967
1000-W lamp standards operated at 7.70A		
1	100.94	7234
2	101.04	7398
3	101.16	7350
4	101.03	7238

TABLE 3.1: Total irradiance from three groups of tungsten-filament lamp reference standards. (From Drummond et al., 1970.)

broad interval. An important use for lasers is the determination of proper optical alignment, such as the alignment of the sun calibration mirror of the MSS (Landsat) using a helium-neon laser (Horan et al., 1974).

Light emitting diodes (LED's) can be made to emit light over a relatively precise wavelength interval. Although the intensity of output is often low, the repeatability of output is very good. In addition, the power requirements are generally quite small, thereby permitting their use in space. Arrays of LED's can be used to provide convenient,

λ (nm)	QM-11	QM-12	QM-13	MEAN
250	0.0189	0.0220	0.0207	0.0205
260	0.0340	0.0389	0.0367	0.0365
270	0.0582	0.0650	0.0619	0.0617
280	0.0934	0.103	0.0984	0.0983
290	0.141	0.155	0.148	0.148
300	0.0201	0.221	0.212	0.211
320	0.382	0.416	0.402	0.400
350	0.874	0.937	0.914	0.833
370	1.34	1.43	1.40	1.39
400	2.32	2.46	2.41	2.40
450	4.51	4.76	4.68	4.65
500	7.50	7.76	7.65	7.64
550	10.8	11.2	11.0	11.0
600	14.2	14.7	14.4	14.4
650	17.5	18.1	17.8	17.8
700	20.5	21.0	20.9	20.8
750	22.5	23.1	22.9	22.8
800	23.8	24.4	24.2	24.1
900	24.6	25.2	25.1	25.0
1000	24.0	24.6	24.5	24.4
1100	22.4	23.0	23.0	22.8
1200	20.4	21.0	21.0	20.8
1300	18.4	18.9	18.9	18.7
1400	16.5	16.9	16.9	16.8
1500	14.6	14.9	15.0	14.8
1600	12.9	13.1	13.2	13.1
1700	11.3	11.4	11.5	11.4
1800	9.80	9.90	9.98	9.89
1900	8.49	8.59	8.62	8.57
2000	7.33	7.42	7.45	7.40
2100	6.39	6.50	6.50	6.46
2200	5.69	5.72	5.75	5.72
2300	5.04	5.10	5.14	5.09
2400	4.56	4.60	4.64	4.60
2500	4.18	4.19	4.26	4.21

Table 3.2

Spectral irradiance of 1000-Watt tungsten-filament quartz-iodine lamps in $\mu\text{W}/\text{cm}^2\cdot\text{nm}$ at a distance of 50 cm when operated at 8.30 A. (From STAIR in Drummond et al [1970])

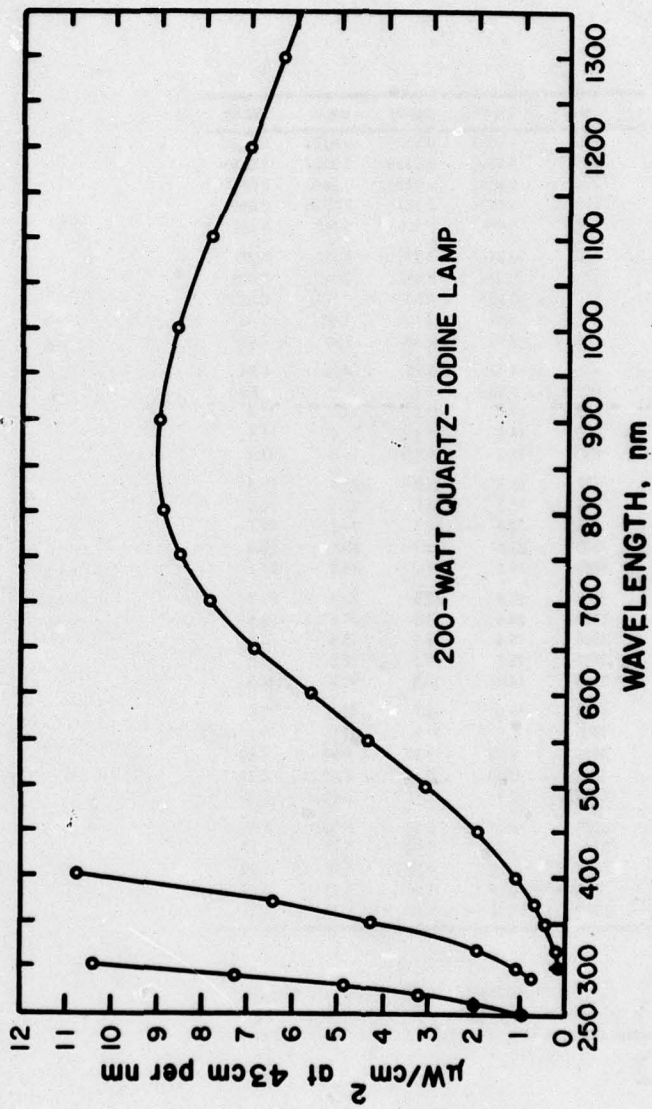


FIGURE 3.1: Spectral irradiance from a 200-W quartz-iodine lamp standard. Irradiance units are $\mu\text{W}/\text{cm}^2 \text{ nm}^{-1}$ with the lamp 43 cm from the detector. (From Drummond et al., 1970.)

repeatable sources for calibration in terms of intensity or spectral distribution. For example, side-by-side arrays of different diode types can give two spectral distributions, and the intensity of radiation from each array may be varied by de-energizing selected LED's in pre-defined patterns.

c. Plasmas

Plasma tubes are high intensity sources of radiation ranging from the ultraviolet through the near infrared. Inert gases or combinations of them may be used to provide light in a narrow or relatively broad spectral interval. Examples of the latter are discussed by Neuder (1970) for the purpose of solar simulation in the interval from 0.25 to 2.5 μ m. The relative contribution from a given portion of the interval may be changed by varying the amount of plasma or current. A diffuse source is obtained through the use of an integrating sphere or diffuse plates.

d. Solar

The sun is the only good natural source of shortwave (visible - near infrared) radiation available for pre-flight calibration. It may be viewed directly, via diffusion plates, through restricted apertures, through filters, or indirectly, i.e., after reflection. Calibration should be performed where the atmosphere is as clear and clean as possible such as on a mountain observatory. Problems of atmospheric effects are reduced considerably if calibration is done in conjunction with coincident viewing by a standard instrument (e.g., cavity radiometer). This second instrument is used to detect variations in solar radiation, thus permitting compensation of changes arising from atmospheric variations.

e. Spectrometer/Monochromator

Spectrometers may be used in conjunction with a lamp and various optical elements to produce a quasi-monochromatic source of radiation. Such a device is described by Fried and Labs (1974). The spectrometer may utilize gratings or prisms for spectral separation. A spectrometer used to produce quasi-monochromatic radiation is often called a monochromator.

f. Solar Simulator

Solar simulators consist of special lamps or plasma tubes that radiate with a spectral distribution or intensity reasonably close to that of the sun over a given spectral interval. Usually a close match is attained only over a small portion of the spectral range of interest. A compact arc lamp is a standard type of solar simulator.

Neuder (1970) investigated the use of plasmas of inert gases which simulated solar radiation from 0.25 to 2.5 μ m, better than compact arc lamps. Increasing the quantity of plasma increased the relative contribution from shorter wavelengths and combinations of gases were best even at lower plasma currents (typical currents varied from less than 100 to more than 250A at 50 to 60 V). Generally the total emitted radiance is similar to the solar value over the desired spectral interval, but there is never an exact match of spectral distribution. Neuder obtained a uniform source of diffuse radiation by use of an integrating sphere.

Jones et al (1965) describe a light source that simulated sunlight in the 0.47 to 0.85 m interval. Two quartz-iodine lamps were placed in front of a cylindrical reflector in a box. The lamps and the reflector were moved to alter the brightness of the light leaving the box through a plate of flashed opal glass. The spectral radiance of the lamps was similar to that of a black body at about 3400°K. Sunlight was approximated by the addition of various filters. However, the spectral distribution of the source was not determined, only the overall output for the given spectral range. This source was used to calibrate television cameras for early Nimbus satellites.

3. Longwave

The devices discussed in this section are used in the laboratory and are often referred to as black bodies. Temperature control frequently involves the use of liquid nitrogen for cooling plus resistive heating or thermoelectric heat pumping for temperatures from about 200 to 350°K.

a. "2π" Cylinder

Karoli et al (1975) describe the cylinder as having a 35.5 cm length and a 35.5 cm diameter. The emissivity of the inner surface may range from about 0.92 to 0.96 yielding

an effective emissivity for a radiometer viewing the 7.5 cm diameter hole at the top of about 0.9999 to 1.005, according to their calculations. (An $\epsilon > 1$ is caused by reflected radiation from the sensor being calibrated.) The authors claim a temperature uniformity of about 0.1°K across the FOV, and an accuracy of the measured temperature of the source of 0.05°K . Table 3.3 presents some further details.

b. Cavities

Cavities include cones, cylinders, and spheres and are generally more desirable (i.e., ϵ closer to 1.0000) than flat plates or grooved surfaces. A honeycomb type black body is really an array of small cavities; Karoli et al (1975) indicate a rough equivalence in ϵ between their 2π cylinder and $4/1$ (length/diameter) honeycomb.

c. Flat Plates

These black bodies have surfaces that have been blackened and, frequently, grooved. Effective emissivity of a flat surface may be about 0.96, and 0.995 or better for a grooved surface (Karoli et al, 1975). Generally, a flat plate is used for wide angle sensors such as on the ERB (see Table 3.3).

d. Honeycombs

Honeycomb sources are basically plates whose surfaces consist of an array of small hexagonal cavities, where the emissivity of the surface of each cavity is about 0.96 for those described by Karoli et al (1975). Effective emissivity of these plates may range from about 0.999 to about 1.005. Karoli et al, claim a temperature uniformity and accuracy of close to 0.1 and 0.05°K respectively. These sources are widely used as may be seen in Table 3.3.

e. Water

A water surface is an inexpensive, readily accessible source. The temperature may be controlled fairly precisely and can be measured by any good immersion thermometer. In general, emissivity of water, without special preparation,

PROJECT	OPERATIONAL RANGE (K)	TARGET SIZE (cm ²)	CONFIGURATION	METHOD OF CONTROL
SIRS	240	330	Honeycomb	Thermoelectric
VTPR	100	340	Honeycomb	LN ₂ + Thermoelectric
VHRR	100	340	Honeycomb	LN ₂ + Thermoelectric
SCMR	260	320	Honeycomb	Thermoelectric
HIRS	100	340	Honeycomb	LN ₂ + Thermoelectric
LRIR	90	320	Honeycomb	LN ₂ + Resistive Heating
ERB	100	390	Concentric	LN ₂ + Resistive Heating
E ³	175	425	1000 [base only]	V Grooves
TOVS	90	340	800	Cylinder (2)
				LN ₂ + Resistive Heating
				LN ₂ + Resistive Heating

TABLE 3.3: Characteristics of Calibration Sources. (From Karoli et al., 1975.)

is about 0.99 for a normal view at selected wavelength intervals (e.g., near 11μm). However, emissivity decreases at other wavelengths and decreases rapidly for larger look or nadir angles (especially those > 40°). Buettner and Kern (1965) present information on emissivity of water.

Most often the water is in a dewar flask or in a flask immersed in a container of liquid which is in turn heated or cooled. Kano and Suzuki (1976) have constructed a

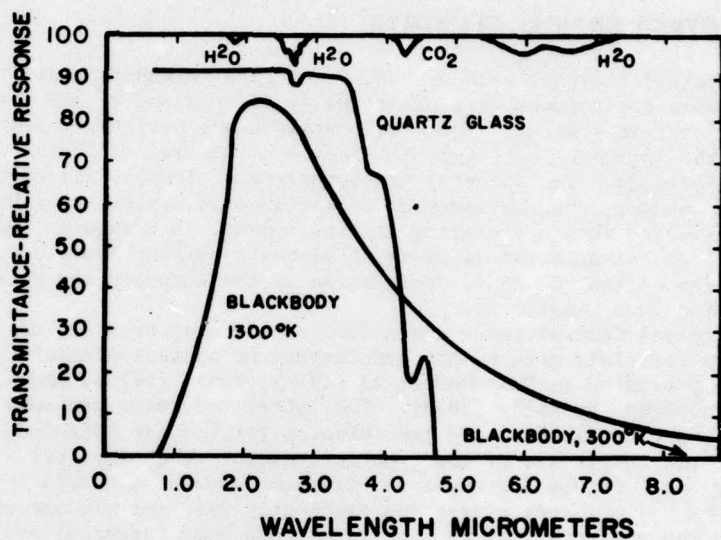


FIGURE 3.2 Spectral irradiance of 1000-Watt tungsten-filament quartz-iodine lamps in $\mu\text{W}/\text{cm}^2\cdot\text{nm}$ at a distance of 50 cm when operated at 8.30 A. (From Drummond et al., 1970.)

special calibration device where the water surface is made rough by the action of numerous tiny water jets, thereby lowering the reflectance. The effective emissivity of their black body is equal to 1.000 ± 0.007 in the wavelength interval between 5 and $100\mu\text{m}$.

4. Microwave

Pre-launch sources for microwave radiometers include grooved plates and "noise" generators. These latter devices input a signal that is equivalent to that produced by a black body at a selected brightness temperature. When the signal is input via the antenna lead, thereby skipping the antenna, errors arising from faults in the antenna are not detected.

C. OTHER OPTICAL ELEMENTS

Optical elements such as lenses, filters, windows, and mirrors are common parts of virtually all radiometer and calibration systems. These elements are not strictly parts of the source or detector, but they are integral to their performance. The spectral transmittance of lenses, filters, and windows, and the spectral reflectance of mirrors must be considered when calibrating any instrument. A change in the optical characteristics of these elements arising from, say, contamination can cause degradation of the accuracy and precision (see Chapter 2).

Typical transmittance and reflectance characteristics of some materials used in the manufacture of optical elements are presented in Drummond et al (1970), Weast (1975), and Wijnbergen and Kelly (1974). The latter reference presents curves of reflection and transmission for the far infrared, but the curves are of the type derived for other spectral regions. Figure 3.2 shows the transmittance of a quartz plate, (i.e., such plates are frequently used for windows of sources and detectors in the visible and near infrared) and compares it with transmittances for 33 cm (STP) paths of water vapor and carbon dioxide. A curve of relative spectral emission of a 1300°K black body is drawn on this figure, permitting the estimation of the approximate percentage of energy transmitted through the plate from such a black body. Similar graphs could be drawn for other sources and windows. Weast (1975) presents more detailed information on spectral transmittance and reflectance for various materials in tabular form.

CHAPTER IV

ERROR MECHANISMS FOR SELECTED SENSOR TYPES

A. SOLAR MEASUREMENTS AND BLACKBODY CAVITY DETECTORS

Potential sources of error in the measurement of solar irradiance and in the use of black body cavity detectors, and the precision with which they can be measured are treated by Kendall and Berdahl (1970), Kendall (1973); and are briefly recounted here.

1. Circumsolar Radiation

This is direct radiation from outside the solar disk from the corona or solar aureole. Error in the measurement thereof is usually less than one percent, but with surface based pyrheliometers having a large angular field of view the error may be as large as 2 to 3% or more. Precision losses of this magnitude, when propagated through a calibration cycle can become highly significant.

2. Loss of Radiation Through Aperture

Radiation can be reflected back or emitted by the cavity out through the aperture, and never contribute to sensor response. For most environmental and cavity temperatures the net loss is probably much less than one percent. While probably usually insignificant, the mechanism for this energy loss must be recognized by instrument designers.

3. Effect of Diffraction

Measured radiation may be increased by diffraction of radiation by the edge of an aperture; a small percentage of this diffracted radiation may enter the cavity. This increase is wavelength dependent (percent "blue" ≈ 0.05 and percent "red" ≈ 0.06), and while small (for solar radiation the increase is probably less than one percent for all principle wavelengths) should be recognized.

4. Effects of Time Constant

The comparison of two radiometers with different time constants requires that close attention be given to the difference.

The time constant (t_c) may be defined as the time needed by the instrument to respond to a signal to within $1/e$ of the total response that would occur after a time tending to infinity. Generally the duration of measurement should be about six times the time constant or more so that the radiometer settles to within a few hundredths of a percent of the "final" or "total" value.

A lag always exists when $t_c > 0$, and an error arises when an instrument with a long t_c is compared with one with a short t_c under changing field of radiation. An example is given in Kendall (1973) for two radiometers with $t_c = 3$ and 6s, a steady variation in solar irradiance of 0.0065 Wcm^{-2} sec and mean value of 0.09 Wcm^{-2} would lead to a difference in measurement of $\approx 0.0007 \text{ Wcm}^{-2}$, or 0.78 percent. Time constants of instruments aboard satellites must of necessity be small and constant to provide meaningful data from fast moving platforms.

5. Time Rate of Change of Radiometer Temperature

Heating of the surface causes heat to flow through the thermal resistor to the body, or heat sink, or the radiometer. This effect is important for radiometers that measure a temperature drop across a thermal resistor. If the surface temperature changes with time the heat capacity of the receiver has a lag in temperature, which combines with the temperature drop across the resistor to cause an incorrect measurement. One can compensate for this "error" by having an equal thermal mass and resistor at the cold junction of the thermopile, i.e., equal temperature lags at warm and cold junctions.

6. Unwanted Thermal Resistance by Coating

It is possible that any sensor or optical element may exhibit a temperature drop across the coating, with a resultant degradation of data signal. However, the size of the error can be expected to be small, probably much less than one percent.

7. Uncertainty in Area Aperture

This source of error involves the computation of heat loss through the aperture (see 2 above). The percentage of error should be much less than one percent.

B. SOURCES OF ERROR FOR A SCANNING RADIOMETER IN SPACE

Some possible causes of sensor degradation, and consequently, instrument error, are discussed by Horan et al (1974) for the MSS carried by the Landsat satellite. These potential causes, which are listed below, may apply to most visible and near infrared radiometers.

1. Change in Calibration Lamp Irradiance

Change in the energy in the output of the calibration lamp should cause a roughly proportional shift in output for all channels.

2. Excitation of Calibration Lamp

Even if the calibration lamp is powered from a source of constant current that is monitored via telemetry, evaporation of filament metal and deposit on bulb envelope could increase resistance and therefore power, leading to a change in brightness and/or color temperature. Evaporated metal also would act as a neutral density filter. If the effects were balanced, a situation which appears unlikely, at least there would be a shift to shorter wavelengths. If they were not balanced, there would be both an irradiance and a spectral shift.

3. Photo-Multiplier Tube (PMT) High Voltage Excitation

The amplification factor of a photomultiplier is extremely sensitive ($\sim v^8$) to the impressed high voltage. Thus small changes in the high voltage supply would bring about changes in the signals from all measurement channels for which the photomultiplier is the sensor.

4. Van Allen Radiation

Radiation damage may affect the glass of the mirrors and other optical components. The optics on the MSS were

enclosed in an aluminum housing, and the calibration wedge lamp and focusing lamp were in a 1 mm thick steel housing. Even though the radiation level at the wedge lamp was estimated at less than 1000 rad, and more probably less than 100 rad, there may have been sufficient damage of the optical components to cause significant errors in the response of the instrument.

5. Partial Blockage of Sun Calibration Mirror or Aperture

A blockage of the source of radiation used for calibration would obviously negate the calibration. The design of sun calibration optics generally makes it unlikely that any material could block the solar beam. However, this source was considered as a possible contributor to problems on the MSS (ERTS-1).

6. Spectrally Selective Contaminant

For the MSS instrument, it was postulated that the sun calibration mirror was contaminated before launch with a material that is transparent in the 0.5-1.1 μ m interval during pre-launch calibration. It appeared that in the post-launch period, unfiltered ultraviolet radiation transformed the contaminant into a material having a spectrally selective reflectance. The evidence for this is as follows:

During thermal vacuum tests some Mylar insulating tape overheated and left a milky deposit on the MSS collimator mirror and several witness mirrors. Tests showed no degradation of performance, but sunlight was not used. The optics were not cleaned prior to launch. The sun mirror receives direct solar radiation, and the scan mirror and internal components may receive scattered ultraviolet radiation through the input aperture. Therefore, transformation of contaminating material would occur relatively slowly for internal optics. This supposition fits with the observed relative stability of the sun calibration while the calibration wedge changed continuously.

A laboratory experiment supported this supposition in that exposure of contaminated mirrors to ultraviolet radiation (< 0.164 μ m) caused degradation, especially at shorter wavelengths. However, in the MSS one would expect degradation of the scene signal and further degradation of the sun calibration signal, along with degradation of the wedge signal,

since these optics are in "front" of the wedge optics and the more forward optics should have been contaminated as well. Nevertheless it did not occur. An answer to this paradox may be outgassing in space from the forward optics, or internal contamination from a source near the wedge optics. In any case, spectrally selective contamination cannot be summarily dismissed as a possible source of error.

C. EXAMPLES

In this section several examples of possible errors in output that may arise from calibration errors are presented, and actual problems with a satellite system are discussed. A typical "every-day" problem involving satellite calibration is shown for the VISSR of the SMS-2.

1. Hypothetical Examples

a. Non-linearity of Instrument Response

Nearly all in-flight calibrations are performed using two data points, a dark (cold) reading and a bright (warm) one. The instruments are usually designed to closely approximate a linear response over the range of brightness or temperature desired. However, for quantitative measurements, even a small deviation from linearity may lead to significant error.

As an example, assume that a narrow window channel is centered at 11μ m with a spectral range sufficiently narrow that a mean wavelength (λ) approximation is valid. For this, channel radiance has been assumed to be linearly related to voltage with zero voltage for the space view and 5V for the maximum radiance (that for a black body at 320°K). This relation is given by $R = a + bV$ where a is the offset, V is the voltage, R is the radiance, and b is the coefficient relating V to R . For simplicity $a = 0$. As with nearly all real sensors, the relation of R to V deviates to a greater or lesser degree from linearity. The relationship now is given by $R = a + bV + f(V)$ where $f(V)$ is some function of V , e.g., $f(V) = c \sin\pi V/V$ where V_m = maximum voltage and c is a constant. Temperature deviations have been computed for values of $f(V)$ of $0.05v$ and $0.1v$ and for temperatures near 200 , 274 , and 300°K ($274^{\circ}\text{K} = T$ of the radiance for $V = 2.5v$, the midpoint of the line given by the linear relation and the point of maximum deviation if $f(V) = c \sin\pi V/V_m$). These

deviations are not unrealistic, as they represent ""errors" of only 1 and 2 percent relative to V . Through the use of the Planck function the following differences in temperature (ΔT) shown in Table 4.1 were computed for the given deviations.

$f(V)$	200	274	300
0.05	3.5	1.1	0.9
0.10	7.2	2.3	1.8

TABLE 4.1: Values of ΔT for two deviations in voltage, $f(V)$, at three values of T . $f(V)$ is in volts and ΔT and T are in $^{\circ}$ K, ΔT to the nearest 0.1° K.

From these crude calculations it is seen that deviations in equivalent black body temperature of the order of 1 or 2° K may arise from relatively minor deviations from linearity for commonly observed radiances.

A similar problem could occur for an instrument operating in the visible spectrum. Figure 4.1 taken from NASA (1972b) shows curves of voltage output versus radiance for the three return beam vidicon (RBV) cameras of Landsat. If no corrections were made for non-linearity of response an error of about $0.14 \text{ mWcm}^{-2}\text{ster}^{-1}$ could occur in the output for camera 3 near a radiance of $0.7 \text{ mWcm}^{-2}\text{ster}^{-1}$. Here we have taken the two reference points as the minimum and maximum voltages on the graph. If 1.0V was the high reference (saturation according to NASA, 1972b), then the resultant maximum error would be about $0.08 \text{ mWcm}^{-2}\text{ster}^{-1}$. These two potential errors in scene radiance expressed as percentages amount to 20 and 16 percent respectively, at the points of maximum deviation.

These two examples suggest the need for verification of total system response, i.e., optics, detector, and electronics, etc. The system should be calibrated at more than two points when in orbit, if at all possible. Three or four suitably chosen reference points should suffice as a check for linearity under most circumstances.

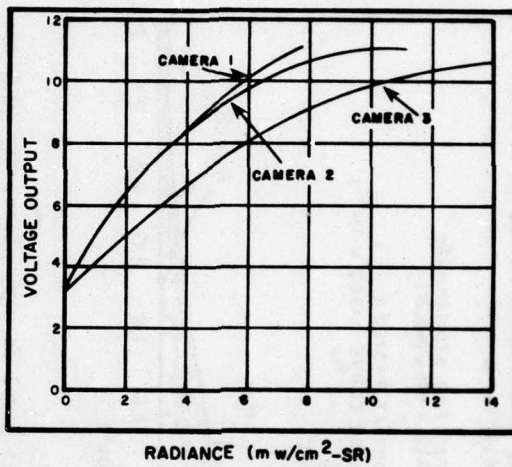


FIGURE 4.1: RBV light transfer characteristics. (From NASA, 1972b.)

b. Incorrect Spectral Response

It has not been unheard of for contamination, degradation, or misalignment of filters or other optical elements to cause a shift in the spectral distribution or interval. Figure 4.2 and Table 4.2 illustrate the solar spectrum for $0.1 < \lambda < 2.6\mu\text{m}$ and $0.115 < \lambda < 50\mu\text{m}$ respectively. For a rectangular filter function an undetected shift in spectral interval from $0.5-0.7\mu\text{m}$ to $0.6-0.8\mu\text{m}$ could cause a change in signal output of about 18 percent. More realistically, a noticeable change could occur for a relatively minor change, say, from $0.48-0.58\mu\text{m}$ to $0.50-0.60\mu\text{m}$. Referring to Table 4.2, the percentage change in received radiance would be about 3 percent. With the aid of this table, and a more detailed one in Drummond and Thekaekara, computations can be made of change in output for more complicated filter functions or for undetected contamination or degradation that is spectrally dependent.

Spectrally dependent degradation may alter the spectral distribution without changing the interval. We may consider a form of degradation that has caused a rectangular filter

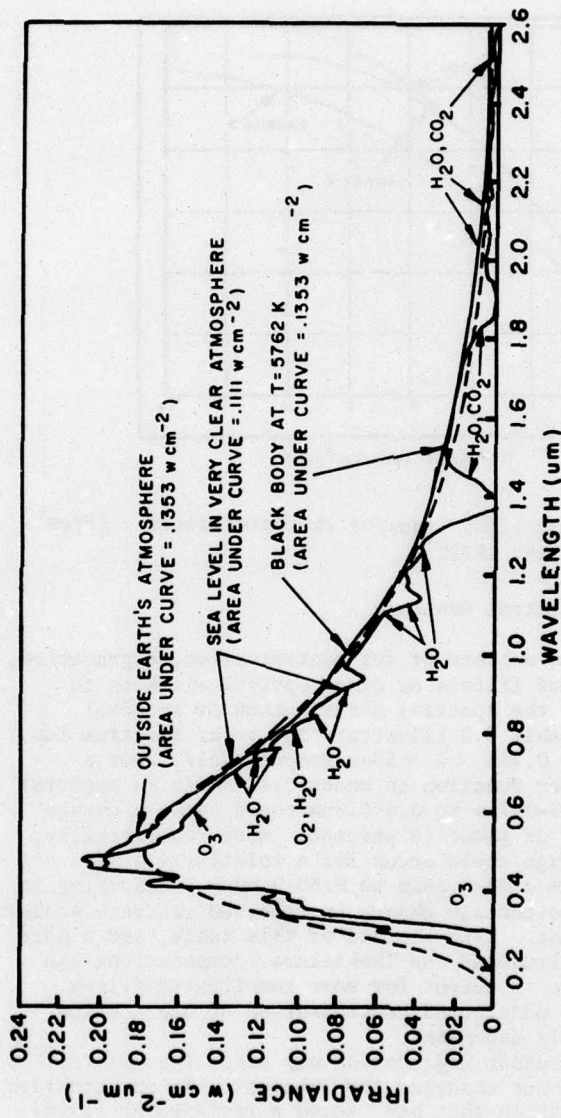


FIGURE 4.2:

Solar spectral irradiance normally incident at sea level on very clear, dry (0.5 cm of precipitable water vapor) days, solar spectral irradiance outside the Earth's atmosphere at 1 AU and black body spectral irradiance curve at $T = 5762\text{K}$ (normalized to 1 AU). (From Drummond and Thekaekara, 1973.)

BEST AVAILABLE COPY

FOR METEOROLOGICAL SATELLITES

47

λ - WAVELENGTH IN μm
 E_λ - SOLAR SPECTRAL IRRADIANCE AVERAGED OVER SMALL BANDWIDTH CENTERED AT λ
 IN $\text{W m}^{-2} \mu\text{m}^{-1}$
 D_λ - PERCENTAGE OF THE SOLAR CONSTANT ASSOCIATED WITH WAVELENGTHS SHORTER THAN
 SOLAR CONSTANT - 1353W m^{-2}

λ	E_λ	D_λ	λ	E_λ	D_λ	λ	E_λ	D_λ
0.115	0.07	1×10^{-4}	0.43	1639	12.47	0.80	891	83.37
0.14	0.3	5×10^{-4}	0.44	1810	13.73	1.00	740	69.49
0.16	2.3	6×10^{-4}	0.45	2006	15.14	1.2	485	70.40
0.18	1.25	1.6×10^{-3}	0.46	2066	16.65	1.4	337	84.33
0.20	10.7	8.1×10^{-3}	0.47	2033	18.17	1.6	245	88.61
0.22	57.5	0.05	0.48	2074	19.68	1.8	159	91.59
0.23	66.7	0.10	0.49	1950	21.15	2.0	103	93.49
0.24	63.0	0.14	0.50	1942	22.60	2.2	79	94.83
0.25	70.9	0.19	0.51	1882	24.01	2.4	62	95.46
0.26	130	0.27	0.52	1833	25.38	2.6	48	96.67
0.27	232	0.41	0.53	1842	26.74	2.8	39	97.31
0.28	222	0.56	0.54	1783	28.08	3.0	31	97.83
0.29	482	0.81	0.55	1725	29.30	3.2	22.6	98.22
0.30	514	1.21	0.56	1695	30.65	3.4	16.6	98.50
0.31	689	1.66	0.57	1712	31.97	3.6	12.5	99.72
0.32	830	2.22	0.58	1715	33.10	3.8	11.1	99.91
0.33	1059	2.93	0.59	1700	34.44	4.0	9.5	99.06
0.34	1074	3.72	0.60	1666	35.60	4.5	5.9	99.34
0.35	1093	4.52	0.62	1602	38.10	5.0	3.8	99.51
0.36	1088	5.32	0.64	1544	40.42	6.0	1.8	99.72
0.37	1181	6.15	0.66	1486	42.66	7.0	1.0	99.82
0.38	1120	7.00	0.68	1427	44.81	8.0	.59	99.88
0.39	1088	7.82	0.70	1369	46.99	10.0	.24	99.94
0.40	1429	8.73	0.72	1314	49.06	15.0	4.0×10^{-2}	99.98
0.41	1751	9.62	0.75	1235	51.69	20.0	1.5×10^{-2}	99.99
0.42	1747	11.22	0.80	1109	56.02	50.0	3.9×10^{-4}	100.00

TABLE 4.2: Zero air mass solar spectral irradiance, standard curve, abridged version. Reproduced with the permission of the Institute of Environmental Sciences from The Extraterrestrial Solar Spectrum (1973) by A. J. Drummond and M. P. Thekaekara.

function to assume a stepped shape, where the affected part has a transmission of 0.9 of the original value and extends over $0.50 \mu\text{m} < \lambda < 0.55 \mu\text{m}$; the unaltered part covers the interval $0.55 \mu\text{m} < \lambda < 0.60 \mu\text{m}$. From Table 4.2 we compute a change in signal of about 5 percent relative to the original

one. Changes of such magnitude have occurred in the output of visible sensors, such as the visible channel of the Scanning Radiometer carried on NOAA satellites.

2. Problems Encountered in the Analysis of Nimbus 6 ERB Data

The Nimbus 6 ERB instrument consists of three separate modules. One of these has a number of channels which measures the solar irradiance (totally and in a number of spectral subdivisions), while another module contains broadband channels which are wide-angle fixed telescopes that view the entire earth's disc visible from the satellite altitude. These radiometers measure the total earth irradiance (emitted plus reflected solar radiation) and the reflected solar radiation. The third module consists of narrow-angle scanning channels (broadband longwave and shortwave) that permit viewing of areas on the earth from a number of different directions. This enables one to obtain the radiation fluxes for synoptic scale areas.

When the data from the ERB were processed their validity was checked. As a result some disturbing facts were discovered. By comparing the wide-angle data over the open ocean areas with those obtained by the scanning channels for a period of one month, it was noticed that the scanning channel fluxes were roughly 11% higher than the wide-angle fluxes. (It should be pointed out that the longwave scanning channels are calibrated in space by means of an internal blackbody. Also, when the total wide-angle channel is shuttered, the radiation temperature is close in value to the monitored shutter temperature.) This observation is quite puzzling. As an additional check an attempt is being made to estimate the solar irradiance with the wide-angle channels during spacecraft sunrise or sunset during which time the detectors are illuminated by the sun. However, an obstacle to a proper comparison of solar and wide-angle channel data is uncertainty in the absolute value of the solar constant as a result of an intercomparison of ERB thermopile sensors with active cavity detectors carried on a rocket. When this problem is resolved, a comparison with the solar irradiance estimates can be made. If the discrepancy between the wide-angle and solar channels is similar to that observed between the wide-angle and scanning channels, then it would appear likely that the results from the wide-angle channels are in error. If there is little discrepancy, then the scanners are most likely in error.

Possibly, they are both in error by an amount greater than that originally expected.

3. Example of an "Every day" Problem - SMS-2

Potential Loss of Infrared Shutter Calibration

An example of a problem that directly affected calibration occurred recently with the VISSR of the SMS-2. The problem and the attempt to minimize its effects are stated in the following two paragraphs taken directly from the notice distributed by the Satellite Operations Control Center of NOAA.
"Subject: SMS-2 VISSR Frame Length

The SMS-2 VISSR has shown evidence of a lubricant buildup problem at the southern end of frame. Consultation with VISSR experts suggest that if no corrective action is taken, the problem will eventually cause the permanent, progressive foreshortening of the VISSR frame and the loss of IR shutter calibration.

In order to preserve IR calibration for as long a period as possible, the following action will be taken effective post eclipse 9/10/76. All normal SMS-2 pictures will be foreshortened by command to 1700 lines. Full length pictures will be taken only for the purposes of enabling calibration and rolling down lubricant buildup. An attempt will be made to provide a calibration picture at least every 48 hours."

CHAPTER V

CALIBRATION STANDARDS, DETECTORS, SCALES

A. STANDARDS

In this chapter the several primary standards are briefly described. The standards maintained by the National Bureau of Standards (NBS) emit in the near ultraviolet through the near infrared, while those of the National Research Council (NRC) of Canada emit in the thermal infrared. Drummond et al (1970) describe these standards in more detail and give further references.

1. NBS (USA) Radiometric References

The fundamental reference is a black body consisting of a cavity of oxidized nickel-chromium alloy maintained at temperatures between about 1273 and 1423°C. The good heat capacity of this furnace produces a very stable temperature, and the low reflectivity of the cavity combined with the small aperture relative to internal surface area yields a very high effective emissivity. Temperature is monitored by a thermocouple (platinum versus platinum and 10 percent rhodium) that is carefully calibrated. Measurements of temperature are checked via an optical pyrometer that agrees with the thermocouple to about 2 or 3°K.

Procedures are disseminated for the use of derived secondary standards of total irradiance at low intensity, e.g., carbon-filament lamps, and such lamps are distributed by the NBS.

The NBS has issued standards of spectral radiance and spectral irradiance applicable to the 0.25 to 2.5 μ m region. The secondary references for radiance are tungsten in quartz lamps, and for irradiance the tungsten source incorporates iodine as an agent to return tungsten deposited on the inner surface of the quartz envelop to the filament. Therefore blackening of the bulb is minimized and stronger emission results, especially in the ultraviolet.

The blackbody for shorter wavelengths is a cylindrical enclosure of high-purity graphite that is heated, to a tem-

perature approaching 2473°K, by induction inside a water cooled coil by a radio-frequency generator operating at 450 KHz. The degradation of the graphite at high temperature is reduced by enclosing the blackbody in an airtight chamber through which dry helium is passed. The concentration of oxygen is reduced further by heating copper coils in the chamber before each operation of the black body. The temperature of the blackbody is measured by a pyrometer. The effective area is much greater than the usual small tungsten enclosures often used in high temperature work. Therefore it is possible to expose the entire slit of the monochromator used to compare spectrally secondary lamps with the primary source.

The older carbon-filament lamps have been supplemented by a series of calibrated 100, 500, and 1000 W tungsten-filament lamps of the projector type. Working radiometers for comparison of primary and working standards consist of a group of cavity blackbody detectors and Eppley thermopiles of the laboratory type, specially constructed to have a uniform response for wavelength up to about 20 μ m.

2. National Research Council (Canada) Radiometric References

A standard of total radiance was derived by Bedford (1960) for the calibration of thermal infrared detectors. The source of a blackbody cavity consisting of a modified cone immersed in a stirred liquid bath controlled over the temperature range of 313 to 423 K. The cavity and the detector being tested are installed in a housing designed to provide a constant temperature surround for the detector, to define the aperture of the system, and to contain a shutter. The calibration procedure essentially entails measuring the output of the detector as exposed alternately to the cavity at the selected temperature and to the shutter at the temperature of the surround.

3. National Physical Laboratory (U.K.) Radiometric Reference

The sensor is a thermopile with a cavity black body receiver, and for which the reflectance is controlled. The thermopile detector is of the compensated type with two receivers side by side, each a spun copper tube with a 3mm bore and 9mm depth. A diaphragm of 2mm diameter over the front end allows radiation to reach the opposite end without hitting the walls. Diffusely reflecting black paint covers

the inside, and the solid angle of the opening is about 0.1 radian, thereby permitting the escape of only $0.1/\pi \sim 1/30$ of reflected radiation. Since the reflectance of the black coating is about 0.05 the effective absorptivity is about 0.998. Since there is a need for uniform sensitivity the walls are thick, and wire thermocouples connected in a series are attached in a manner that gives the best indication of the average rise of temperature. The instrument has a low sensitivity and, therefore, is only good for measurements of high radiative flux density.

B. DETECTORS

In this section primary detectors are briefly discussed, and the standard detector maintained by the National Physical Laboratory (NPL) of the U.K. is described. More detailed information is provided by Drummond et al (1970) along with further references. A newer type of primary detector, the cavity radiometer, is briefly described (see Kendall, 1973; and Kendall and Berdahl, 1970). The devices described herein measure solar radiation, i.e., nearly all radiation at wavelengths less than $3\mu\text{m}$, and are spectrally non-selective.

1. Angstrom Electrical Compensation Pyrheliometer

This instrument is usually designated as the Angstrom Scale of Pyrheliometry. In operation, heat is absorbed by a thin, blackened manganin strip exposed to the sun's rays. The strip is located at the bottom of a tube to restrict stray light. The received radiation is determined by measuring the electrical energy necessary to warm a similar, but shielded, strip to the same temperature. The rate of generation of heat in the electrical circuit is equal to the rate of absorption of heat by the exposed strip. The equality of temperature of both strips is verified by thermocouples attached to the strips and connected in opposition through a sensitive null detector.

2. Abbot Silver-disk Pyrheliometer

This instrument is usually designated as the Smithsonian Scale of Pyrheliometry. It consists of a blackened relatively massive disk of silver at the lower end of a diaphragmed tube which has an aperture angle of about 6° . A bent mercury thermometer graduated in 0.1°K and read to the

nearest 0.01°K is immersed, from the side of the tube, into a mercury filled hole in the silver disk. A thin steel jacket isolates the mercury and silver, but permits rapid heat transfer. The unit is thermally insulated. In operation, a triple shutter is opened and closed every two minutes, systematically exposing and isolating the disk from the solar beam. It is important to explicitly follow the procedure described by Abbot and his co-workers in order to obtain accurate readings.

3. Cavity Radiometers

Within the past decade a new type of radiometric standard has been developed, the cavity radiometer. This type of instrument is spectrally non-selective, contains a cavity receptor (black body cavity), and operates by electrical equivalence. One of the more accurate versions of this class of detectors is the Primary Absolute Cavity Radiometer (PACRAD). The PACRAD is illustrated and described more fully in Kendall and Berdahl (1970). In addition to the aforementioned features the PACRAD has a view-limiting aperture, tube and "muffler" that prevents nearly all stray radiation from entering the cavity aperture and wind currents from disturbing the functioning of the radiometer. Other parts include a massive thermal guard (heat sink) and thermal resistors. Cavities and thermal resistors are made from pure silver about 0.13 mm thick.

In operation the viewing aperture is alternately capped and opened for electrical calibration of the system and measurement of radiation respectively. The time constant of the system, 7 sec, is such that an accurate measurement, to within 0.05 percent of the final value, requires about one minute. The absolute accuracy of the PACRAD is about ± 0.3 percent. This accuracy depends on the accurate measurement of electrical power (which is equivalent to radiative heating of the cavity), the output of the thermopile, and the aperture area. Frohlich and Brusa (1975) estimate the emissivities of several cavities, an important factor for the correction of systematic error. Kendall (1975) provides additional information on the PACRAD and Willson (1975) describes the number of cavity radiometers aside from the PACRAD.

The PACRAD and similar instruments are the basis for a new international standard being proposed to replace the one

currently in use. The new scale should have a greater accuracy and precision.

C. INTERNATIONAL RADIOMETRIC SCALES

The current International Pyrheliometric Scale (IPS) and the newly proposed Solar Constant Reference Scale (SCRS) are briefly discussed herein; more detailed descriptions are found in the appropriate references. In addition, a brief comparison is made of the two scales and various reference standards. A possible cause is suggested for the apparent difference in determinations of the solar constant using the two scales.

1. International Pyrheliometric Scale

The IPS involves a comparison between the two scales defined by the Smithsonian and Angstrom pyrheliometers. The general value of the ratio of the readings from the two instruments with the sun as the source is 1.035 (Smithsonian: Angstrom). A ratio of 1.028 is indicated when an artificial source is used. It is considered that measurements on the uncorrected Angstrom scale increased by 1.5 percent almost certainly will be within ± 1 percent (maybe within ± 0.5 percent) of the best approximation of the true absolute scale of radiation. The IPS is described and discussed by Drummond et al (1970) and Drummond and Thekaekara (1973).

2. Solar Constant Reference Scale

The SCRS is based on an absolute electrical unit, the Watt, and utilizes measurements by cavity radiometers such as the PACRAD discussed above. The absolute accuracy of this scale is about ± 0.3 percent, the maximum deviation from a true SI Watt (White, 1976).

3. Intercomparison of Scales

The new value of the solar constant proposed by White (1975) and based on the SCRS is approximately $1377 \pm 20 \text{ Wm}^{-2}$ compared with about 1358 Wm^{-2} based on the IPS from a critical compilation of measurements by many investigators. This difference of about 1.4 percent is comparable to the present 1.6 percent difference between the radiometric and pyrometric determination of the lumen per Watt in photometry.

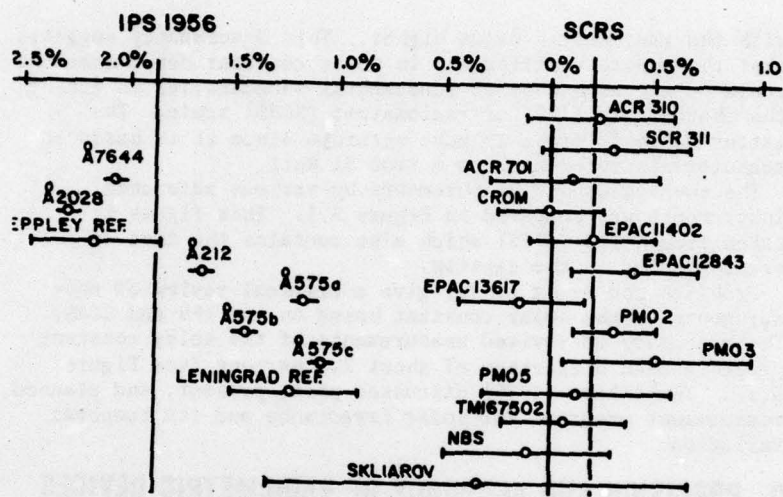


FIGURE 5.1: Relation of different realizations of radiometric scales to PACRAD 3:

- The Angstrom pyrheliometers are referenced by their serial numbers. Å 7644 and Å 2028 are the base for the Eppley Laboratory reference (according to results of IPC III 1970). Å 212, the USSR standard and Å 575, the Leningrad University instrument are the base for the Leningrad reference [according to results of comparisons at Davos (Å 212, Å 575c), at Byurakan (Å 575a) and Terskol (Å 575b)].
- The absolute radiometers are referenced by appropriate abbreviations and serial numbers. The results are from IPC IV (1975) except for the NBS instrument, which participated together with PACRAD 3 in IPC III (1970).
- The International Pyrheliometer Scale (IPS 1956) is shown as it is realized during IPC IV (1975). The Solar Constant Reference Scale (SCRS) is the best available representation of the SI scale of total irradiance, the absolute accuracy is estimated to be $\pm 0.3\%$.
- Details on the instruments can be found in: ACR: Willson (1971), CROM: Crommelynck (1973), NBS: Geist (1972), PACRAD: Kendall and Berdahl (1970), PMO: Brusa and Frohlich (1975), SKLIAROV: Skliarov (1964), EPAC and TMI are commercial versions of PACRAD, made by Eppley Laboratory and Technical Measurement Inc., respectively. (From White, 1976.)

with the radiometric value higher. This discrepancy suggests that the apparent difference in solar constant determinations could be a consequence of fundamental inaccuracies in either the photometric (IPS) or radiometric (SCRS) scale. The latter scale is probably more accurate since it is based on measurements referenced to a true SI Watt,

The two scales and measurements by various reference instruments are compared in Figure 5.1. This figure is taken from White (1975) which also contains the list of references noted in the caption.

Frohlich and Brusa (1975) give a critical review of measurements of the solar constant based on the IPS and SCRS. Their summary of revised measurements of the solar constant yields a mean difference of about 2.0 percent (see Figure 5.1). Thekaekara (1975) discusses past, present, and planned measurement programs for solar irradiance and its temporal variation.

D. PRECISION AND ACCURACY OF RADIOMETRIC DEVICES

Accuracy may be defined as "the absolute uncertainty in a measurement" or the "degree of conformity to the true value" (Drummond et al, 1970).

Precision is "connected with the response of a measuring instrument or system to changes in the parameter under investigation". It has components of reproduction, resolution, and repeatability (Drummond et al, 1970).

The primary physical laboratories reproduce their own radiometric reference to within 1 or 2 parts per thousand, and there is a similar repeatability with working standards on a routine basis. However, the fixation of the true absolute reference of radiometry is not so good, at best probably about ± 0.5 percent (as of the date of the writing of Drummond et al, 1970). When these scales are applied on a transfer basis for greater generality a realistic reliability is about 1 percent in derived secondary references. The same holds for the IPS; over a 10 year period the IPS was evaluated at Newport with a constancy relative to the Davos (Switzerland) primary standards of ± 0.2 percent, but such an absolute accuracy is not implied.

In the comparison of NBS and IPS radiometric references, care is taken to avoid significant errors arising from the temperature dependence of the instruments and non-linearity of response over the range of radiative flux encountered.

FOR METEOROLOGICAL SATELLITES

57

The agreement between the two references is less than ± 1 percent despite the several transfer operations involved.

The newer cavity radiometers have an absolute accuracy of about ± 0.3 percent relative to the SI Watt (White, 1976). A series of 35 measurements presented by Kendall (1973) suggests a precision for the PACRAD of about ± 0.1 percent. Thus it appears that the precision and accuracy of these newer instruments represent an improvement over the older Angstrom and Smithsonian types.

CHAPTER VI

CALIBRATION PROCESSES

A. GENERAL

In general, a radiometer is exposed to a source at one or more predetermined positions under normal atmospheric conditions or in a vacuum. Sources for thermal infrared radiation range from simple blackened surfaces to complex cavities, where their temperatures are more or less accurately measured. These sources in turn are usually calibrated against primary or secondary standards of one of the national laboratories (e.g., NBS, NPL, etc). Calibration of sources takes place via various transfer agents such as a thermopile. For visible and near infrared radiation the source may be the sun or a calibrated lamp, viewed through an integrating sphere, a diffuse plate, or some other arrangement to assure uniform illumination of the detector to as great a degree as possible. These sources are generally calibrated against primary or secondary standards through transfer agents. For microwaves the source is either a black body similar to that used for thermal infrared calibration of a "noise generator" that simulates a black body at a given brightness temperature.

The general goals of pre-launch calibration include the determination of linearity of response, sensitivity of the system, stability of the system, output in voltage or digital counts per quantity of radiation, and a checkout of the electronics. The accuracy of in-flight calibration depends in part on the quality, stability and accuracy of internal calibration sources, which normally should be calibrated prior to launch by reference to appropriate standards.

Drummond et al (1970) illustrate radiometric calibration procedures with particular reference to a joint JPL-Eppley project involving the use of multi-channel (solar) radiometers on-board aircraft. The overall procedure involving comparisons with primary standards via working standards, is shown in Figure 6.1. A similar procedure would be followed in a good calibration of a visible or near infrared radiometer prior to launch in a satellite.

In-orbit calibration of satellite sensors is as important, if not more so, as pre-flight calibration, even though some major satellite systems contain no on-board calibration. An in-orbit check of performance is necessary for maintaining

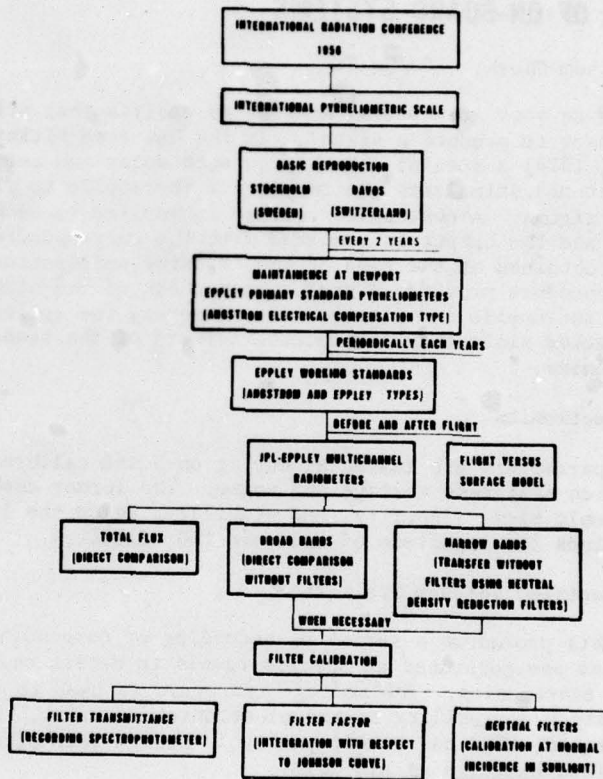


FIGURE 6.1: Radiometric calibration procedures (after Drummond et al, 1970).

both accuracy and repeatability of measurements, and to correct for whatever degradation or change in a system that may occur after launch. In this section we consider a number of methods and sources utilized for calibration in space including those conducted internal to the satellite and those using various natural targets.

B. USE OF ON-BOARD SYSTEMS

1. System Checks - Go/No Go

These devices are special heating assemblies that stimulate the sensor to produce a signal. In the ERB (see Hickey and Karoli, 1974) a special assembly in each solar and earth flux channel stimulates the respective thermopile to produce a test signal. A controlled voltage is applied to each heater and the output is compared with the corresponding values obtained at the time of the transfer calibrations. This procedure provides a good, quick check of the stability of the thermopile and electronics. However, the optics are not checked since they are located forward of the sensor and electronics.

2. Electronics

Two parameters are looked at during on-board calibration, precision staircase voltage and noise. The former checks electronic bias, linearity, and stability, while the latter determines the magnitude of noise in the circuitry.

a. Precision Voltage Staircase

In this procedure a series of ascending or descending step voltages are generated at precise levels to detect changes in the electronics. The voltage staircase is used to verify linearity and stability of the electronic circuitry. For example, the VTPR has 7 voltage levels plus a zero offset level (see McMillin et al, 1973).

b. Noise Check

The noise of the system may be determined for high and low radiances by noting the fluctuations during a view of the uniform FOV's provided by the housing and space "looks". Longer period variations such as the 200 Hz waveform, caused by pickup from the spacecraft clock, noted by E. J. Williamson (1970) for the HRIR may be detected by comparison of successive looks or by noting periodic changes in signal during a single view, if sufficiently long. The noise in the output signal is a measure of the precision of the system.

3. Sensor

a. View of Space

Deep space is the only source that is relatively uniform, fills the FOV, and has an accurately known radiance (i.e., close to 0). It is presumed unchanging during a mission, and is always "on". A space "look" is generally considered vital for absolute radiometric calibration of most detectors, though its use is more as a noise estimator rather than as a calibrator. The radiant contribution of stars, moons, planets, comets, galaxies, interspace dust, meteorites, and other technological satellites is presumed to be negligible in space looks, as discussion or consideration of such appears non-existent. This presumption is probably most always valid, as the radiant contribution from these phenomenon probably remains well outside the dynamic range of most sensors. It should not be taken for granted, however, that such sources cannot contribute to some anomalies in the data, especially in the instances of narrow angle or high power telescope optics.

The sensor commonly views space by means of a scanning mirror or antenna, or the spin of the whole satellite. Usually a view of space is part of the scan sequence for each scan line with scanning radiometers (e.g., VHRR and VISSR). Sounders may be calibrated in an automatic mode (e.g., optional for VTPR; every 7 min.) or on command (e.g., second mode for VTPR; once per orbit).

An important consideration is whether the calibration procedure involves a static or dynamic, i.e., scanning, look. If the instrument is scanning, errors from microphonics can occur. A comparison of space views while scanning with others in a static, i.e., stopped, position provides an assessment of the effect of microphonics.

b. View of Internal Targets

(1) Comparison to Normally Shuttered Standard Channels

In this procedure it is assumed that the shuttered channel remains uncontaminated and does not degrade over the normal lifetime of the system. Furthermore, the two channels should be as identical as possible at the beginning of operations. The working channel is checked for degradation or contamination by comparison with occasional "looks" by the shuttered

channel. The scene should be the same for both channels whether it consists of a view of an internal source, an external source such as the sun, or a uniform area on the earth's surface. The procedure is very useful when a channel is likely to degrade on exposure to the space environment. In some systems the shuttered channel may become the working one if the initial channel fails.

(2) Diffuse Plates

These plates are used with sunlight or a solar simulator and consist of specially made plates that either transmit or reflect solar radiation diffusely. Radiation is diffused over the FOV of the detector and the intensity is reduced so as to avoid overloading the sensor.

Degradation of plates in space is a serious problem, since the calibration source, i.e., the sun plus the plate, would degrade. Absolute calibration would be ruined, but channel-to-channel comparisons still could be made. On the ERB the plate is covered except when in use, when a door is opened to allow sunlight to fall on it.

(3) Standard Lamps

For a short term mission a lamp is probably the best practical source for visible and near infrared sensors, provided that proper attention is taken to uniformly fill the FOV, regulate the current, maintain optical alignment, and properly age the source beforehand. The lamps are specially constructed with, perhaps, a quartz envelope and a tungsten or carbon filament. Generally arc lamps or plasma tubes require too much power for satellite applications, and the peripheral equipment may be too heavy. When lamps are used an attempt is usually made to match the magnitude and spectral distribution of solar radiation over a fairly broad spectral range (e.g., 0.4 to 2.5 μ m as on the S191). However, even with special filters, one lamp cannot suffice over the visible and near infrared, nor is the match precise in any case. In addition, over a long term mission, a standard lamp may change in unknown ways and therefore one needs to calibrate the lamp with some regularity.

(4) Thermal Infrared Black Bodies

These are simpler and more accurate than lamps on an absolute scale. The most common black bodies for internal calibration are blackened flat plates which are grooved or honeycombed. The shutter, chopper, or part of the filter wheel may serve as a black body (see Karoli et al, 1975; Lansing and Cline, 1975). The black body may be heated or cooled (Nichols et al, 1975), but usually it is maintained at the ambient temperature of the system. Black bodies for individual systems are described and illustrated in the various User's Guides (e.g., Sissala, 1975) and some descriptive articles. Especially complicated black bodies such as cones or cylinders (e.g., 2π black body described by Karoli et al) are not often used on satellites because of space and/or weight restrictions.

Major factors to consider when using black body sources are as follows: (a) insure that the measured temperature represents the actual radiance temperature of the black body; (b) insure that the temperature distribution across the surface and (if a cavity or honeycomb) into the source is uniform; (c) obtain an accurate measurement of the spectral emissivity of the black body, not merely that of the paint or flat surface, for the wavelength of the sensor; (d) eliminate or account for all thermal background radiation reflected off the source and into the FOV of the sensor; and (e) make sure emissivity of the source remains constant over a long mission, or at least monitor the change.

It is worth noting that black bodies are used for other wavelengths, particularly the microwave. Grooved plates are used by the SCAMS described in Sissala (1975) for wavelengths from about 0.5 to 1.3 cm.

4. Intercomparison Between Instruments

A good check of calibration accuracy is the comparison of measurements of the same surface in the same spectral region by similar independent instruments. If two satellite systems sensitive to radiation in, say, the 0.4 to $0.8\mu\text{m}$ interval had a claimed accuracy of ± 1 percent, but their output for the same target, e.g., the White Sands, differed by 10 percent, then one could infer that one or more significant discrepancies existed in one or both systems. Of course there would be a small but finite chance that an error, or a combination of various errors, in both instruments could

cause both to give incorrect readings within ± 1 percent of each other.

Intercomparison is the most commonly used method of in-flight calibration for ultraviolet sensors, perhaps the only one (D. Bede, private communication, 1976). Two instruments of the same type and model are compared, where one has been recently calibrated. The new system may be on a newly launched satellite (or a rocket, which is frequently used). Some problems are present in this method. A significant mismatch of spectral distribution within the same interval could be a cause of widely different readings; such a mismatch could be expected for different instrument types, but not for successive units of the same type. Care must be taken to insure the same viewing geometry for both instruments. For example, variation in solar zenith and azimuth angles should result in real differences in received radiation in different regions of the spectrum. Furthermore, instruments with the same relative spectral response may have a different absolute response.

C. USE OF NATURAL TARGETS

Natural surfaces can be useful calibration targets for satellite instruments after launch. A brief discussion on calibration via natural targets by K. Coulson (private communication, 1976) utilizing an existing facility is followed by discussion of specific surfaces, both terrestrial and extraterrestrial.

"In some cases there is a need to detect instrument changes following pre-launch calibration. One serious problem is the drift of instrument response with time in orbit, and another is the possibility that instrument characteristics might be modified during the launch itself. Unless these changes are detected and appropriate corrections applied, the data can become unreliable and misleading.

One way to check the instrument calibration while it is in orbit is to use an area of the earth's surface as a calibration standard. Such a 'standard surface' might be a large uniform area of desert or the white gypsum sand of the White Sands National Monument in New Mexico. In any case, the standard surface can be viewed repeatedly by the radiometer as the satellite passes over, thereby yielding many measurements for the calibration check. By knowing the reflectance properties of the surface and characteristics of the intervening atmosphere, it is possible in principle to compute

the intensity of radiation directed to space over the standard surface. In practice, it is necessary to establish a ground station at the site in order to determine atmospheric properties in sufficient detail to compute the effects of the atmosphere on the outgoing radiation.

Although this method is most applicable to calibration checks of instruments for measuring solar radiation, there is no basic reason why it could not be used for longwave instruments as well. In this case, however, it would be necessary to determine profiles of temperature, water vapor, and perhaps ozone over the area in order to compute the field of terrestrial radiation directed outward from the top of the atmosphere." (Coulson, 1976)

1. Earth Surface Targets

a. Dark Objects

Viewing dark surfaces may have a use such as the determination of atmospheric effects by acting as a crude indicator of solar backscatter. A good example is the lava area to the north of White Sands which is very dark in the visible.

b. Manmade Objects

Useful objects would be costly to build and maintain, and therefore probably are not useful except as targets of opportunity when accompanied by ground truth measurements. Examples include large airfields or artificial lakes and reservoirs.

c. Water Bodies

Water surfaces are excellent sources for thermal infrared calibration. The surface is often reasonably uniform away from the boundaries, and the emissivity is high, as high as 0.99 for a nadir view near $11\mu\text{m}$ (Buettner and Kern, 1965) and for a broad thermal band under special conditions (e.g., Kano and Suzuki, 1976). A water surface is about the most uniform natural surface on the earth for thermal infrared. However, the process requires the measurement of surface radiation temperature "in situ" for ground truth.

Reflectivity and geometry are important for visible and infrared radiation. An example of such a phenomenon is sun-glint. In a study by Whitehead (1971), reflection apparently

caused the brightness temperature (measured from an aircraft) to be 3°K higher when viewing the water surface in the direction of the sun than when looking away from the sun. A direct look into sunglint at 80° from nadir by a shipboard radiometer gave an apparent increase in temperature of up to 34°K.

A program for obtaining ground truth measurements for the EREP of Skylab is discussed in a report by NASA (1973). Measurements were made of the radiance temperature of the surface and the temperature and humidity of the overlying atmosphere for several lakes with different surface temperatures.

d. Reflection Discontinuities

These discontinuities may be useful for obtaining time constants of instrument response. However there are few natural targets of sufficient size and contrast or sharpness. Some possible choices include cloud shadow, if sufficiently well defined, lake or sea surfaces adjacent to barren land, or bright clouds over the sea or lava beds. In this latter case there may be a problem with reflection from the clouds (Hulstrom, 1973).

e. Bright Surfaces

Few natural surfaces are uniformly bright enough to act as calibration targets in the visible and near infrared. Two possible sites are the White Sands of South Central New Mexico (white gypsum sand) and the Solar de Uyuni in Bolivia (salt flat). The solar constant, direct reflectivity of the surface, and optical thickness of the overlying atmosphere are needed to determine intensity of radiation reaching a satellite from such a natural target. Direct reflectivity and optical thickness may be measured directly as proposed by Coulson and Jacobowitz (1972), and performed by Jacobowitz and Gruber (1975) and Reynolds and Vonder Haar (1976). The intensity component for diffuse transmission or backscatter may be obtained by measuring global flux incident at the surface and applying realistic radiative transfer theory to the turbid atmosphere over the site. Appendix A presents a fuller treatment of this procedure.

For the EREP of Skylab two desert areas were used, Wilcox Playa and the Great Salt Lake Desert (see NASA, 1973). The measured quantities were direct solar radiance, optical

depth, diffuse solar radiance, total target radiance, target directional (i.e., normal) reflectance, target hemispherical reflectance, and near-surface meteorology. A spectroradiometer was used to measure the radiances and reflectances. This instrument was calibrated using a ribbon filament tungsten lamp. The absolute accuracy of the instrument was about $\pm 4\%$ ($0.4 - 0.75 \mu\text{m}$) and about $\pm 7\%$ ($0.75 - 1.3 \mu\text{m}$) over the spectral interval of interest. The repeatability was about 1 to 3% depending on wavelength; the recorded data were only read to the nearest 0.5%.

f. Uniform Surfaces of Known Characteristics and Constancy

Calibration by reference to known surfaces can be useful if the surfaces are relatively uniform over the FOV, and if atmospheric conditions are favorable. "In situ" measurements are also necessary. It would be desirable to have light and dark surfaces close together, such as White Sands and the nearby lava beds, to properly account for the atmosphere. The assumptions of a uniform atmosphere over sites separated by, say, a few tens of kilometers is probably good away from active weather zones or major topographical boundaries (i.e., near the shore of a major water body).

A facility for the collection of ground-and-air-truth data for comparison with satellite measurements is currently in operation at White Sands Missile Range as part of the Atmospheric Sciences Laboratory of the US Army. A description of this site, its instrumentation, and some uses are presented in Appendix III.

2. Clouds and the Atmosphere

In general clouds are far too variable to serve as radiance or reflectance calibration targets. Their radiative properties in the infrared are particularly sensitive to their height and thickness and the precision with which these properties are known is generally indefinite. Cloud shape and size are important at most all wavelengths, and some properties change with sun elevation and azimuth, especially in the near infrared and visible. The contrast between cloud and cloud shadow, or cloud and an underlying dark surface, may be useful for determining such factors as response time of the instrument, provided that the cloud edge is sufficiently sharp.

The atmosphere is, in general, too variable for use in calibration. Variable quantities, all affecting emission or transmission in one or more spectral bands include humidity, temperature, pressure, and aerosols. In addition clouds may partially fill the FOV or be optically thin with an unknown emissivity. Scattering of visible and infrared radiation is also highly variable and is usually overwhelmed by (1) radiation reflected (visible and near infrared) or emitted (thermal infrared) from the surface of the earth, or (2) clouds. While these two items do not provide calibration targets, in the usual sense, it is recognized that they comprise the ultimate in calibration reference targets. Most meteorological satellite data is, in fact, radiance data from cloud tops and the atmosphere. In addition the atmosphere - at least some portions of it - are intensely measured and therefore the atmosphere can be interpreted as something of a secondary standard. To say the least, if satellite measurements cannot be meaningfully compared or related to conventional atmospheric measurements, then this new technology faces a dubious future. While at the present time the atmosphere can be said to be more of a problem than a solution in the calibration process, this present situation does not necessarily describe that of the future. One concept that implies that the atmosphere can become part of a systematic calibration process is suggested. The advent of the SPACELAB, wherein a manned space facility and a ground-to-space-to-ground interchange of equipment is practical, suggests a more absolute method of determining atmospheric effects. The capability of laboratory comparison of ground and space instruments before and after an experiment will greatly enhance the usefulness of such an experiment. One such experiment might be the transmission of one or more signals (e.g., a laser beam) whose attenuation characteristics are adequately understood, from the surface to the spacecraft (and possibly back to the surface). Absolute control can be exercised on the entire signal generation and transmission (at the ground) and reception (at the SPACELAB) processes. Simultaneous measurements of critical atmospheric parameters with balloons, rockets, etc. can be conducted. These data may then permit the atmospheric effect to be determined with high precision. This knowledge can then be applied to the data from any other satellite which observed through the same atmospheric column, to minimize the atmospheric contribution to that data. Thus a combined ground-atmosphere-space process becomes a calibration entity appli-

cable to other orbiting systems.

3. Extraterrestrial

a. The Moon

Instruments on satellites generally need no atmospheric correction for viewing the moon, except when viewing through the earth's limb. Certain lunar mares produce nearly uniform reflectances and thermal emittances just before and after a full moon (Soule, 1974). Except for the period just before and after full moon, data generally are not useful because of shadowing effects and non-linearities in target radiation characteristics. For times less than \pm one day from full moon, intensities are undefined by Soule (1974) because of eclipsing by the earth, and the change in intensity (very close to full moon) was too rapidly rising for meaningful interpolation. Use of lunar mares along with deep space offer widely different low and high temperature targets; the maximum brightness temperature of some mares is near 400°K. Also, spectral reflectivity of these areas was in excellent agreement with the reflectances of lunar soil samples. Because of the rapid change in radiance with time, adequate application of these data requires accurate measurements of thermal and luminance characteristics as a function of phase angle as well. Soule states that the uniformity of the surface is probably a result of the dust cover. The albedo of various surfaces changes from about 0.05 (darkest part of mare) to 0.18 (brightest part of crater Aristarchus) with an average value of about 0.09.

b. The Sun

The sun is a relatively constant source for all wavelengths from the ultraviolet to the far infrared and is always "on". Fröhlich (in White-1975) and Fröhlich and Brusa (1975) discuss the solar constant and evaluate its measurement by various investigators. It may be viewed through a diffuser or off a diffusing reflector; the signal can be precision attenuated in the pre-amplifier; the data may be collected in a low gain mode; or the aperture may be restricted (e.g., pinhole). The solar beam may be acquired via the normal optics, a special set of optics, or on the back (return) scan of a spin scan system, depending on the requirements of the calibration process. The sun look provides a check of the response of

the radiometer and the constancy of the internal source. The output from the sun view may be used to measure the degradation of the sensor. The radiation from the internal source may be checked by using the sun as a primary source and the radiometer as the transfer agent. Unfortunately, a diffusion plate, precision attenuator, or other means of reducing the solar signal may degrade the signal and appropriate consideration must be applied in the system design. Also, changes in energy flux due to earth/sun geometry must be addressed in any long term (months) "sun look" calibration process.

CHAPTER VII

CALIBRATION OF SPECIFIC INSTRUMENTS

In this section specific instruments, one from each of five classes of instruments identified in Chapter 3, A, and their calibration, are presented.

A. SCANNERS

1. Operational Linescan System (OLS)

Description: This system is the primary package flown on current DMSP satellites. The system contains four sensors, two with very high resolution in both the visible and infrared spectral regions (VHR and WHR respectively) and two with high resolution in nearly those same regions (HR and MI). Six scan lines of very high resolution data are acquired for each one of high resolution (see Figure 7.1). Spectral interval and FOV data are given below in Table 7.1.

SYSTEM	SPECTRAL INTERVAL	NOMINAL FOV
HR and VHR	0.4 - 1.1 μ m	0.8 km
MI	7.7 - 13.1 μ m	4.4 km
WHR	7.9 - 13.1 μ m	0.64 km

TABLE 7.1

Figures 7.2 and 7.3 show the relative spectral distribution of the HR and MI channels.

Calibration:

Pre-flight

Visible: Minimum information is available. The preparation involves a check-out of the inflight system using simulated solar radiation.

Infrared: Standard black body sources are probably used. The instrument is calibrated so that there is a linear response in equivalent black body temperature, specifically for the range 210-310°K.

In-flight

Visible: Data are normalized with respect to solar illumination by use of zero-resolution "super hemispheric" radiometer (see Dickenson et al, 1974 and Spangler, 1974) that is oriented 180° from the OLS nadir (i.e., looks upward from sub-satellite point). The sensor gain has a relative range of about 1 to 10. Gain is automatically altered when the satellite crosses the terminator to compensate for changing illumination along the scan lines.

Infrared: Calibration is performed by reference to black body sources on each end of every infrared scan. There are two sources, a cold "clamp" source and a warm source that is attached to the housing. The clamp is cooled by radiation to space through a conduction rod. This source cools

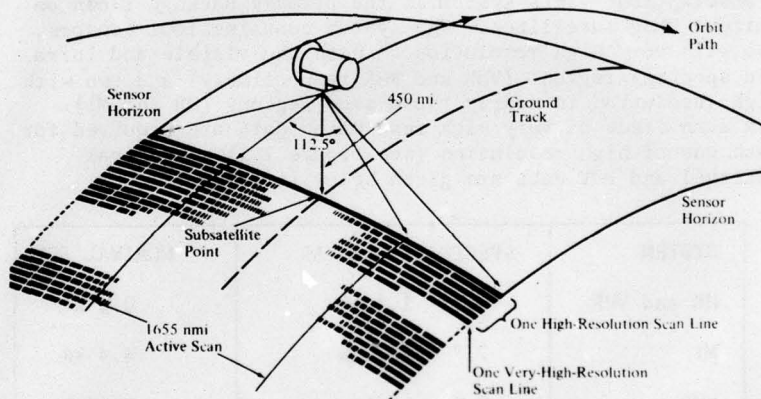


FIGURE 7.1
Space perspective of DMSP viewing geometry.
Rotating mirrors in the sensor provide the cross-track scan of approximately 1600 nautical miles. Along-track scanning is provided by the forward motion of the spacecraft. Since the scanning mirrors rotate at a constant angular velocity, geometric resolution on the ground decreases as the distance from the satellite sub-point increases in the cross-track direction. Also a picture produced from video signals would appear foreshortened at the edges unless rectified by the ground equipment. (From Spangler, 1974.)
Courtesy of Westinghouse Electric Corporation.

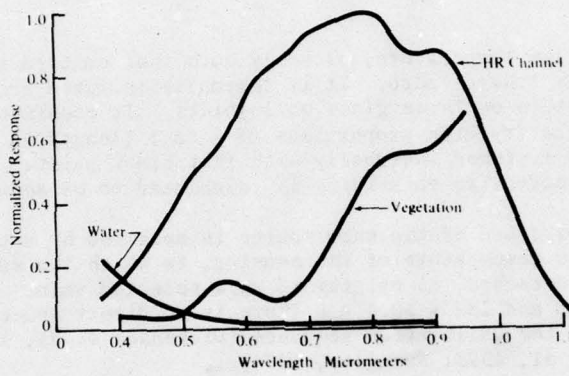


FIGURE 7.2

The spectral bandwidth of the visual channel is 0.4 to 1.1 micrometers, a range that optimizes the distinction between clouds, ground, and water.

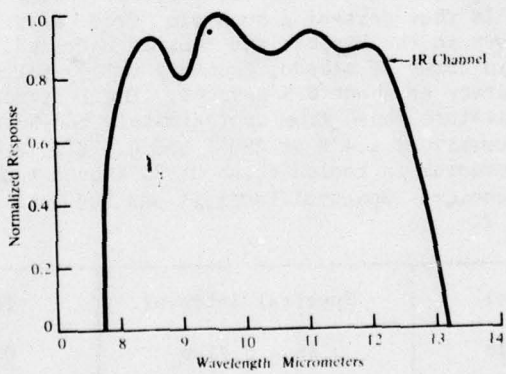


FIGURE 7.3

The spectral bandwidth of the infrared channel is 8 to 13 micrometers. (From Spangler, 1974.) Courtesy of Westinghouse Electric Corporation.

to a very low temperature, probably such that emitted radiation tends towards zero. It is thermally isolated from the main structure on three glass ball joints. It consists of a conical cavity with proportions of 4 to 1 (length to diameter), finished internally with flat black paint. The resultant effective emissivity is calculated to be about 0.99.

The temperature of the warm source is measured by a thermistor. The temperature of the housing, to which the warm source is attached, is maintained at a selected value between 278 and $283^{\circ}\text{K} \pm 0.1^{\circ}\text{K}$. There is no direct space look as part of the calibration sequence (Dickenson et al, 1974; Nichols et al, 1975; Spangler, 1974).

2. Visible Infrared Spin Scan Radiometer (VISSR)

The VISSR is carried on the SMS and GOES. The instrument scans perpendicular to the earth's axis using the rotational motion of the satellite, which spins at 100 rpm. A scanning mirror provides the pole to pole movement. From geosynchronous height, about 35,600 km, the earth scene at the equator fills that part of a scan $\pm 10^{\circ}$ from nadir. The radiometer senses in the visible and thermal infrared. Visible output is in terms of albedo, from 0.5 to 100 percent, implying an accuracy of about 0.5 percent. The infrared channel has a temperature range from approximately 180°K to 315°K with an accuracy of 1.4°K at 200°K and 0.4°K at 300°K . The infrared detector is cooled to about 95°K by a two-stage radiative cooler. Spectral interval and FOV data are shown in Table 7.2.

Channel	Spectral Interval	FOV
Visible	$0.55 - 0.75\mu\text{m}$	0.9 km
Infrared	$10.5 - 12.6\mu\text{m}$	7.2 km

TABLE 7.2

Calibration:

Pre-flight

No "hard" calibration data were obtained other than on spectral response and drift. Absolute calibration was performed on the prototype model which was not launched. The

absolute spectral response of the flight model for SMS-1 was compared with that of the prototype. Differences in the responses have not been explained.

The visible channel staircase voltage approximated a square root function, expressed as $C = 28.1 \sqrt{V}$ where C = digital counts and V = volts. This equation converts volts to digital counts. Volts computed from the above equation were used to compute albedo, A , in percent, by the following equation: $A = 0.2 V \times 100$. This linear equation permits calibration using two points.

The thermal channel staircase is used directly to evaluate linearity. If deviations are noted in a thermal detector more than two points will be needed for calibration. Sea surface temperature and the thermal channel solar image have been suggested as additional targets.

In-flight

There are several provisions for calibration as listed below. Visible: (1) Sun and space "looks", (2) Check on electronics gain and linearity. Infrared: (1) Sun and space "looks", (2) Check against calibrated black bodies, (3) Check on electronic gain and linearity.

Visible: The sun is viewed with a reduced size "side-looking" prism. An area the size of 10^{-5} of radiometer aperture provides a signal equivalent to 50 percent albedo. FOV of the calibration point leads the primary one by 15° to avoid a recovery problem in the earth scan. The prism has three facets that increase the effective north-south FOV at 0° and $\pm 32^\circ$ to assure a scan of the sun within the normal scan displacement. Thus inflight calibration of the visible channel is nominally assured for each frame of every day, except during solar eclipses. Electronic gain calibration makes use of a precision staircase voltage applied to the pre-amplifier input.

In reality the absolute response of the first flight model was unknown in the visible channel. The prism facets were improperly orientated on the SMS-1; and the sun did not fill the FOV of the sensor. Consequently, this sun calibration apparatus only gave relative changes. An attempt is being made to determine absolute response by comparing the data with known measurements by pyrheliometers during the GATE (E. Smith and T. Vonder Haar, private communication, 1976), and a complete description is being prepared by Smith and Vonder Haar. Lienech has described the variation of solar energy during the year. This annual variation amounts to ± 3.4 percent of the solar energy level that is used for

normalization of the visible channels.

Infrared: The sun signal is attenuated in the pre-amplifier to prevent saturation of the channel. An attenuation factor of 400 yields a signal of about 50 percent of maximum. Sun calibration is limited to about 25 days before and after the equinoxes. Electronic gain calibration is the same as with the visible channel.

The second infrared calibration is via a space view and by the shutter acting as a black body, which is activated by command. The shutter is in the FOV near the filter and detector assembly; thus it cannot be used to detect a gain change caused by the primary optics. The temperature is monitored. The sequence includes a look at the shutter entirely closed (solid) and partially closed (slotted). Consequently there are three calibration points, two shutter positions and a space view. The slotted shutter is used only when the instrument views space, providing an intermediate level.

In an attempt to insure accuracy in the infrared channel, comparisons were made with ground truth measurements, particularly of the sea surface temperature. Critical comparisons of the thermal infrared data with sea surface temperature showed that the VISSR underestimated the sea temperature by about 3°K even after accounting for atmospheric attenuation. At this time the scanner was subjected to large temperature gradients which decreased during the first year of operation. Later calibration using the shutter yielded data in somewhat closer agreement to surface measurements of sea temperature. Typical differences of about 3 to 5°K were observed, about equal to the corrections for atmospheric attenuation.

Lienesch has also provided additional information on the calibration of the thermal channel, including data quality and corrections for various errors following insertion of the VISSR into orbit. The VISSR calibration sequence is initiated by command except for the sun calibration. A typical sequence is as follows:

Scan line 1 - frame start ID of 10KHz
2 - electronics staircase calibration
3 - slotted shutter
4 - solid shutter
5 - zero line scan
6 to 1821 - normal frame

1st retrace scan - frame end ID of 5KHz

Note that line 5 probably includes the space view. (Smith and Vonder Haar, 1976; Pipkin, 1971.)

3. Scanning Radiometer (SR)

The Scanning Radiometer is carried on NOAA satellites, and is redundant in that there is nearly a complete back-up system (two radiometers, processors, and recorders). The system operates in both the visible and infrared, and yields radiance temperatures between 185°K and 330°K with a purported accuracy of about $\pm 4^{\circ}\text{K}$ near 185°K and $\pm 1^{\circ}\text{K}$ near 330°K . Radiation is reflected from a mirror and separated into the relevant components by a dichroic beam splitter. Changes have been made in certain aspects of the SR, as indicated in Table 7.3.

Channel	Spectral Interval	FOV
Old Visible	0.52 - 0.73 μm (NOAA-1,2,3)	3.7km
New Visible	0.4 - 1.2 μm (NOAA-4,5)	3.7km
Infrared	10.5 - 12.5 μm	7.4km

TABLE 7 3

Calibration:

Pre-flight

Infrared: The infrared calibration target is a heavy copper plate with deep V-grooves. The temperature of the target ranges from 180 to 320°K and is varied in steps of 20°K . The gradient of temperature is claimed to be only about 0.1°K . The target temperature is monitored by thermocouples, and a new reading is taken every half-hour (time is allowed for thermal stabilization). A complete set of target temperatures takes about 12 hours and one set is taken for each of a series of instrument temperatures. A typical instrument temperature and accuracy are about 288°K and $\pm 2^{\circ}\text{K}$. The entire procedure is performed in a thermal vacuum.

Views of the housing are made during the "back" scan. The housing is specially prepared to give reliable information, and temperature sensors are imbedded in it.

The curves that are fitted to the resultant data are very nearly linear. No effort is made to check the histories of the target and the instrument.

Visible: For the visible calibration the procedure is performed in the air, not in a vacuum. The target source is

similar to that used for earlier Nimbus satellites (see Jones et al, 1965) where the light source fills the entire mirror. The brightness of the surface is measured with a photometer concurrently with measurements of signal level in volts. Brightness levels are from about 21,000 to 118,000 lux (~2000 to 11000 ft. - lamberts), i.e., up to saturation. A curve is drawn from a series of these measurements. The photometers are calibrated and traceable to NBS standards. The voltage output decreased by 5 to 10% from initial ground calibration to the last calibration of the spacecraft model, a period of about two years. It is not clear whether this decrease was compensated for by internal correction or not.

The new SR's used a more rigorous determination of the radiation distribution of the source over the spectral interval of the visible channel. For the calibration source an equivalent albedo was determined (from the Handbook of Geophysics) for the spectral distribution of sunlight outside the atmosphere, and an equivalent albedo of 100 percent was computed for radiation from 0.4 to 1.2 μ m. The instrument is calibrated in terms of albedo. For this procedure the spectral distribution of the source and response of the radiometer are considered.

Both old and new calibration sources utilized tungsten illumination. For the old SR a "light box" was used where the lamps are inside the box and light is transmitted to the radiometer through diffuse opal glass (see Jones et al, 1965). The intensity was varied by moving the instrument from the source. Unfortunately the box "aged" or degraded due to darkening of the interior white paint which was allowed to deteriorate for several years. When the "box" was new the spectral distribution was independent of distance, but became somewhat dependent when the paint aged.

In-flight

Infrared: Digital counts are compared with radiance for views of the housing during the back scan and at space looks (near zero radiance). Specially prepared sections of the housing act as black bodies, and their temperatures are monitored. A linear relationship is assumed between radiance and digital counts. A more detailed description of calibration procedures for Direct Readout Infrared (DRIR) is given in the Appendix by Brower.

Visible: No calibration of the visible sensor is performed in space for either the old or new SR. (Horowitz and Davis, 1975; Jones et al, 1965; Harper, 1976.)

4. Electrically Scanning Microwave Radiometer (ESMR)

This instrument is carried on the Nimbus 6 satellite and consists of the following main components: (1) a phased array antenna with an aperture area of 83.3×85.5 cm and linear polarization parallel to the velocity vector of the satellite, (2) a beam steering computer which determines the coil current for each phase shifter for each beam position, (3) a microwave receiver with a center frequency of 19.35 GHz and an IF bandpass of 5 to 125 MHz, and (4) timing, control, and power circuits. The unit scans perpendicular to the sub-satellite track $\pm 50^\circ$ from left to right in 78 steps every 4 sec. The beam width is 1.4° near nadir degrading to 2.2° crosstrack x 1.4° downtrack at the scan extremes. Complete global coverage is obtained in 12 hours. The absolute accuracy is about 2° K in the temperature range of 50 to 330° K. Spectral and FOV information is in Table 7.4.

Wavelength	Frequency	FOV
≈ 1.55 cm	19.225 to 19.475 GHz (except for 10 MHz gap at center band)	Nadir 27km Scan Extreme 160 km x 45 km (crosstrack x downtrack)

TABLE 7.4

Calibration:

Pre-flight

Bench test equipment for the ESMR consisted of two main items: (1) a spacecraft telemetry simulation unit, and (2) a variable cold load source. The former unit provided signals for power, clock, digital A (primary data) timing, and command relay drive. It also accepted and displayed data of three types: digital A, digital B, and analog. The latter unit produced a variable temperature by two closed cycle cryogenic coolers with helium as the coolant. One cooler was used to simulate the temperature of space at the cold horn input to the radiometer, while the other provided a means to calibrate the radiometer input. Temperature varied from about 40 to 350° K.

Several models of the ESMR were subjected to engineering, thermal vacuum, and vibration tests. For the engineering test the protoflight model was placed in a vacuum chamber that was cooled by liquid nitrogen in a shroud and heated by an array of heat lamps. The radiometer was heated to 55.5°K $\pm 0.5^{\circ}\text{K}$, allowed to stabilize, and then cooled by turning off the lamps, simulating the eclipse of the satellite by the earth. Temperature was recorded using 41 thermocouples, and intensity and uniformity of lamp radiation was measured by 5 radiometers. Both power-on and power-off tests were performed. The results indicated that all components remained within acceptable limits. Necessary modifications and repairs were made as a result of the vibration tests and the thermal vacuum tests. Note that these three tests served mainly to insure delivery of a serviceable unit to NASA, and not to calibrate the instrument for launch (see NASA, 1973b).

In-flight

The sources for in-flight calibration were an ambient load (a black body at ambient temperature) and a space view via the "cold horn". These two reference points provide data for a linear interpolation scheme to determine brightness temperature from antenna temperature. In-flight calibration procedures are summarized as follows: (1) read eight scan lines of data (including calibration data); (2) using the multiplex data (e.g., switch temperatures), calculate the calibration temperatures of the cold load and ambient load, and the error due to variation in signal leakage between even and odd scans ($\sim 3^{\circ}\text{K}$); (3) average the four ambient and the four cold calibration temperatures; (4) convert all data for the 78 beam positions for all 8 scans to brightness temperatures at the radiometer input; (5) using the measured antenna thermodynamic temperature and tabulated antenna losses as a function of beam position, as corrected for phase shifter temperature, calculate the gain function for the averaged brightness temperature; and (6) using the modified matrix for sidelobe correction, correct each scan for the sidelobe contribution.

Wilheit (in Sabatini, 1972) provides a more detailed summary of in-flight corrections including a number of tables and figures. (Sabatini, 1972; NASA, 1973b.)

B. FIXED - SKYLAB S-194

The S-194 was flown on Skylab and is an L-band microwave

radiometer. This passive radiometer has a fixed antenna with a 15° (half-power) beam width, and a 36° (.9 power) beam width, centered at nadir. It responds to brightness temperatures in the nominal range from near 0° to 350°K, and is ascribed an accuracy of $\pm 1.0^{\circ}$ K. The beam is in the form of a solid triangle. Spectral and FOV data are given in Table 7.5.

Wavelength	Frequency	FOV
≈ 21.2 cm	1.4135 GHz	15° 110km
		36° 270km

TABLE 7.5

Calibration:**Pre-flight**

The system was checked out using calibration sources at various effective brightness temperatures. These sources are not specified, but probably consist of the output from a "noise" generator that produces loads equivalent to specified temperatures. The signal from the generator would replace that from the antenna, thus the electronics were included in the calibration, but not the antenna.

In any case a system processing algorithm was devised that was used to convert voltage output into brightness temperature. The algorithm includes terms for various losses, e.g., antenna terms, some of which are not entirely independent.

In-flight

The internal network is referenced to a fixed hot or cold load input. An absolute calibration is acquired by viewing space which has a normal background temperature of 2.8°K.

Lerner and Hollinger (1975) found that the measured antenna temperature and the space temperature differed greatly. The system processing algorithm was re-worked using the known cosmic background temperature and the temperature of the hot source used for pre-flight calibration. It was assumed that two independent loss terms were responsible for error, and those were adjusted. However, a second iteration was required. The two loss terms were adjusted again using the cosmic temperature and the antenna temperature for the Gulf of Mexico taken on pass 56. Because a system offset of 3.6°K was noted, a further refinement was made using the

cosmic temperature (2.8°K) and an adjusted value (95°K) for the Gulf of Mexico. These latter procedures appeared appropriate since the measurements for the Gulf of Mexico used in the calibration were taken under nearly ideal conditions of clear weather and calm seas. Furthermore, excellent ground truth data were available from ships and aircraft. New values gave close agreement between measured and calculated values. The newest values of the loss terms are not in the released data, and must be applied to each output value. Thus the overall in-flight calibration of the S-194 involved the use of fixed reference sources, a space view, and a view of a uniform natural target. (Lerner and Hollinger, 1975; NASA, 1972.)

C. RESTRICTED SCAN-EARTH RADIATION BUDGET (ERB)

The ERB instrument is a multichannel (22) radiometer flown on the Nimbus 6 satellite. It measures incoming solar radiation in 10 fixed channels and outgoing total radiation from the earth in 4 fixed channels. Eight scanning channels are used to measure the angular dependence of emitted and reflected earth radiation and have relatively narrow FOV's. Of these eight channels, four are sensitive to shortwave and four to longwave radiation.

The total spectral range of the 22 channels is from 0.2 to over $50\mu\text{m}$. Sissala (1975), and Figure 7.4 provide details on the various spectral intervals, some narrow channels (e.g., channel 10: $0.25\text{-}0.3\mu\text{m}$) and other very broad channels (e.g., channel 3: $0.2\text{-}50\mu\text{m}$). The scan patterns of the eight scanning channels is complex and variable on command. The FOV of the scanning channels (at nadir) is about $0.25 \times 5.25^{\circ}$ representing approximately a 5×100 km rectangle from the nominal orbit of 1100 km. The wide angle channels have an "unlimited" FOV (i.e., view the whole earth).

Calibration:

Pre-flight

Because absolute values of radiation are important for this application, calibration for this instrument was a more rigorous process than for most satellite radiometers. Reference for calibration is the new Cavity Radiometric Scale (CRS) referenced in turn to other viable radiometric standards (i.e., International Pyrheliometric Scale (IPS) 1956 and radiometric standards at the US Bureau of Standards).

Solar modules used natural and simulated solar light to establish operational levels and reference points. Primary

BEST AVAILABLE COPY

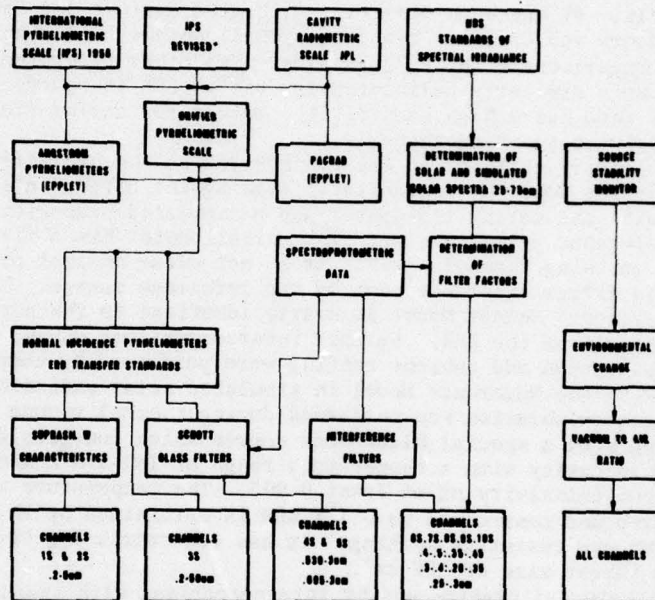


FIGURE 7.4

Calibration traceability diagram for ERB solar channels and their spectral intervals. (From Hickey et al., 1973.)

calibration was by simultaneous viewing of the sun by the modules and a self-calibrating cavity radiometer of the Primary Absolute Cavity Radiometer (PACRAD) type. This procedure was mainly used for the total shortwave and broad bandpass channels. A Normal Incidence Pyrheliometer was the transfer instrument for indoor calibration with simulated solar radiation. This instrument was calibrated against the new Cavity Radiometric Scale and by direct comparison with an Angstrom electrical compensation pyrheliometer (traceable to IPS of 1956).

The primary ERB reference instrument is a Normal Incidence Pyrheliometer having a 'Suprasil W' window matching the ERB channels. It has been directly calibrated against the Epply Laboratory and Canadian standard pyrheliometers, all with intercomparisons with IPS standards. Two other pyrheliometers were similarly calibrated for use as ERB standards. One of them has a high sensitivity, mainly for calibration of shortwave scanning channels.

The primary calibration was transferred to the ERB Reference Sensor Model by sequentially viewing the direct solar beam with the cavity radiometer and a simulated beam with the reference pyrheliometer. The pyrheliometer has a filter wheel matching channels 4-10. It is not clear whether or not the filter wheel was part of the reference source. The ERB Reference Sensor Model is nearly identical to the actual flight unit of the ERB. Further intercomparisons during thermal vacuum and ambient testing were performed by comparison with the Reference Model in simulated solar radiation. Longwave calibration was performed during thermal vacuum testing with a special black body source which consists of a double cavity with a temperature range of 180-390°K and an apparent emissivity of at least 0.995. The temperature is measured and controlled to 0.1°K and is maintained by LN₂ cooling and resistive heating. It has concentric V-grooves and a target size of 125 cm².

Shortwave calibration was by intercomparison with standard pyranometers that have been calibrated against the above pyrheliometric standards. Intercomparison was made by measuring diffuse radiation in integrating hemispheres and outdoors by the solar shading technique. "Suprasil W" partial hemispheres were employed on channels 11 and 12 and the reference pyranometers were fitted with FOV reduction collars to match those of the ERB channels. For channel 14 the standard pyranometer was fitted with a special hemisphere matching that of the channel. Subsequently, channels of the flight unit were compared with those of Reference Sensor Model during thermal vacuum testing. The Reference Sensor Model and flight units were sequentially irradiated in the controlled light of the 'Shortwave Earth-Flux Channel Comparator'.

In-flight

Electronic linearity and gain are checked by replacing scene signals with fixed staircase input signals. If needed, corrections are applied to any channel from 1 to 14.

In-flight checks of degradation of solar and earth flux channels are made by occasionally unshuttering reference

channels 1 and 11. (Duplicates of 2 and 12, respectively.) Occasionally channel 12 is shuttered for comparison with normally shuttered channel 11.

Channel 13 is checked against 12 over the illuminated pole, since channel 12 at that time is dominated by shortwave and near infrared radiation ($0.2\text{-}4\mu\text{m}$). An additional daily check of channel 13 is made by integrating shortwave scanning data obtained in the normal scan mode. Zero level signals for channels 13 and 14 are obtained over the dark pole. Calibration of channel 13, with correction for energy from 3.0 to $4.0\mu\text{m}$ (as determined from longwave scanning data), is used to check pre-flight calibration of channel 14.

Calibration of shortwave scanning channels 15 through 18 is done by viewing a diffusely-reflecting scatter plate that is illuminated by the sun. The apparent reflectance of the plate is known.

Longwave scanning channels 19 through 22 are calibrated by viewing space and internal reference black bodies on command during each scan sequence. The scan "head" can be commanded to view space constantly. (Sissala, 1975; Karoli et al, 1975; Hickey and Karoli, 1974; Hickey et al, 1973.)

D. SOUNDERS

1. Vertical Temperature Profile Radiometer (VTPR)

The VTPR is an instrument used on the NOAA and DMSP series of satellites. It consists of a scanning infrared radiometer with eight channels that uses a filter wheel to separate the various intervals. Radiance values obtained in these spectral intervals permit the computation of vertical profiles of temperature and humidity, if cloud conditions permit. Spectral intervals and FOV data are presented in Table 7.6.

Spectral Interval	Wavelength	FOV
CO ₂ Band	15 μm 6 channels	at Nadir
H ₂ O Rotational Band	18.7 μm	68 x 68 km
Window	12.0 μm	

TABLE 7.6

Calibration:**Pre-flight**

All channels were exposed to an external reference source that was calibrated against standard sources. The external sources were used during thermal vacuum tests. Honeycombed plates were maintained at a fixed temperature between 180 and 340°K, and had a target size of 135 cm² with liquid nitrogen and thermoelectric control. Six thermocouples indicated that thermal gradients across the surface were less than 0.1°K. These external sources were calibrated against low temperature black body of the Canadian National Research Council (NRC) standard using calibrated thermopile detectors as transfer standards. Thermopile output from VTPR references were approximately 1% higher than output from the NRC reference. Two external sources were placed in the FOV of the VTPR for the calibration of the internal source at the extremes of the scan (scan spots 1 and 23). Temperature of one source was varied between 180 and 340°K, the other was held constant. The procedure was repeated for a series of instrument temperatures. The VTPR was then put into the automatic calibration mode to compare internal and external sources.

In-flight

The sources used were a black body at the instrument temperature and a view of space. A linear relationship was assumed between radiance and digital counts. The linearity of output was verified by tests of each instrument. While the optics and shroud contribute to the radiance at the detector, temperature dependence was assumed linear because of narrow range of operating temperature. The coefficients for the optics and shroud for each channel were determined by regression during the pre-flight tests in the thermal vacuum. The temperatures of the various components were taken during each scan, and values of the coefficients were checked periodically. When in error they can be adjusted. If necessary, the automatic calibration mode is used and new coefficients are determined through the use of the mean values of the digital counts for a number of views of space and the internal black body (see McMillin et al, 1973). A calibration sequence lasts 37.5 seconds. Normal calibration is activated once per orbit on command, in the automatic mode, the sequence occurs every seven minutes. During the sequence electrical calibration is performed using staircase voltage counts to verify the linearity and stability of the electronic circuitry. Means and standard deviations are

AD-A041 662 ARMY ELECTRONICS COMMAND WHITE SANDS MISSILE RANGE N--ETC F/G 4/2
CALIBRATION TECHNOLOGY FOR METEOROLOGICAL SATELLITES. (U)
JUN 77 L E WILLIAMSON

UNCLASSIFIED

MONOGRAPH SER-3

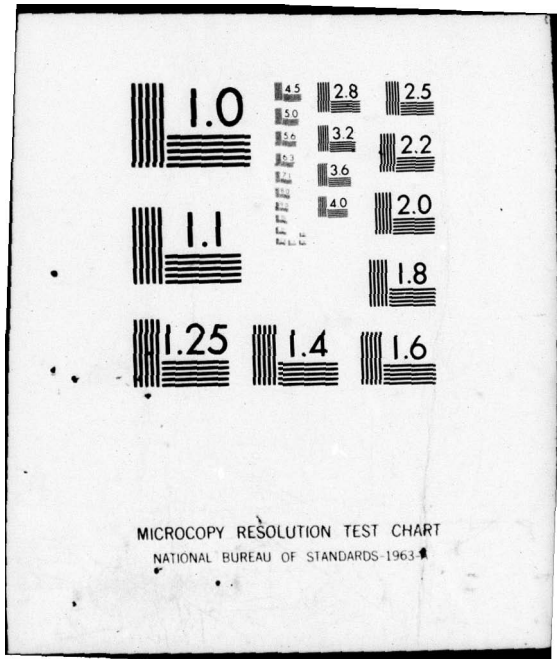
NL

2 OF 2
AD
A 041662



END

DATE
FILMED
8-77



computed for each phase (i.e., electronic voltage staircase, space view, and view of the internal black body). During the retrace period of 1 second during each mirror scan, digital counts representing temperature are recorded for the primary optics, secondary optics, and shroud. (Karoli et al, 1975; McMillin et al, 1973.)

2. Limb Radiance Inversion Radiometer (LRIR)

This instrument is on the Nimbus 6 and is used to vertically scan the earth's atmosphere at the limb. The scan range is about $\pm 1^{\circ}$ for a complete view of the atmosphere. The goals of the mission are to obtain global values of temperature, ozone, and humidity in the stratosphere and mesosphere. In addition the geostrophic wind component is computed for heights up to 1 mb (~48km) via the thermal wind equation. Spectral, FOV, and accuracy information are shown in Table 7.7. Accuracies claimed for the instrument are $\pm 3^{\circ}$ K for altitudes above 15 km, and 20% for ozone and 15% for water vapor at 1 mb.

Band	Spectral Interval	FOV
CO ₂	14.6 - 15.9 μ m	2 x 20 km
CO ₂	14.2 - 17.1 μ m	2 x 20 km
O ₃	8.5 - 10.2 μ m	2 x 20 km
Water Vapor Rotational	23.0 - 27.0 μ m	2.5 x 25 km

TABLE 7.7:

Calibration:

Pre-flight

The absolute accuracy is about one percent. The procedures may be summarized as follows: (1) Determine optical characteristics of in-flight calibration sources; (2) Calibrate encoder used to measure angular position of scan mirror; (3) Determine response of LRIR system to variable black body source for: (a) 10 points over dynamic range of all channels, (b) 3 environmental temperatures of the spacecraft; (4) Deter-

mine spectral response of each channel; and (5) Determine FOV response of each channel in the scan plane.

The first two procedures are critical to the absolute accuracy and interpretation of the data. Procedure (3) determines the response expected range of scene radiances and probable spacecraft temperatures. Linearity of the instrumental response is determined and once estimated for the operating environment on the spacecraft is assumed to hold throughout the mission. The black body itself is a honeycombed plate with a target size of 400 cm^2 and an operating range of 90° to 320°K . This source is kept at a selected temperature by liquid nitrogen and resistive heating.

In-flight

Two calibration points are needed, "zero" radiance from a space view and a large radiance from the in-flight calibration source. The relation between radiance and output is assumed linear between these two points. In the automatic mode calibration occurs every 30 seconds. The mirror rotates up to 8° above its nominal centerline for a 1 second look at space. Then it moves to 30° above the centerline for a 2 second look at the in-flight calibration source. It then returns to the centerline where it remains for 1 second before returning to the scan mode. (Total calibration sequence takes 4 seconds.) The scan mirror may be held on command at the position for a space or in-flight calibration source view. (Sissala, 1975; Karoli et al, 1975; Horowitz and Davis, 1975.)

3. Pressure Modulated Radiometer (PMR)

This instrument is carried on the Nimbus 6 satellite. Each of its two channels views the earth through a cell of carbon dioxide which has a variable pressure. The two channels are closely similar; one has a 1 cm cell of CO_2 (at 0.5 to 3.0 mb) for measuring radiances emitted at heights from 60 to 90 km, and the other has a 6 cm cell (at 1 to 4 mb) for heights from 40 to 60 km. The deduced temperatures are nominally accurate to $\pm 2^\circ\text{K}$ at 65 km and $\pm 0.2^\circ\text{K}$ near 50 km.

The instrument operates via two scanning modes; pressure scanning whereby the pressure of CO_2 in the cells is varied, and Doppler scanning where the mirror scans $\pm 15^\circ$ along the direction of flight causing the relative speed to vary and, therefore, introducing various Doppler shifts.

Calibration:**Pre-flight**

The sensor alternately views a radiation source and its CO₂ cell.

In-flight

The sensor views space and an internal black body. The calibration sequence occurs every 32 minutes. (Sissala, 1975; Horowitz and Davis, 1975.)

E. ACTIVE MICROWAVE—SKYLAB S-193

The S-193 Radiometer/Scatterometer/Altimeter was carried on the Skylab. This microwave instrument has a mechanically scanning antenna with a parabolic reflector, and can scan in various continuous or discrete-step modes. The instrument operates passively as a radiometer and actively as an altimeter or scatterometer. The half-power beam width of the antenna is 1.5° in a conical pencil shape. As a scatterometer the radar transmits a 5.0 ms pulse at a pulse repetition rate of 125 s⁻¹ with a minimum power of 8W. The system has a dual polarization of a 23 db signal to noise ratio. As an altimeter the radar transmits 130,100 or 10 ns pulses at a pulse repetition rate of 250 s⁻¹ and a peak power of 2 kW. Additional features of the system in this mode of operation are a 20 db signal to noise ratio, a 10 to 100 MHz bandwidth, waveform sampling capability, and operation in a pulse compression mode.

As a radiometer it operates with the spectral density of thermal noise and a bandwidth that yields enough independent samples to obtain a temperature resolution of 1.0°K. The radiometer receiver responds to a range of temperature from 50° to 350°K. The spectral and FOV information are as follows: Wavelength ≈ 2.15 cm; Frequency = 13.9 ± 0.1 GHz. FOV on earth's surface at nadir at a nominal altitude of 435 km: about 12 km for the 1.5° half-power beam width.

Calibration:**Pre-flight**

No published information has been obtained, but the radiometer was probably calibrated by using known sources of noise representing certain temperatures.

In-flight

In general, calibration data were obtained by viewing cold sky conditions. Also in the radiometer mode, mean noise values (i.e., measurements) are compared with the mean noise

from a source of known temperature. When operating as a radar a number of independent samples of both signal plus noise, and noise alone, are taken to insure a measurement of sufficient accuracy. (NASA, 1972a.)

REVIEW AND COMMENTARY

Review of the literature has indicated that the nature of calibration can be described as an electrical, mechanical, mathematical or optical process which can be applied to an instrument or series of instruments for the purpose of evaluating its output or performance. The status of calibration can be described as an extension of processes which have served the science well during past generations and which are presumed to suffice for the present. It is suggested that the historical processes, suited to the laboratory and to earth-bound systems alone, are not necessarily translatable into space technology, wherein all or parts of a system have been removed from the laboratory, and indeed from the earth itself. It is further suggested that the concept of calibration be broadened to include all processes involved in the collection and interpretation of remotely-sensed data.

The science of meteorology has advanced rapidly during the past decade, at least partly because of existence of observations from space platforms. Its continued advance will be effected by our ability to interpret data from space. This fact demands that the most careful scientific processes be applied to the total system calibration, or quality assurance of the total performance monitoring process. Calibration, as contemporarily interpreted, is an engineering term used primarily in the fabrication and delivery of instrumentation between a manufacturer and a requiring (usually Government) agency. The term is applied to certain functions of specific systems dealing with performance monitoring. Rarely is the term applied to a total system. The brevity and/or absence of documented processes, for the calibration of complete satellite systems, produces the conclusion that a total system calibration exists only in a bare and fragmentary mode in meteorological satellite technology.

This document has reviewed some sources of errors that may occur in satellite data acquisition. The current state-of-the-art of calibration of satellite systems has been discussed in the light of available literature, including various aspects of pre-flight and in-flight calibration. Calibration procedures for both these stages of operation, and

brief descriptions were given of some of the present and possible future systems and reference scales were reviewed. The description of calibration tools and procedures for some specific satellite instruments demonstrated the application of the methods and sources to typical cases. This report suggests some deficiencies in present calibration practice, i.e., that generalities, assumptions and lack of specifics are probably too prevalent.

Notable among the deficiencies in the calibration process is the failure to document in sufficient detail the procedures used, if in fact any were used. Intercomparisons of similar instruments, as a general process, is not evident. Long-term, i.e., life-cycle, duration processes are the exception, rather than the rule. The combined use of on-board, in space and earth/natural targets in the calibration of specific instruments is rarer still. Little use is made of ground and air truth data in the calibration process, and there is less reference still to signal and data processing. Other problems are the lack of common procedures for given types of instruments and the non-use of standardized calibration sources. The lack of common procedures and sources occurs in both pre-flight and in-flight calibration, but especially the former. Calibration appears to be accepted as a fragmented and sporadic function rather than as a total system process that could be used to improve the state of affairs.

It is suggested that a total system calibration process should include more than a pre-flight check out and occasional in-flight reference to some arbitrary "standard". Atmospheric and target (ground) truth data, and continuity of correlated (simultaneous satellite and ground target) data analysis over the life time of the equipment system are proposed to be effective in improving the process.

Several specific suggestions are offered to aid in alleviating some deficiencies in calibration of satellite instruments, and in the establishment of better total system calibration. One factor to be considered is that agencies requiring the construction of space instruments should pay more critical attention to the calibration criteria in writing contracts. Better documentation and procedures can be accomplished if required by the funding agency. Another factor is for each agency and experimenter to emphasize calibration to its acquisition and analyses systems and to more thoroughly document in detail the procedures followed. Such detailed documentation should be readily available to users.

of the data in User's Guides, or in easily acquired open literature technical reports.

Each experimenter or instrument developer should make use of some central facility to compare the response of his instrument with similar ones of known characteristics. This central calibration facility is a necessary step towards the initiation of the total system calibration concept. Such a facility should be readily available for investigators to calibrate their sensors and compare them with others of a similar nature. The facility should be equipped with a full range of radiation sources and detectors with carefully documented characteristics. Primary and secondary instruments should be included so as to lower costs and to provide an adequate number of references, while maintaining good accuracy and precision through periodic intercomparison of secondary with primary standards. An important part of such a facility would be an outdoor component, the objective of which would be the provision of a realistic operating environment, e.g., real atmospheric and solar radiation data, as required. In addition, the facility would promote the construction and use of standardized sources for both pre- and in-flight calibration. The use of standardized sources would aid the meaningful comparison of data from different instruments of the same general type (e.g., SR and VISSR), and from successive instruments of the same series (e.g., the SR on NOAA-4 and NOAA 5).

There is no existing or planned facility on the ground that can duplicate exactly the operating environment of space. Furthermore, the response of radiometers after a period in space cannot be checked or re-calibrated by any existing method to the same accuracy as in pre-flight calibration. A direct observation of the degradation or contamination of an instrument in space is not now possible except at a prohibitive effort and cost. A solution to these problems would be the construction of a calibration facility for use in space. Such a facility could be included in the SPACELAB planned for launch via the space shuttle. Instrument response in space could be compared with that for the same instrument at a ground based facility such as that proposed in the preceding paragraph. A sample of satellite instruments could be recovered and re-calibrated. The degradation or contamination of sensors and calibration sources could be checked by direct observation, possibly leading to better and more efficient instruments. Most importantly, sample instruments could be calibrated under their actual

operating conditions. For satellites carried by the shuttle, calibration could take place aboard the space station prior to insertion into independent orbit, but after the trauma of launch into initial orbit. In any case, a relatively inexpensive space facility used in conjunction with a complete ground (and perhaps aerial) facility may permit many current calibration problems to be minimized if not eliminated.

Consideration should also be given to experiments that combine the capabilities of appropriate ground-based and space platform facilities which yield improved mechanisms for calibration processes. One such procedure would include the establishment of a vertical pointing laser or sounder facility at a ground target site below the space calibration station (SPACELAB) trajectory. The ability to transmit radiative signals of known properties, i.e., frequency, duration, intensity, etc. and receive them at the satellite as it passes over the target station can yield data on the structure, composition and dynamics of the atmospheric column which could then serve as a "calibrated" atmospheric column for other instruments on other satellites. The presence of personnel aboard the space facility combined with the ability to return the receiving instruments to the ground laboratory for post-operative comparison with the ground instruments appears to be a realistic project for the immediate future. As a minimum, such a facility would represent a great stride toward a total system calibration capability.

APPENDICES

The first two articles are presented to illustrate (1) a method used for calibrating visible sensors on satellites using the natural target of the White Sands and (2) a summary of the calibration process for direct readout data from the infrared channel of the scanning radiometer of NOAA-1 and 2. The latter report is useful in demonstrating the calibration procedures for a specific channel of one instrument, even though the instrument is somewhat dated. In this report the reader should note the many possibilities for error arising from various compromises and assumptions (e.g., assumption of accurate thermistor measurements that are in reality only good to $\pm 1^{\circ}\text{K}$). It was written while the author was temporarily assigned to the Environmental Prediction Research Facility of the US Navy in Monterrey, CA. The author of the former report was the Chief, Radiation Budget Section, Radiation Branch, NOAA, NESS.

Both of these reports illustrate a type of written information not generally available to most investigators because of extremely limited distribution.

The third report describes a unique facility for collection of ground truth data for comparison with satellite measurements, which is being operated at the White Sands Missile Range. The paper describes briefly the sites, currently available instrumentation, and some applications. This paper was presented at the Symposium on Radiation in the Atmosphere on 19-28 August 1976 at Garmisch-Partenkirchen, Germany.

APPENDIX I

Estimation of the Solar Radiation Reflected from White Sands and Transmitted Back to Space for Use in Calibrating Radiometers Aboard Meteorological Satellites

Herbert Jacobowitz, Chief, Radiation Budget Section,
Radiation Branch, NOAA-NESS.

The report that is appended lists all the equations that are needed for estimating the amount of solar radiation that is scattered from White Sands and back out to space. Included are the equations needed for computing the various solar and satellite viewing angles as well as the means for computing reflectivity of White Sands as a function of solar zenith angle from the laboratory data on the bidirectional reflectance. Also, the means for computing the diffuse reflectance (isotropic source of radiation) of White Sands is given.

Following this are the equations needed for determining the solar irradiance at the top of the atmosphere for the spectral band of interest, the optical thickness of the atmosphere above White Sands and the flux reaching the surface due to the scattering of the incoming radiation by the atmosphere.

Rather than relying upon the absolute values of the bi-directional reflectance of White Sands as measured in the laboratory using a sample taken from the surface, only the relative variation with angle is used. A scale factor is computed by matching the predicted upward scattered flux with that actually measured (Equation 12). Equations (13) through (18) permit computation of the components and of the total radiation that is scattered by White Sands up to the satellite level. As described in the text, the flux transmissivity and reflectance of the atmosphere should be sufficiently well described by Rayleigh scattering corresponding to the optical thickness determined by Equation (10). It should be pointed out that the components approximated by Equations (15) and (16) assume that the radiance field after scattering from the surface is isotropic, which is a pretty fair approximation. Since these terms account for less than 15% of the total estimated radiance, small deviations from this assumption will cause only small errors in the total estimated radiance.

Following these equations is presented a reasonable first approximation which neglects the components given by Equations (15) through (17), and assumes that the scale factor is unity. Satellite measurements over White Sands made with the NOAA-2 Scanning Radiometer simultaneously with surface measurements are presented along with the predicted radiance values. Comparison of the ratios of the radiance divided by the cosine of the solar zenith angle on two separate days with the maximum SR counts observed with the satellite, shows that they are consistent. Inclusion of the missing terms

would lower the ratio of the predicted radiances and yield a better agreement with the ratios of the counts.

Plans call for completing the software for computing the three remaining terms. Also, an analysis will be undertaken for assessing the influence that the location of the field of view has on the recorded brightness. In other words, how much does the reflectivity of White Sands vary with location and how does this influence the measured brightness?

NOTATION

- ϕ_v = Latitude of viewed spot
 λ_v = Longitude of viewed spot
 ϕ_{sat} = Latitude of subsatellite point
 λ_{sat} = Longitude of subsatellite point
 θ_o = Solar zenith angle
 α_o = Solar azimuth angle (eastward from north)
 θ_{sat} = Satellite zenith angle
 α_{sat} = Satellite azimuth angle (eastward from north)
 δ = Declination of the sun
 h = Hour angle of the sun
 R = Mean radius of the earth
 H = Altitude of the satellite
 λ = Wavelength of radiation
 $\phi(\lambda)$ = Spectral weighting function of the filter used at White Sands
 $S(\lambda)$ = Solar spectral irradiance (air mass = 0)
 $F_o(\theta_o)$ = Solar irradiance at the top of the atmosphere (for the spectral interval measured)
 $F_D(\theta_o)$ = Normal incidence pyrohelioelectric reading at White Sands

- F_g^+ = Global radiation incident on a unit horizontal surface at White Sands measured with an upward looking pyranometer
 F_g^\downarrow = Global radiation reflected from a unit horizontal surface at White Sands measured with a downward looking pyranometer
 F_{scat} = Global sky radiation impinging on a unit horizontal surface at White Sands
 $\zeta(\theta_v, \theta_{sat}, \alpha_v, \alpha_{sat})$ = Bidirectional reflectance of White Gypsum Sand measured in the laboratory
 R_d = Reflectance of White Sands to global diffuse radiation
 τ = Optical thickness of the atmosphere over White Sands
 $T(\tau, \theta_{sat})$ = Flux transmissivity of diffusely reflected radiation
 $S(\tau, \theta_o, \theta_{sat})$ = Reflectivity of radiation scattered back by the atmosphere itself
 I_{DD}^+ = Radiance at the satellite level resulting from solar radiation that was directly transmitted to the surface (unscattered), reflected, and directly transmitted back through the atmosphere
 I_{dd}^+ = Radiance at the satellite level due to diffusely (scattered) transmitted radiation, which after reflection was directly transmitted back through the atmosphere
 I_{Dd}^+ = Radiance at the satellite level due to directly transmitted radiation, which after reflection was diffusely transmitted back
 I_{dd}^+ = Radiance at the satellite level due to diffusely transmitted radiation, which after reflection was diffusely transmitted back
 I_s^+ = Radiance at the satellite level resulting from solar radiation that was scattered back by the atmosphere alone
 I^\downarrow = Total radiance at the satellite level resulting from solar radiation reflected from White Sands
 $\Gamma(\theta_o)$ = Directional reflectance of White Gypsum Sand

a = Reflectance scale factor

COMPUTATIONS REQUIRED

A. Geometrical Equations

1. Solar Zenith and Azimuth Angles

$$\cos\theta_o = \sin\phi_v \sin\delta + \cos\phi_v \cos\delta \cosh \quad (1)$$

$$\sin\alpha_o = -\cos\delta \sinh / \sin\theta_v \quad (2)$$

2. Satellite Zenith and Azimuth Angles

$$\cos\theta = \sin\phi_{sat} \sin\phi_v + \cos\phi_{sat} \cos\phi_v \cos(\lambda_v - \lambda_{sat}) \quad (3)$$

$$S^2 = R^2 + (R + H)^2 - 2R(R + H) \cos\theta \quad (4)$$

$$\sin\theta_{sat} = \frac{(R + H)}{S} \sin\theta \quad (5)$$

$$\sin\alpha_{sat} = \frac{\sin(\lambda_v - \lambda_{sat})}{\sin\theta} \cos\phi_{sat} \quad (6)$$

B. Reflectance Equations

$$\Gamma(\theta_o) = \frac{1}{\pi} \int_{\phi=0}^{2\pi} \int_{\theta=0}^{2\pi} \zeta(\theta_v, \theta, \phi) \cos\theta \sin\theta d\theta d\phi \quad (7)$$

$$R_d = \frac{2}{\pi} \int_0^{2\pi} \Gamma(\theta_o) \sin\theta_o \cos\theta_o d\theta_o \quad (8)$$

C. Radiation Equations

1. Solar Irradiance

$$F_o(\theta_o) = \int_0^\infty S(\lambda) \phi(\lambda) d\lambda \quad (9)$$

2. Optical Thickness

$$\tau = -\cos\theta_o \ln\left(\frac{F_D(\theta_o)}{F_o(\theta_o)}\right) \quad (10)$$

3. Sky Radiation

$$F_{scat} = F_g - \cos\theta_o F_D(\theta_o) \quad (11)$$

4. Scale Factor Equation

$$F_g^+ = a[\cos\theta_o \Gamma(\theta_o) F_D(\theta_o) + R_d F_{scat}] \quad (12)$$

5. Radiance Components

$$I_{DD}^+(\theta_{sat}, \alpha_{sat}) = a \cos\theta_o \zeta(\theta_o, \theta_{sat}, \alpha_o - \alpha_{sat}) F_D(\theta_o) e^{-\tau/\cos\theta_{sat}} \quad (13)$$

$$I_{dD}^+(\theta_{sat}, \alpha_{sat}) = \frac{a R_d F_{scat}}{\pi} e^{-\tau/\cos\theta_{sat}} \quad (14)$$

$$I_{Dd}^+(\theta_{sat}, \alpha_{sat}) = a \cos\theta_o n(\theta_o) \frac{F_D(\theta_o)}{\pi} T(\tau, \theta_{sat}) \quad (15)$$

$$I_{dd}^+(\theta_{sat}, \alpha_{sat}) = \frac{a R_d F_{scat}}{\pi} T(\tau, \theta_{sat}) \quad (16)$$

$$I_s^+(\theta_{sat}, \alpha_{sat}) = F_o(\theta_o) S(\tau, \theta_o, \theta_{sat}) \quad (17)$$

$$I^+ = I_{DD}^+ + I_{dD}^+ + I_{Dd}^+ + I_{dd}^+ + I_s^+ \quad (18)$$

A reasonable approximation to the transmissivity function, $T(\tau, \theta_{sat})$, can be obtained by assuming the atmosphere can be described by Rayleigh scattering with an optical thickness of τ . The function T can be computed from the tables of Rayleigh scattering compiled by Coulson, Dave, and Sekera, by integrating the downward entries corresponding to τ and θ_{sat} over all azimuth angles, ϕ , and all zenith angles, θ . Surface albedo, A , must be set equal to zero. The function S can be computed by integrating the upward entries corresponding to τ, θ_o , and θ_{sat} over all azimuth angles, ϕ . Surface albedo, A , should be set equal to R_d .

A reasonable first approximation to I^+ is obtained by considering only the terms I_{DD}^+ and I_{dD}^+ which probably accounts for over 85% of the total. Also one can set $a = 1$. Then,

$$I^+ = [\cos\theta_o \zeta(\theta_o, \theta_{sat}, \alpha_o - \alpha_{sat}) F_D(\theta_o) + \frac{R_d F_{scat}}{\pi}] e^{-\tau/\cos\theta_{sat}} \quad (19)$$

FOR METEOROLOGICAL SATELLITES

101

where R_d can be approximated by averaging over a number of values of F_g^+/F_g^- .

For two cases considered below, the value of ζ corresponding to a wavelength of 6000 Å was used. Actually one should integrate over wavelength weighted by $\phi(\lambda)$ to obtain the appropriate value of ζ . Also R_d was set equal to .7. The results are tabulated below.

DATE	ϕ_v	λ_v	ϕ_{sat}	λ_{sat}	
9/20/73	32.87°	106.28°	32.6°	115.1°	
10/31/73	32.87°	106.28°	34.8°	103.9°	
DATE	θ_o	α_o	θ_{sat}	α_{sat}	
9/20/73	41.77°	132.83°	9.12°	-89.69°	
10/31/73	59.02°	136.11°	14.55°	45.03°	
DATE	$\alpha_o - \alpha_{sat}$	δ	h		
9/20/73	222.52° (-137.48)	1.40°	29.25°		
10/31/73	91.08°	-13.86°	37.75°		
DATE	$F_o(\phi_o)$	$F_D(\phi_o)$	F_g^+	F_{scat}	$\pi\zeta$
9/20/73	0.478	0.363	0.275	0.0043	0.698
10/31/73	0.478	0.388	0.225	0.0253	0.722
DATE	R_d				
9/20/73	0.70				
10/31/73	0.70				

DATE	τ	I_{DD}^{\uparrow}	I_{dD}^{\uparrow}	I^{\uparrow}
9/20/73	0.205	0.0467	0.00074	0.0474
10/31/73	0.107	0.0373	0.0034	0.0407

DATE	$I^{\uparrow}/\cos\theta_0$	Max SR Counts
9/20/73	0.0636	149
10/31/73	0.0791	183

$$\frac{(I^{\uparrow}/\cos\theta_0)_{10/31}}{(I^{\uparrow}/\cos\theta_0)_{9/20}} = 1.24$$

$$\frac{(\text{Max counts})_{10/31}}{(\text{Max counts})_{9/20}} = 1.23$$

The three missing terms I_{DD}^{\uparrow} , I_{dD}^{\uparrow} , and I_s^{\uparrow} are strongly dependent upon $\tau/\cos\theta_{sat}$

$$\frac{(\tau/\cos\theta_{sat})_{10/31}}{(\tau/\cos\theta_{sat})_{9/20}} = 0.437$$

Therefore I^{\uparrow} may be even greater on 9/20 relative to that on 10/31 and the same thing can be said for $I/\cos\theta_0$. This would tend to make the ratio of $I^{\uparrow}/\cos\theta_0$ on the two days even less than that given above.

APPENDIX II

DRIR* Calibration

Robert L. Brower, National Environmental Satellite Service,
National Oceanic and Atmospheric Administration, US Department
of Commerce, Suitland, MD

INTRODUCTION

The Improved TIROS Operational Satellite (TOS) system contains a two channel scanning radiometer (SR) which operates in the .52 to .73 micron visible range and the 10.5 to 12.5 micron infrared (IR) water vapor window. TIROS M, the prototype in the ITOS series and now designated ITOS-1, was launched on January 23, 1970. The second spacecraft in the series, NOAA-1, was launched on December 11, 1970. The next spacecraft in the series will be consecutively numbered NOAA satellites.

The scanning radiometers aboard these satellites provide an optical scan perpendicular to the direction of spacecraft path of travel by means of a mirror rotating at 48 RPM. Energy from a single data spot, which is the field of view element at any instant, passes through a beam splitter and spectral filters to provide the input for 10.5 to 12.5 micron IR channel. System optics provide a 5.3 milliradian field of view for the IR detector. It will therefore "see" a 6 to 7 km data spot at the sub-satellite point. This spot size increases to 15 to 21 km at a local zenith angle of 60 degrees. The effective range of thermal sensitivity of the sensor is 180° to 330°K. The SR instrument can provide data on a global scale by storage of the data on onboard tape recorders or on a geographical area reference scale by direct readout.

Temperature measurements of a reasonable accuracy can be obtained from the IR channel of this sensor. In order to do so, the factors which can effect data precision must be accounted for in the logic of the data processing system.

* DRIR - Direct Readout of Infrared channel data from ITOS scanning radiometer. Current terminology is APT/SR - Apparent Picture Transmission from the Scanning Radiometer.

Discussion in this paper is directed at the calibration of the direct readout data of the infrared channel (DRIR). Analysis conducted on the ITOS SR system reveals other factors which will effect accuracy of the end product (Leese et al, 1971). Among the more prominent of the factors which must be dealt with are:

- Analog to digital conversion
- Atmospheric Attenuation Correction
- Earth location
- Signal noise

Realtime users of DRIR data beginning with ITOS "D" data will have the necessary parameters available in the data stream to affect electrical and thermal calibration. Earlier satellites lacked necessary parameters in the DRIR data stream to directly compute inflight calibration.

CALIBRATION PROCESS

The calibration requirements for the SR sensor are best viewed in two segments; (1) electronic calibration, and (2) thermal calibration. The process of electronic calibration establishes a standard relationship of the received data in digital format (digital count) to the analog voltage signal generated by the sensor. This type of calibration is necessary to account for shifts introduced into the analog signal as it proceeds through the data path from the radiometer to the processing facility. The process of thermal calibration accounts for behavioral changes in the SR instrument produced by variations in operating temperatures of the spacecraft.

ELECTRONIC CALIBRATION

Infrared scanning radiometer data arrives at a receiving station as an FM signal and is recorded in its analog form. The analog data is then passed through a digitizing unit to convert the analog form to a digital format via a signal discriminator. Discriminator level settings on this signal are critical to the overall accuracy of the IR temperature value. If the signal level is not adjusted or compensated for properly, the effect will be reflected in a deviation from the standard curve for converting from analog volts to digital counts. The standard curve commonly in use is a linear relationship zero to six volt analog range into an

eight bit byte digital count with a range of 256 counts. It is estimated that the equipment available for manual adjustment of level settings in observed handling systems could provide an accuracy no better than 5% over the total temperature range. This accuracy could contribute to a temperature error of 6°C at 300 K. This example was based on assumption that there is no change in slope of the Volts-to-Count curve. A slope change would produce an additional error in the digitized data.

COMPENSATING APPROACHES

It is apparent that dependence upon manual adjustments to a standard curve is inadequate with present equipment. An alternative to using manual adjustment entirely is to make coarse adjustments within prescribed limits and then use automated processing techniques to achieve the precision required. This technique which is referred to as "Electronic Calibration" can be accomplished by using the stepwedge signal included in the DRIR data stream on each scan line. The stepwedge wave form provides reference voltage levels which can be used to compute the magnitude and slope of the deviation from the standard volts-to-count curve. These computed deviations are then applied to the raw digital data to obtain a set of data "Electronically Calibrated" to the standard curve.

Computation of magnitude and slope of the deviation from the standard curve can be accomplished by several techniques, including

- Least square fit a linear curve to data points
- An nth order fit to the points of the stepwedge
- Stepwise linearity between adjacent voltage levels.

Which of these techniques to employ depends on the degree of accuracy needed as opposed to the temperature range to be considered. Where a specific temperature range accuracy may be specified, such as in the study of sea-surface temperature where cloud temperatures are not a consideration, a least squares fit is best used. If a relative accuracy is needed over the entire range of temperatures, then a stepwise linear interpretation may be adequate.

Determination of true representation of a count value assigned an individual level on the stepwedge can produce some difficulty in maintaining stability estimates from stepwedge to stepwedge due to notable low frequency coherent noise patterns. To achieve stability in the stepwedge levels,

a floating mean value for each level can be taken from several adjacent stepwedges.

THERMAL CALIBRATION

Two basic approaches have been used to provide thermal calibration for these instruments, "static" and "dynamic".

A "static" mode thermal calibration process, which incorporates the prelaunch calibration curves, was utilized by the National Environmental Satellite Service (NESS) for ITOS-1 and NOAA-1 infrared data. Prelaunch bench and vacuum thermal tests of each IR instrument establish measurements of the relative sensor response function and calibration curves. Samples of this data are found in Figures 1 and 2. The technique produced a temperature differential of 2 to 4°C between thermister measurement and the IR instrument viewed measurement on an on-board black body. This differential was also verified to exist in earth surface temperature retrievals.

A "dynamic" inflight thermal calibration technique has been developed by the Product Development Branch of NESS. This thermal calibration technique is accomplished in two segments;

first, it establishes the relationship of the radiational energy received by the sensor to effective temperature of the scene being viewed; and secondly, it calculates the calibration curve which relates the radiant input energy to the sensors output voltage.

SENSOR ENERGY TO TEMPERATURE RELATIONSHIP

The relationship to black body radiation received by the IR sensor to effective temperature measured at the top of the atmosphere is computed by the radiative transfer equation

$$N = \int_{\lambda_1}^{\lambda_2} B(\lambda, T_s) \phi(\lambda) d\lambda \quad \text{Equation (1)}$$

when transmissivity and emissivity equal one.
Where B is the Planck's formula:

$$B(\lambda, T) = \frac{2C^2 h}{\lambda^5} \left(e^{\frac{Ch}{k\lambda T}} - 1 \right)^{-1} \quad \text{Equation (2)}$$

where:

C = velocity of light
 h = Planck's constant
 k = Boltzman constant
 λ = wave length
 B = energy in ERGS units
 φ = the relative spectral response function of the sensor.

Analytically the procedure as defined by the radiative transfer equation, which relates sensor input energy to temperature, and the thermal calibration transformation equation relate output voltage to input sensor energy. The radiative transfer equation may be further reduced to the Planck's formula when the response function, φ, is scaled to equal one and \bar{T} is substituted for λ. The infrared spectrum curve is a nearly linear function for the bandpass and temperature range being used. NOTE: Use of the scaled approach to the calibration problem should be based on limited computer space and accuracy requirements. Some error will be introduced with this mean response technique particularly at the higher scene temperatures.

For application purposes it is useful to compute a reference table relating sensor energy to temperature equivalents for the form of the radiation transfer equation required. The reference table should cover the full effective temperature range of the IR sensor, 160.0°K. Once computed, this table is applicable for the lifetime of the sensor for it has no dependency on any yet observed phenomena which would alter the response function. Any degradation of the sensor optics should be linear and would not affect the output of this approach. A scaling factor of 10 for the energy unit index of the reference table will reduce storage requirements while maintaining accuracy to within 0.1°C for most of the viewed temperature range.

THERMAL CALIBRATION TRANSFORMATION ALGORITHM

The thermal calibration algorithm establishes the calibration curve and relates Input Radiant energy to output voltage. Three assumptions are made in the thermal calibration procedure:

1. A linear relationship is maintained between voltage output and energy output.
 2. The relative response function of the IR sensor is constant.
 3. On-board electrical measurements by thermistors (temperature sensors) are accurate.
- The calibration curve can be computed utilizing three data points from the spacecraft:
1. Radiometer output voltage value of space, in terms of digital counts.
 2. Radiometer output voltage value of housing scene viewed during backscan in terms of digital count.
 3. Output voltage of housing thermister in terms of digital count.
- The slope (m) of the calibration curve is computed by equation:

$$m = \frac{E_1 - E_2}{C_1 - C_2} \quad \text{Equation (3)}$$

where:

- E_1 = radiance energy equivalent computed from housing thermister output voltage.
 E_2 = radiance energy value of space, accepted as being 0.
 C_1 = viewed digital count value of housing scene.
 C_2 = viewed digital count value of space.

The calibration curve intercept point is computed by

$$B = -mC_2 \quad \text{Equation (4)}$$

Thermal calibration is then affected by relating the sensor output voltage to the calibration curve to produce an equivalent black body energy value. Mathematically this is:

$$E(T_s) = mC + b \quad \text{Equation (5)}$$

where:

- $E(T_s)$ is the equivalent black body energy and C is the digital count representation of the sensor output value.
 $E(T_s)$ is then converted to effective scene temperature, T_s , by the energy to temperature table.

APPENDIX III

A United States Facility for the Collection of Satellite-Correlated Air and Ground Truth Data

L. Edwin Williamson, Atmospheric Sciences Laboratory, U S Army Electronics Command, White Sands Missile Range, NM

BACKGROUND

The Atmospheric Sciences Laboratory of the United States Army began in 1973, the establishment of a facility for the collection of surface radiation data for comparison, correlation and/or calibration of data acquired by meteorological satellites. The facility, located on and near the White Sands Missile Range, in South Central New Mexico, USA, now consists of three* distinct target areas from which surface radiation and meteorological data are collected, and other nearby locations from which balloonsonde and rocketsonde data are acquired. These air and ground truth data are collected simultaneously with selected satellite overpasses for the purpose of monitoring and/or evaluating the performance of certain satellite sensors.

SITE CRITERIA

The initial process for the establishment of a calibration data facility is the determination of site criteria. These criteria basically include visibility, composition and geometry. Regarding visibility, the site must be observable from satellites of different orbital modes, i.e., polar orbiters, and equatorial orbiters (including geostationary). In essence, this means the site should be between 50°N and 50°S latitudes, and in the Western hemisphere (for consideration of the US geosynchronous satellites). In addition, the sites should have minimal obscuration by clouds. The composition of the site should insure a uniformity in its structure such that the determination of its emissive or radiative character at one point would be reasonably repre-

* A fourth target site, representing the desert background surrounding the sites described herein, began operation in January 1977.

sentative of the whole. The site should be readily identifiable by its geographic features to aid in location and registration, and should have a large enough geometry to meet the resolution criteria of the various sensors.

WHITE SANDS TARGET SITE

There is an area of gypsum (hydrous calcium sulphate) in South Central New Mexico, which was proposed as a calibration data target and which is in the boundaries of the White Sands Missile Range. The coincidence of scientific interest, purpose, and geographic availability provided adequate justification for the laboratory to initiate the program. The gypsum field is located on one of the most cloud-free areas in the USA. It covers approximately 350 sq. miles and is level and vegetation-free on the west. It consists of sand dunes approximately 4-8 meters high on the east.

INSTRUMENTATION

Following selection of the site, consideration was given to the parameters to be monitored and the instrumentation and resources available to perform the task. The interpretation of visible imagery is one of the principle areas of meteorological satellite technology, and there were several instruments available suited to the collection of visible data. Therefore, the sites originally were equipped to collect data applicable to visible radiometry. Subsequently, measurements of longer wave radiation, as well as conventional meteorological parameters were included. The current instrumentation array consists of those described in Table I.

TARGET SITE ARRAY AND CHARACTER

Once the first site at White Sands was established, additional targets on surfaces of different albedoes and compositions were deemed appropriate and were subsequently established on lava, fresh water and desert surfaces. The technical and logistical merits of having a wide variety of targets within this geographic area are substantial. First, the proximity of the targets permits satellite radiometer viewing of all of them through a very small atmospheric

FOR METEOROLOGICAL SATELLITES

111

column (while this does not eliminate atmospheric effects on energy being received, the effect becomes common to all sites). Second, the nearness of the sites permits centralized logistics and manpower administration (which implies a minimal economic burden). Thirdly, the atmosphere up to 60 km over White Sands Missile Range is one of the most densely measured atmospheric envelopes on the globe, and this upper atmospheric data is available to the satellite community at minimal effort and expense. The general characteristics of the primary target sites are as shown in Table II.

DATA APPLICATION

Data are routinely collected at these sites on a weekly basis on a schedule coincident with one or more of the US national meteorological satellites. The site data are combined with the rocket and balloon data and are distributed to researchers and analysts in Governmental, academic, defense and industrial agencies who deal with the satellite data. The data are also archived and published annually and form the only known climatology of satellite-correlated air-and-ground truth data. While the primary schedule of data collection adheres to the principal polar orbiting US meteorological satellites, numerous other satellite systems are supported on an irregular schedule. These other programs represent a broad spectrum of satellite observations including special instrumentation aboard manned space experiments (SKYLAB), the LANDSAT program, and the Synchronous Meteorological Satellites which routinely observe the target sites at one half-hour intervals, and consequently do not require special scheduled observations. The data are used in both domestic and international programs.

SUMMARY

There is in operation within the United States a facility dedicated solely to the purpose of collection of satellite-correlated ground truth data on a continuing basis. The data consists of meteorological (both surface and upper air), radiative (visible and infrared wavelength), and other pertinent parameters intended primarily to aid in the interpretive meteorological process. The data are, or can be, provided to national and international programs involved in the interpretation of satellite data for these and other applications.

<u>MEASURED PARAMETERS</u>	<u>INSTRUMENT USED</u>
<u>METEOROLOGICAL - Surface</u>	
Air Temperature (standard USWB shelter height)	Thermocouple and thermometer
Dew Point (standard USWB shelter height)	Wet and dry bulb thermometer
Dew Point (25 meters above ground)	Wet and dry bulb thermometer
Wind Speed and Direction (4 meters above ground)	Standard USWB airport indicator
Atmospheric Pressure	Sosman transducer and converter
Sky Condition (observed)	Trained meteorological observers
<u>METEOROLOGICAL - Upper Air</u>	
Balloon - surface to 30 km	Standard Hypsometric Radiosonde
Rocket - 30 to 60 km	Lokisonde and Arcasonde - US Meteorological Rocket Network
<u>RADIATIVE - Visible and Near IR</u>	
Incoming Global Radiant Flux - .285-.800 microns	Eppley Precision Spectral Pyranometer (WG285) (GG495)
" " ".500-.2,800 microns	" "
" " ".700-.2,800 microns	" "
Outgoing Global Radiant Flux - .285-.800 microns	" "
" " ".500-.2,800 microns	" "
" " ".700-.2,800 microns	" "
Normal Radiant Flux - .285-.4,000 microns	Eppley Model 15 Pyrheliometer w/crystal quartz window w/GG495 filter
" " ".500-.4,000 microns	" "

MEASURED PARAMETERS	INSTRUMENT USED
<u>ABSORB</u> - Visible and Near IR	
Normal Radiant Flux	Eppley Model 15 Pyrheliometer w/RG530 filter
" "	" " " w/RG630 filter
" "	" " " w/RG655 filter
" "	" " " "
RADIATIVE - Long Wave	
Apparent Radiant Surface Temperature-9.5-11.5 microns	Barnes Precision Radiation Thermometer PRT-5
" "	" Barnes Radiation Thermometer PRT-10
RADIATIVE - Radiative Measurements in the 11-15 micron band	
PLANNED	
Soil Temperature (1 mm below surface)	Thermocouple embedded in surface
Soil Moisture	Gravimetrically determined - soil sample
UTIL	

Table I (continued)

TABLE II

	NETSAT 1A White Sands FLATS	NETSAT 1B White Sands DUNES	NETSAT 1I LAVA	NETSAT 1II FRESH WATER
Nominal Emissivity (measured) 9.0-11.5/0.5-20	.98/.96	.97/.91	.96/.96	.97/.97
Average Albedo (.285-.800 micron)	.47	.35	.10	.9
Average Albedo (.300-.600 micron)	.51	.36	.11	.9
Average Albedo (.700-.100 micron)	.53	.65	.13	.5
Average Noon Surface Radiant Temperature (°C) (winter) (summer)	12.3 42.4	13.0 43.4	16.7 47.3	4.8 20.7

*after Davies et al.

ACRONYMS AND DEFINITIONS

- albedo: ratio of the amount of electromagnetic radiation reflected by a body to the amount incident upon it, commonly expressed as a percentage.
- apogee: the point in the orbit at which the satellite is farthest from the center of the earth.
- APT: Automatic Picture Transmission
- ascending node: the point on the equator at which the satellite crosses from the southern to the northern hemisphere measured in degrees longitude westward from Greenwich.
- ATS: Applications Technology Satellite
- attenuation: reduction in intensity.
- attitude: position or orientation of a satellite as determined by the relationship between its axis and some reference line or plane or some fixed system of reference axes.
- AVCS: Advanced Vidicon Camera System
- AVHRR: Advanced Very High Resolution Radiometer
- AWS: Air Weather Service
- AZ: Azimuth
- blackbody: a radiant source from which no energy is reflected or transmitted for any wavelength, i.e., a body that radiates for every wavelength the maximum amount of radiation possible at a given temperature.
- BSU: Basic Sounder Unit
- BUV: Backscatter Ultraviolet Spectrometer
- CDA: Command and Data Acquisition Station
- CZCS: Coastal Zone Ocean Color Scanner
- DCP: Data Collection Platform
- DCS: Data Collection System
- DMS: Defense Meteorological Satellite Program. Unclassified title of the DOD program for obtaining world wide weather coverage for strategic operations.
- effective radiation: net radiation on a horizontal, upward (or downward) facing black surface at the ambient temperature.
- emissivity: ratio of the flux emitted by a body to the flux emitted by a black body at the same temperature.
- emittance: measure of the total radiant energy emitted per unit area of emitting surface.
- enhancement: the capability of varying the signal voltage to give a non-linear display of gray shades.
- equatorial satellite: artificial satellite whose orbital

plane is inclined at zero degrees to the equator.

ERB: Earth Radiation Budget. A NIMBUS instrument that will measure reflected and emitted terrestrial radiation fluxes in conjunction with solar radiation.

EREP: Earth Resources Experiment Package (SKYLAB)

ERTS: Earth Resources Technology Satellite (early name for LANDSAT).

ESMR: Electrically Scanning Microwave Radiometer. For use in measuring the earth's microwave emission at 37 GHz. Liquid water content of clouds, distribution and variation of sea ice cover, and gross characteristics of land surfaces are some applications.

FOV: Field Of View

gain: ratio of voltages, powers, or currents.

geosynchronous: positioned such that the sub-satellite point remains fixed (over the equator).

global solar radiation: downward direct and diffuse solar radiation as received on a horizontal surface from a solid angle of 2π .

GMS: Geosynchronous Meteorological Satellite (Japan). Planned for fall 1977, to be positioned at 140° E.

GOES: Geostationary Operational Environmental Satellite (USA). Two GOES currently operative, one at 75° W and one at 135° W, see SMS.

gray scale: various shades of gray which can be incremented (square root of a 2-step function) by the optics or sensors of a satellite for imagery.

ground track: projected track of an orbiting body on the ground plane, i.e., the line formed by the intersection of the vertical projection of the track and the ground plane.

GVHRR: Geosynchronous Very High Resolution Radiometer

HIRS: High-resolution Infrared Radiation Sounder

HR: High Resolution (visible) on DMSP-OLS.

HRIR: High Resolution Infrared Radiometer.

HRPT: High Resolution Picture Transmission

IDCS: Image Dissector Camera System

IPS: International Pyrheliometric Scale. Recommends suitable corrections to the Angstrom (+1.5%) and Smithsonian (-2.0%) standard instruments to bring them into line with each other and to make the units of the radiation measurements more nearly equal to the rigidly defined physical units.

IR: Infrared. Wavelengths in the electromagnetic spectrum which are longer than visual light, $> .75 \mu\text{m}$ and generally shorter than $100 \mu\text{m}$.

IRIS: Infrared Interferometer Spectrometer. For measurement of emission spectra of earth - atmosphere system.

IRLS: Interrogation, Recording and Location System

irradiance: the quotient of the flux of radiation incident on an infinitesimal element of surface containing the point under consideration, to the area of that element.

ITOS: Improved TIROS Operational Satellite

ITPR: Infrared Temperature Profile Radiometer. Used to obtain temperature profiles and total water vapor content in the troposphere and lower stratosphere with sensing taking place in 6 intervals in the 15μ CO₂ band, 1 interval in the water vapor rotational band near 20μ and 2 intervals in the atmospheric window near 3.8 and 11μ .

LACATE: Lower Atmospheric Composition And Temperature Experiment

LANDSAT: modified version of NIMBUS satellite formerly called ERTS.

LRIR: Limb Radiance Inversion Radiometer. Will provide calibrated radiance versus altitude profiles by sensing the following intervals:

(1) 14.6 to 15.9μ CO₂

(2) 14.2 to 17.3μ CO₂

(3) 8.8 to 10.1μ ozone

(4) 20 to 25μ water vapor rotational band

CO₂ and water vapor measured in the stratosphere and lower mesosphere.

MAPS: Measurement of Air Pollution from Satellites

MDCTS: Meteorological Data Collection and Transmission System (also known as Data Collection System)

METEOSAT: Meteorological Satellite. This synchronous meteorological system is planned for launch during the summer of 1977 by the European Space Agency (ESA), formerly ESRO, to be positioned at 0° longitude.

MI: High Resolution (infrared) on DMSP-OLS.

MRIR: Medium Resolution Infrared Radiometer

MSS: Multi-Spectral Scanner

MSSCC: Multi-color Spin Scan Cloud Camera

MSU: Microwave Sounding Unit

MUSE: Monitor Ultraviolet Solar Energy

NBS: National Bureau of Standards

NEMS: NIMBUS E Microwave Spectrometer

NESS: National Environmental Satellite Service of NOAA.

NIMBUS: the name given to a family of NASA earth-observing research and development satellites.

NIP: Normal Incidence Pyrheliometer

- NOAA: National Oceanographic and Atmospheric Administration
noise: any unintelligible signals in a system that tend to interfere with a desired signal return.
- OLS: Operational Linescan System
perigee: point in a satellite's orbit where it is closest to the earth's center.
- PMR: Pressure Modulated Radiometer
polar orbit: orbit of an earth satellite that passes over or near the earth's poles with an inclination of 90°.
- polarization: the state of electromagnetic radiation when transverse vibrations take place in some regular manner due to the nature of the emitting source or to some process to which it is subjected after leaving the source (i.e., scattering).
- PRT: Precision Radiation Thermometer
pyrgeometer: instrument for measuring net atmospheric radiation (long-wave) on a horizontal upward-facing black surface at the ambient air temperature.
- pyranometer: a type of pyradiometer which may include hemispheres of optical glass and filters for various wavelengths.
- pyrheliometer: instrument for measuring direct solar radiation.
- pyrradiometer: instrument for measuring total radiation falling from the solid angle 2π on a plane surface.
- radiometer: instrument for measuring radiation.
- RBV: Return Beam Vidicon Camera System
reflectivity: the ratio of the energy (of a particular wavelength) reflected by a body (at a given temperature) to the energy incident upon the body.
- resolution: a measure of the ability of an instrument to distinguish targets separated by very small angular distances.
- REV: revolution
roll: rotation or oscillatory movement of a satellite about the velocity vector.
- SAM-II: Stratospheric Aerosol Measurement - II
SAMS: Stratospheric and Mesospheric Sounder
satellite subpoint: intersection of the local vertical passing through the satellite with the earth's surface, with the image plane, and with the celestial sphere.
- SBUV/TOMS: Solar and Backscatter Ultraviolet/Total Ozone Mapping System
- SCAMS: Scanning Microwave Spectrometer
SCMR: Surface Composition Mapping Radiometer

SCR: Selective Chopper Radiometer

SCRS: Solar Constant Reference Scale

SEM: Space Environmental Monitor

SIRS: Satellite Infrared Spectrometer

sky radiation: downward diffuse solar radiation as received on a horizontal surface from a solid angle of 2π with the exception of the solid angle subtended by the sun's disk.

SMMR: Scanning Multispectral Microwave Radiometer

SMS: Synchronous Meteorological Satellite (see GOES)

solar constant: solar radiation received on a surface perpendicular to the solar beam outside the earth's atmosphere when the earth is at its mean distance from the sun.

SPM: Solar Proton Monitor

SR: Scanning Radiometer. Basic ITOS imaging system. Image is formed by using a continuously rotating mirror which scans perpendicular to the satellite's orbital path and produces one scan line of the picture for each rotation of the mirror as the satellite progresses along the orbital path.

SSCC: Spin Scan Cloud Camera

SSH: Supplementary Sensor Package H. A scanning infrared radiometer on DMSP satellite.

SSTIR: Sea Surface Temperature Infrared Radiometer

SSU: Stratospheric Sounding Unit

sun-synchronous: an orbit which maintains a constant angular relationship between its ascending node and the solar subpoint.

terrestrial radiation: radiation emitted by the planet Earth.

THIR: Temperature-Humidity Infrared Radiometer. NIMBUS instrument to detect thermal radiation in the IR window (10.5 to 12.5μ) for the measurement of cloud top temperatures; during cloud-free times may produce thermal gradients on land and water surfaces (night and day); also measures water vapor in upper troposphere and stratosphere primarily at night at 6.5 to 7.0μ .

TIROS: Television Infrared Observation Satellite

TOVS: TIROS Operational Vertical Sounder. Measures infrared radiation emitted from earth and atmosphere to indirectly determine vertical distribution of temperature, water vapor, and ozone.

transmittance: measure of the amount of radiation propagated through a given medium; ratio of the transmitted radiation to the total radiation incident upon the medium.

TWERLE: Tropical Wind Energy Conversion and Reference Level Experiment

VCS: Vidicon Camera System

VHR: Very High Resolution System (visible) on DMSP-OLS.

VHRR: Very High Resolution Radiometer. Measures surface temperature of earth, sea, and cloud tops during the day and night with a 9 km resolution at $.6\text{-.}7\mu$ for reflected radiation and 10.5 to 12.5μ for emitted radiation.

VISSR: Visible-Infrared Spin Scan Radiometer. A sensor on GOES that provides night and day observations of cloud cover and earth/cloud radiance temperature measurements using a common optics system with 2 channels IR (10.5 to 12.5μ) and visible ($.55$ to $.75\mu$); resolutions are 9 km for IR and .9 km for visible, radiance temperatures measured between 180 and 315°K .

visual: wavelengths in the electromagnetic spectrum to which the human eye is sensitive (.4 to $.7\mu$) bounded by the ultraviolet at the short end and infrared on the long end.

VTPR: Vertical Temperature Profile Radiometer. Senses radiant energy from atmospheric CO_2 in several spectral regions.

WHR: Very High Resolution (infrared) on DMSP-OLS.

REFERENCES AND BIBLIOGRAPHY

Not all of the following references are cited in the text, and few of them deal exclusively with the subject of calibration. Typically, each contains some discussion of errors, data quality, or calibration, and collectively they illustrate the concepts and principles that define both the nature and status of calibration.

- Alexander, G. D., 1974: Comparison of Three Iterative Methods for Inverting the Radiative Transfer Equation, Sixth Conference on Aerospace and Aeronautical Meteorology, Preprint, pp. 231-238.
- Allison, L. J., Arking, A., Bandeen, W. R., Shenk, W. E. and Wexler, R., 1974: Meteorological Satellite Accomplishments, U. S. Quadrennial Report to the IVGG, 1971-1975, Greenbelt, MD, 60 pp.
- Allison, L. J., 1975: Meteorological Satellite Accomplishments, U. S. National Report, 1971-1974, Reviews of Geophysics and Space Physics, Vol. 13, No. 3, American Geophysical Union.
- Backus, G. E. and Gilbert, J. F., 1967: Numerical Applications of a Formalism for Geophysical Inverse Problems, Geophysical Journal of the Royal Astronomical Society, Vol. 13, pp. 247-276.
- Backus, G. E., 1970: Uniqueness in the Inversion of Inaccurate Gross Earth Data, Phil. Trans. Roy. Soc. London, 266, pp. 123-192.
- Barnett, T. L., 1969: Application of Non-Linear Least Squares Method Atmospheric Temperature Sounding, J. Atmos. Sci., Vol. 26, No. 3, pp. 457-461.
- Baumhefner, D. P. and Julian, P. R., 1974: The Structure and Growth of Initial and Forecast Error Introduced by Remotely Sensed Temperature Profiles, NCAR MS. 0102-74-3, National Center for Atmospheric Research, Boulder, CO, 34 pp.
- Bede, D., 1976: Private Communication.
- Bedford, R. E., 1960: A Low Temperature Standard of Total Radiation, Can. J. Phys., 38, pp. 1256-1278.
- Broderick, H. J. and Hayden, C. M., 1972: Verification of Operational SIRSB Temperature Retrievals, NOAA Tech Rep. NESS 63, National Oceanic and Atmospheric Administration, Washington, DC.

- Brower, R., 1977: "DRIR Calibration", Private Communication, (See Appendix).
- Bruce, R. E. and Duncan, L. D., 1974: The Effect of Atmospheric CO₂ Variations on Satellite-Sounded Temperatures, ECOM Research and Development Technical Report, ECOM-5552, US Army Electronics Command, White Sands Missile Range, NM, 12 pp.
- Buettner, K. J. K. and Kern, C. D., 1965: The Determination of Infrared Emissivity of Terrestrial Surfaces, J. Geophys. Res., 70, pp. 1329-1337.
- Canfield, L. R., Johnson, R. G. and Maddin, R. P., 1973: NBS Detector Standards for the Far Ultraviolet, Appl. Opt., 12 (7), pp. 1611-1617.
- Chahine, M. T., 1968: Determination of the Temperature Profile in an Atmosphere from its Outgoing Radiance, J. Opt. Soc. Am. 58 (12), pp. 1634-1637.
- Chahine, M. T., 1970: Inverse Problems in Radiative Transfer: Determination of Atmospheric Parameters, J. of Atmos. Sci., Vol. 27, No. 6.
- Chahine, M. T., 1972: Recent Developments in the Inversion by the Method of Relaxation, Proceedings of the NASA Workshop on the Mathematics of Profile Inversions, L. Colin, Editor, pp. 1-57 to 1-66.
- Chahine, M. T., 1974: Remote Sounding of Cloudy Atmosphere. I. The Single Cloud Layer, J. Atmos. Sci., 31, pp. 233-243.
- Chahine, M. T., 1975: An Analytical Transformation for Remote Sensing of Clear-Column Atmospheric Temperature Profiles, J. Atmos. Sci., 32, pp. 1946-1952.
- Chen, Y. M., Woolf, H. M. and Smith, N. L., 1974: Vertical Resolution of Temperature Profiles for HIRS, NOAA Technical Report NESS 67, NESS.
- Chow, M. D., 1975: A study of the Effects of Vertical Resolution and Measurement Errors on an Iteratively Inverted Temperature Profile, J. Atmos. Sci., 32.
- Comsat, 1976: Comsat Technical Review, CTR-CG(1)-1-218 (1976), 6(1), 217 pp.
- Conrath, B. J., 1972: Vertical Resolution of Temperature Profiles Obtained From Remote Radiation Measurements, J. Atmos. Sci., 29, pp. 1262-1271.
- Conrath, B. J. and Revah, I., 1971: A Review of Nonstatistical Techniques for the Estimation of Vertical Atmospheric Structure from Remote Infrared Measurements, Proceedings of a Workshop held at Ames Research Center, Mathematics of

- Profile Inversion, L. Colin, Editor, pp. 1-36 to 1-49,
NASA Tech Memo.
- Coulson, K. L., and Jacobowitz, H., 1972: Proposed Calibration Target for the Visible Channel of a Satellite Radiometer, NOAA TR NESS 62, NOAA/NESS, Washington, DC, 27 pp.
- Coulson, K. L., 1975: Solar and Terrestrial Radiation - Methods and Measurements, Academic Press, New York, 322 pp.
- Crosby, D. S. and Weinreb, M. P., 1974: Effect of Incorrect Atmospheric Statistics on the Accuracy of Temperature Profiles Derived from Satellite Measurements, J. Statis. Comput. Simul., Vol. 3, pp. 41-51.
- Crosby, D. S., Fleming, H. E. and Mark, D. E., 1973: Covariance Matrices and Means . . . Satellite Measurements, J. Atmos. Sci., Vol. 30, No. 1, pp. 141-144.
- Curtis, P. D., Moughton, J. T., Peskett, D. G. and Rodgers, C. D., 1974: Remote Sounding of Atmospheric Temperature from Satellites V. The Pressure Modulated Radiometer for NIMBUS F, Proc. Roy. Soc. A, 337, pp. 135-150.
- Davies, J. A., Robinson, P. J. and Nunez, M., 1971: "Field Determinations of Surface Emissivity and Temperature for Lake Ontario", Journal of Applied Meteorology, Vol 10, #4, pp. 811-819.
- Davis, P. A., 1972: Universal Transmittance Representations for Application to ITPR Measurements, Final Report prepared for NOAA/NESS, Contract 2-35136, Stanford Research Institute, Menlo Park, CA, 45 pp.
- Davis, P. A., 1974: Atmospheric Transmittance Models for Infrared Radiometer Measurements, Final Report for NESS Contract 3-35208.
- Davis, P. A., Hadfield, R. G. and Wiegman, E. J., 1973: Infrared Emissivities and Upper Tropospheric Cloud Motions, Stanford Research Inst. Rpt. No. 2014, 55 pp.
- Dickenson, L. G., Boselly, S. E. III and Burgman, W. S., 1974: Defense Meteorological Satellite Program (DMSP) User's Guide, HQ, Air Weather Service, USAF, Scott AFB, IL, 109 pp.
- Drayson, R. S. and Young, C., 1966: Theoretical Investigations of Carbon Dioxide Radiative Transfer, U. S. Department of Commerce Contract No. Qwb-11106, Washington, DC.
- Drummond, A. J., Landsberg, H. E. and Van Meighem, J. (Eds), 1970: Advances in Geophysics, Vol. 14: Precision Radiometry and its Significance in Atmospheric and Space Physics, Academic Press, New York and London, 415 pp.

- Brummond, A. J. and Thekaekara, M. P. (Eds), 1973: The Extraterrestrial Solar Spectrum, Institute of Environ. Sci., Mount Prospect, IL, 169 pp.
- Duncan, L. D., 1976: SATFAL - The Application of Meteorological Satellite Data to Nuclear Fallout Predictions, Presented at the Army Science Conference, West Point, NY, 14 pp.
- Duncan, L. D., 1973: A Geometric Investigation of the Effect of Viewing Angle on the Ground Resolution of Satellite Borne Sensors, ECOM Research and Development Technical Report, ECOM-5502, US Army Electronics Command, White Sands Missile Range, NM, 14 pp.
- Duncan, L. D., 1974: An Iterative Inversion of the Radiative Transfer Equation for Temperature Profiles, ECOM Research and Development Technical Report ECOM-5534, US Army Electronics Command, White Sands Missile Range, NM, 18 pp.
- Duncan, L. D., 1974: Approximations in Inverting the Radiative Transfer Equation, ECOM Research and Development Technical Report, ECOM-5545, US Army Electronics Command, White Sands Missile Range, NM, 7 pp.
- Ellis, P., Holan, G., Houghton, J. T., Jones, T. S., Peckham, G., Peskett, G. D., Pick, D. R., Rodgers, C. D., Roscoe, H., Sandwell, R., Smith, S. D. and Williamson, E. J., 1973: Remote Sensing of Atmospheric Temperature from Satellites IV. The Selective Chopper Radiometer for Nimbus 5, Proc. Roy. Soc. A, 337, pp. 149-170.
- Falcone, V. J. Jr., 1974: Atmospheric Temperature Inferring from Passive Radiometry, Sixth Conference on Aeronautical Meteorology, Preprint, pp. 239-240.
- Fastie, W. G. and Kerr, D. E., 1975: Spectroradiometric Calibration Techniques in the Far Ultraviolet: A Stable Emission Source for the Lyman Bands of Molecular Hydrogen, Appl. Opt., 14 (9), pp. 2133-2142.
- Fleming, H. E., 1972: An Algorithm for the Approximate Solution of a Non-linear Integral Equation of the First Kind, SIAM Review, 14 (3).
- Fleming, H. E. and Smith, W. L., 1972: Inversion Techniques for Remote Sensing of Atmospheric Temperature Profiles, Temperature its Measure and Control, Vol. 4, H. H. Plumb, Ed-in-Chief, Part 3, Thermocouples, Biology and Medicine, Geophysics in Space, D. I. Finch, G. W. Burns, K. L. Bersen and T. E. Van Zandt, Eds., Inst., Soc. of Amer., pp. 2239-2250.

- Fleming, H. E., Weinreb, H. M., Fritz, S., Soules, S., Luebbe, R., Hill, M., Nevendorffer, A., Morse, B., Hayden, C., Lienesch, J., McMillin, L., Johnson, K. and Crosby, D., 1975: An Analysis of the Soundings from the NOAA 2 VTPR Instruments, NOAA Tech Rep., National Oceanic and Atmospheric Administration, Washington, DC.
- Foster, M. R., 1961: An Application of the Wiener-Kolmogorov Smoothing Theory to Matrix Inversion, J. SIAM, 9, pp. 387-392.
- Fried, J. and Labs, D., 1974: Quasi-Monochromatic Calibration Source for the Wavelength Range from $0.22\mu\text{m}$ to $7.0\mu\text{m}$, Appl. Opt., 13 (1), pp. 197-199.
- Fritz, S., 1969: On the Question of Measuring the Vertical Temperature Distribution of the Atmosphere from Satellites, Mon. Wea. Rev., 97, pp. 712-715.
- Fritz, S., Wark, D. Q., Fleming, H. E., Smith, W. L., Jacobowitz, H., Hilleary, D. T. and Alishouse, J. C., 1972: Temperature Sounding from Satellites, NOAA Technical Report NESS 59, National Environmental Satellite Service, National Oceanic and Atmospheric Administration, Washington, DC, 49 pp.
- Fröhlich, C. and Brusa, R. W., 1975: Measurement of the Solar Constant, A Critical Review, Proc. of the Workshop on the Solar Constant and the Earth's Atmosphere, Big Bear Solar Observatory, Big Bear City, CA, pp. 112-126.
- Garing, J. S. and McClatchey, R. A., 1973: AFCRL Atmospheric Line Parameters Compilation (AFCRL-73-0096).
- Gautier, D. and Revah, I., 1975: Sounding of Planetary Atmospheres: A Fourier Analysis of the Radiative Transfer Equation, Journal of the Atmos. Sci., 32, No. 5, pp. 881-892.
- Goddard Space Flight Center, 1972: NIMBUS 5 User's Guide, Greenbelt, MD, 162 pp.
- Goldberg, I. L., 1974: Analysis of the Vertical Temperature Profile Radiometer (VTPR) Radiometric Problem, Document X-726-74-213, Published by Goddard Space Flight Center, Greenbelt, MD.
- Goody, R. M., 1964: Atmospheric Radiation, The Clarendon Press, Oxford, 436 pp.
- Green, A. E. S. (Ed), 1966: The Middle Ultraviolet: Its Science and Technology, John Wiley and Sons, Inc., NY, 390 pp.
- Halem, M. and Chow, Ming-Dah, 1976: Sounder Design Considerations in the Selection of Temperature Sensing Channels, J. Appl. Meteor., 15, pp. 394-401.

- Hickey, J. R., Hilleary, D. T. and Maschhoff, R. A., 1973: Solar Radiation Measurements Capability of the Earth Radiation Budget Experiment of NIMBUS F Satellite, Proc. of Sym on Solar Radiation, Measurements and Instrumentation, Smithsonian Inst., Radiation Biology Laboratory, Washington, DC, pp. 127-150.
- Hickey, J. R. and Karoli, A. R., 1974: Radiometric Calibrations for the Earth Radiation Budget Experiment, Appl. Opt., 13 (3), pp. 523-533.
- Horan, J. J., Schwartz, D. S. and Love, J. D., 1974: Partial Performance Degradation of a Remote Sensor in a Space Environment, and Some Probable Causes, Appl. Opt., 13 (5), pp. 1230-1237.
- Hogan, J. S. and Grossman, K., 1972: Tests of a Procedure for Inserting Satellite Radiance Measurements into a Numerical Model, J. Atmos. Science, 29, pp. 797-800.
- Horowitz, R. and Davis, L. R. (Eds), 1975: 1975 Report on Active and Planned Spacecraft and Experiments, National Space Sci. Data Ctr./World Data Ctr. A for Rockets and Satellites, NASA/GSFC, Greenbelt, MD, 312 pp.
- Houghton, J. T. and Smith, S. D., 1972: The Selective Chopper Radiometer (SCR) Experiment, The Nimbus 5 User's Guide, Goddard Space Flight Center, Greenbelt, MD, pp. 131-139.
- Mulstrom, R. L., 1973: The Cloud Bright Spot, Photogrammetric Engineering, pp. 370-376.
- Idso, S. B., Fuchs, M., and Tanner, C. B., 1971: "Comments on Errors in Infrared Thermometry and Radiometry", J. Amer. Met., Vol 10, pp. 1041.
- Jacobowitz, H. and Gruber, A., 1975: Calibration of the Visible Channel of the NOAA-2 Scanning Radiometer, Abstracts of the Second Conference on Atmospheric Radiation, Arlington, VA, p. 67.
- Jacobowitz, H., 1973: "Estimation of Solar Radiation Reflected from White Sands and Transmitted Back to Space for use in Calibrating Radiometers Aboard Meteorological Satellites", Private Communication, (See Appendix).
- Jastrow, R. and Hale, M., 1973: Accuracy and Coverage of Temperature Data Derived from the IR Radiometer on the NOAA-2 Satellite, J. Atmos. Sci., 30, pp. 958-964.
- Johnson, K. W., 1975: Information Content of Vertical Temperature Profile Radiometer Data, Preprint, 3rd Symposium on Meteorological Observations and Instrumentation, Washington, DC, published by Amer. Meteor. Soc., Boston, MA.

- Joint Planning Staff (JPS), 1973: Global Atmospheric Research Program (GARP), Indirect Measurements of Temperature and Humidity from Satellites (1972), Appendix III GARP Publications Series No. 11, The First GARP Global Experiment Objectives and Plans, World Meteorological Organization, pp. 63-68.
- Jones, G. D., Hilleary, D. T. and Fridovich, B., 1965: A Diffuse Light Source for Calibrating Meteorological Satellite Television Cameras, Appl. Opt., 4 (3), pp. 307-309.
- Kaflan, L. D., 1959: Inference of Atmospheric Structure from Remote Radiation Measurements, J. of the Optical Soc. of Amer., Vol. 49, No. 10, pp. 1004-1007.
- Kano, M. and Suzuki, M., 1976: On the Calibration of the Radiometer for Longwave Radiation (II) - The Case of Pyrgeometer, Papers in Met. and Geophy., 27 (1), pp. 33-39.
- Karoli, A. R., Hickey, J. R. and LeBlanc, L. R., 1975: Low Temperature Blackbody Sources for Use in the Calibration of Satellite Infrared Radiometers, Abstracts of the Second Conf. on Atm. Rad., Arlington, VA, pp. 86-91.
- Kendall, J. M. Sr., 1973: Factors Affecting Accuracy of Radiometer Measurements of Solar Irradiance and Results of a Measuring of the Solar Constant, Proc. of Sym. on Solar Radiation, Smithsonian Instit., Rad. Bio. Lab., Washington, DC, pp. 190-202.
- Kendall, J. M., 1975: Measurements of Stefan-Boltzman Constant, Circumsolar Irradiance, and Solar Constant Made with PACRAD Radiometer, Proc. of the Workshop on the Solar Constant and the Earth's Atmosphere, Big Bear Solar Observatory, Big Bear City, CA, pp. 141-156.
- Kendall, J. M. Sr. and Berdahl, C. M., 1970: Two Blackbody Radiometers of High Accuracy, Appl. Opt., 9 (5), pp. 1082-1091.
- Koffler, R., De Cotis, A. G. and Rao, P. K., 1973: A Procedure for Estimating Cloud Amount and Height from Satellite Infrared Radiation Data, Mon. Wea. Rev., 101, pp. 240-243.
- Kuhn, P. M. and Stearns, L. P., 1974: Infrared Radiation Observations vs Calculations in the Atmosphere During Skylab, Preprint, Sixth Conference on Aerospace and Aero-nautical Meteorology, pp. 120-124.
- Kuhn, P. M., Weickmann, H. K., Lojko, M. J. and Stearns, L. P. 1974: Transfer of Infrared Radiation Through Clouds, Appl. Opt., Vol. 13, No. 3, pp. 512-517.

- Lansing, J. C. Jr. and Cline, R. W., 1975: The Four-and Five-Band Multispectral Scanners for Landsat, Opt. Engineering, 14, pp. 312-322.
- Lerner, R. M. and Hollinger, J. P., 1975: Analysis of Micro-wave Radiometric Measurement from SKYLAB, N76-18611 (mf), Nav Res Lab, Washington, DC, 102 pp.
- Lienesch, J. H., 1976: Private Communication.
- Lo, R. C. and Johnson, D. R., 1971: An Investigation of Cloud Distribution from Satellite Radiation Data, Mon. Wea. Rev., 99, pp. 599-605.
- Lowry, W. P. and Gay, L. W., 1971: Reply, J. Amer. Met., Vol 10, pp. 1042.
- Lowry, W. P. and Gay, L. W., 1970: Errors in Infrared Thermometry and Radiometry, J. Appl. Meteorology, Vol 9, pp. 929-932.
- Ludwig, G. H., 1974: The NOAA Operational Environmental Satellite System, Status and Plans, Preprint, Sixth Conf. on Aerospace and Aeronautical Meteorology, pp. 120-124.
- McClatchey, R. A., Benedict, W. S., Clough, S. A., Burch, D. E., Calfee, R. F., Fox, K., Rothman, L. S. and Garing, J. S. 1973: AFCRL Atmospheric Absorption Line Parameters Compilation, Air Force Cambridge Research Laboratories, L. G. Hanscom Field, Bedford, MA, 78 pp.
- McCulloch, A. W., 1972: The Temperature Humidity Infrared Radiometer (THIR) Subsystem, The Nimbus 5 User's Guide, Goddard Space Flight Center, Greenbelt, MD, pp. 11-47.
- McMillin, L. M., Wark, D. Q., Siomkajio, J. M., Abel, P. G., Werbowetzki, A., Lauritsen, L. A., Pritchard, J. A., Crosby, D. S., Woolf, H. M., Luebbe, R. C., Weinreb, M. P., Fleming, H. E., Bittner, F. E. and Hayden, C. M., 1973: Satellite Infrared Soundings from NOAA Spacecraft, NOAA Tech Rep. 65, National Oceanic and Atmospheric Administration, Washington, DC, 197 pp.
- Moller, F., 1951: Long Wave Radiation, Compendium of Meteorology, published by the American Meteorological Society, Boston, MA, pp. 34-49.
- Moller, F. and Raschke, E., 1964: Evaluation of TIROS III Radiation Data, NASA Contractor Report CR-112, NASA Research Grant NsG-305, University of Munich, Germany, for National Aeronautics and Space Administration, Washington, DC, 84 pp.
- NASA, 1972a: SKYLAB, EREP Investigator's Data Book, Principal Investigator Management Office, Sci. and Appl. Directorate, Manned Spacecraft Center, Houston, TX, 106 pp.

- NASA, 1972b: Data Users Handbook, Appendices A and G, Payload and Data Calibration, GSFC, NASA, Greenbelt, MD, 20 and 18 pp.
- NASA, 1973a: SKYLAB Program Earth Resources Experiment Package: Ground Truth Data for Test Sites (SL-2), N75-30628 (mf), JSC/NASA, prepared by Martin Marietta Corp., Contract NAS8-24000, 85 pp.
- NASA, 1973b: Final Report for the Electrically Scanning Microwave Antenna for NIMBUS E, prepared by Aerojet Electro-systems Co. for NASA, Goddard Space Flight Center, Greenbelt, MD, 45 pp.
- NASA, 1976: Satellite Situation Report, Vol. 16, No. 3, Goddard Space Flight Center, Greenbelt, MD.
- National Environmental Satellite Center, 1969: The Improvement of Clear Column Radiance Determination with a Supplementary 3.8 μ Window Channel, Technical Memorandum NESCTM 16, Washington, DC, 17 pp.
- Neuder, S. M., 1970: Spectral Modification for Solar Simulation, Appl. Opt., 9 (5), pp. 1014-1018.
- Nichols, D. A., 1975: Primary Optical Subsystem for DMSP Block 5D, Opt. Engineering, 14, pp. 279-283.
- Nichols, D. A., Elsby, C. N. and Schultz, E. G., 1975: Block 5D Compilation, Def. Met. Sat. Prog., HQ, Space and Missile Systems Organization, AF Systems Command, USAF, 522 pp.
- Ott, W. R., Fieffe-Prevost, P. and Wiese, W. L., 1973: VUV Radiometry with Arcs. I: Principle of the Method and Comparison with Black Body Calibration from 1650 Å to 3600 Å, Appl. Opt., 12 (7), pp. 1618-1629.
- Paresce, F., Kumar, S. and Bowyer, C. S., 1971: Continuous Discharge Line Source for the Extreme Ultraviolet, Appl. Opt., 10 (8), pp. 1904-1908.
- Pierluissi, J. H. and Gomez, R. B., 1974: Study of Transmittance Models for the 15 micron-CO₂ Band, Sixth Conference on Aerospace and Aeronautical Meteorology, Preprint, pp. 200-204.
- Pipkin, F. B., 1971: Synchronous Meteorological Satellite System Description Document, Vol. 2, Goddard Space Flight Center, NASA, Greenbelt, MD, 157 pp.
- Platt, C. M. R., 1973: Lidar and Radiometric Observations of Cirrus Clouds, J. Atmos. Sci., 31, pp. 1191-1204.
- Platt, C. M. R., 1974: Structure and Optical Properties of Some Middle-level Clouds, J. Atmos. Sci., 31, pp. 1079-1088.
- Proc. Intl. Radiation Symposium (IAMAP, IUGG), 1972: Sendai, Japan, pp. 554-557.

- Reeves, R. G., Anson A. and Landen, D., 1975: Manual of Remote Sensing, 2 Vols., American Society of Photogrammetry, Falls Church, VA, 867 pp.
- Renne, D. S. and Marlatt, W. E., 1974: A Comparison of Several Atmospheric Infrared Radiation Transfer Models, Preprint, Sixth Conference on Aerospace and Aeronautical Meteorology, pp. 127-130.
- Reynolds, D. W. and Vonder Haar, T. H., 1976: A Bispectral Method for Cloud Parameter Determination, Atmos. Sci. Paper No. 239, Colorado State University, Fort Collins, CO.
- Rodgers, C. D., 1970: Remote Sounding of the Atmospheric Temperature Profile in the Presence of Cloud, Qlty. J. of the Royal Meteorological Society, Vol. 96, No. 410, pp. 654-666.
- Sabatini, R. R. (Ed), 1972: The Nimbus 5 User's Guide, Goddard Space Flight Center, NASA, Greenbelt, MD, 162 pp.
- Samson, J. A. R., 1967: Techniques of Vacuum Ultraviolet Spectroscopy, John Wiley and Sons, Inc., NY, 348 pp.
- Scoggins, J. R., 1976: "The Determination of Atmospheric Structure from Quantitative Satellite Data", Progress Report #2, Center for Applied Geosciences, Texas A&M University, US Army Research Office DAA629-76-G-0078.
- Scoggins, J. R., 1974: Comparisons Between Nimbus 5 and Rawinsonde Temperature Data Obtained in the AVE II Pilot Experiment, prepared for Aerospace Environment Division Space Sciences Laboratory, Marshall Space Flight Center, NASA Contract NAS8-26751.
- Shenk, W. E. and Salomonson, V. V., 1970: Visible and Infrared Imagery from Meteorological Satellites, Applied Optics, Vol. 9, No. 8, pp. 1747-1760.
- Shenk, W. E. and Salomonson, V. V., 1972: A Simulation Study Exploring the Effects of Sensor Spatial Resolution on Estimates of Cloud Cover from Satellites, J. Appl. Met., 11, pp. 214-220.
- Shirfrin, K. S., 1955: Thermal Radiation Transfer in Clouds, Trudy GGO, No. 46.
- Sikla, G. J., 1974: Spectral Signatures of Several Cloud Types and Information Extracted from Very High Resolution Visual Satellite Radiances, presented at the Sixth Conference on Aerospace and Aeronautical Meteorology.
- Sissala, J. E. (Ed), 1975: The Nimbus 6 User's Guide, Landsat/Nimbus Project, CA, pp. 56-63.
- Smith, E. A. and Vonder Haar, T. H., 1977: Calibration of SMS Flight 1 Model VISSR Data from GATE, Colorado State University, Fort Collins, CO, (in preparation).

- Smith, W. L., 1967: An Iterative Method for Deducing Tropospheric Temperature and Moisture Profiles from Satellite Radiometer Measurements, Mon. Wea. Rev., Vol. 95, No. 6, pp. 363-369.
- Smith, W. L., 1970: Iterative Solution of the Radiative Transfer Equation for the Temperature and Absorbing Gas Profile of an Atmosphere, Appl. Opt. 9 (9), pp. 1993-1999.
- Smith, W. L., 1968: An Improved Method for Calculating Tropospheric Temperature and Moisture Profiles from Satellite Radiometer Measurements, Mon. Wea. Rev., 96 No. 6, pp. 387-396.
- Smith, W. L., 1969: A Polynomial Representation of Carbon Dioxide and Water Vapor Transmission, ESSA Technical Rpt. NES 47, National Environmental Satellite Center, Washington, DC, 20 pp.
- Smith, W. L., 1972: Calculation of Clear Column Radiances Using Airborne Infrared Temperature Profile Radiometer over Partly Cloudy Areas, NOAA Technical Memorandum, NESS 28, Washington, DC, 74 pp.
- Smith, W. L., 1972: Satellite Techniques for Observing the Temperature Structure of the Atmosphere, Bull. Amer. Met. Soc., 53, pp. 1074-1082.
- Smith, W. L., Woolf, H. M. and Jacob, W. D., 1970: A Regression Method for Obtaining Real-time Temperature and Geopotential Height Profiles from Satellite Spectrometer Measurements and its Application NIMBUS III SIRS Observations, Mon. Wea. Rev., Vol. 98, No. 8, pp. 582-603.
- Smith, W. L., 1971: Calculation of Clear Column Radiances Using Airborne Infrared Temperature Profile Radiometer Measurements over Partly Cloudy Areas, NOAA Technical Memorandum NESS 28, Washington, DC.
- Smith, W. L. and Fleming, H. K., 1972: Retrieval of Atmospheric Temperature Profiles from Satellite Measurements for Dynamical Forecasting, J. of Applied Meteor., Vol. 11, No. 1, pp. 113-122.
- Smith, W. L., Hilleary, D. T., Baldwin, E. C., Jacob, W. J., Jacobowitz, H., Nelson, G., Soules, S. D. and Wark, D. Q., 1972: The Airborne ITPR Brassboard Experiment, NOAA Technical Report, NESS 58, 74 pp.
- Smith, W. L., Howell, H. B., Fischer, J. C., Chalfaut, M. C. and Hilleary, D. T., 1972: The Infrared Temperature Profile Radiometer (ITPR) Experiment, The Nimbus 5 User's Guide, Goddard Space Flight Center, Greenbelt, MD, pp. 107-130.

- Smith, W. L. and Rao, P. K., 1972: The Determination of Satellite Temperature from Satellite "Window" Radiation Measurements, Temperature Its Measure and Control, Vol. 4, H. H. Plumb, Ed-in-Chief, Part 3, Thermocouples, Biology and Medicine Geophysics in Space, D. I. Finch, G. W. Burns, R. L. Berger and T. E. Van Zandt, Eds., Instrument Soc. of America, Pittsburgh, PA, pp. 2251-2257.
- Smith, W. L., Hilleary, D. T., Fischer, J. C., Howell, H. B. and Woolf, H. M., 1974: Nimbus 5 ITPR Experiment, Applied Optics, Vol. 13, No. 3, pp. 499-506.
- Smith, W. L., Wydick, J., Howell, H. B. and Pellegrino, P. P., 1974: Results from the CV-990 ITPR Experiment during BESEX, NOAA Technical Report.
- Smith, W. L., Woolf, H. M., Abel, P. G., Hayden, C. M., Chalfant, M. and Grody, N., 1974: Nimbus 5 Sounder Data Processing System Part I: Measurement Characteristics and Data Reduction Procedures, NOAA Technical Memorandum, NESS 57.
- Soule, H. V., 1974: Deep Space and the Moon as Radiometric Standards for Space-Borne Sensors, Proc. Soc. Photo-Optical Instrumentation Engineers, Vol. 51, Scanners and Imagery Systems for Earth Observations, San Diego, CA, pp. 56-63.
- Spangler, M. J., 1974: What's the Weather Down There, Preprint 186, from the Westinghouse Engineer, Westinghouse Information Services, Baltimore, MD, 10 pp.
- Staelin, D. H., Kunzi, K. F., Pettyjohn, R. L., Poon, R. K. L., Wilcox, R. W., and Waters, J. W., 1976: "Remote Sensing of Atmospheric Water Vapor and Liquid Water with the NIMBUS 5 Microwave Spectrometer", Journal of Applied Meteorology, Vol. 15, November 1976, pp. 1204-1214.
- Staelin, D. H., Barath, F. T., Blin, J. C. III and Johnston, E. J., 1972: The Nimbus E Microwave Spectrometer (NEMS) Experiment, The Nimbus 5 User's Guide, Goddard Space Flight Center, Greenbelt, MD, pp. 141-157.
- Staelin, D. H., 1974: Review of Nimbus 5 Microwave Spectrometer Results, Preprint, Sixth Conference on Aerospace and Aeronautical Meteorology, pp. 146-149.
- Strand, O. N., 1971: Optimization of Frequencies Used in Indirect Sensing by Inversion, NOAA Tech. Report ERL 202-WPL 14, 22 pp.
- Strand, O. N., 1973: Expected Accuracy of Tropopause Height and Temperature as Derived from Satellite Radiation Measurements, NOAA Technical Report ERL 295-WPL 28, Boulder, CO, 67 pp.

- Strand, U. N. and Westwater, E. R., 1968: Minimum - RMS Estimation of the Numerical Solution of a Fredholm Integral Equation of the First Kind, SIAM J. Numer. Anal., 5, pp. 287-295.
- Stull, V. R., Wyatt, P. J. and Plass, G. N., 1963: The Infrared Absorption of Carbon Dioxide, Infrared Transmission Studies Final Report, Vol. III, Contract AF 19 (604) --7479, Aeronutronic Division, Ford Motor Company, 36 pp.
- Tarakanova, V. P., 1974: The Accuracy of Satellite Temperature Sounding of the Atmosphere, NASA Tech Transl. F-15, 690, translated from the Russian Meteorologivai Gidrologiva, pp. 76-78.
- Taylor, S. E. and Williamson, L. E., 1973: Satellite Calibration Site Has Brightness Equivalent to Clouds, Bull. of the American Meteorological Society, Vol. 54, No. 6, p. 551.
- Thekaekara, M. P., 1975: The Total and Spectral Solar Irradiance and Its Possible Variations, Proc. of the Workshop on the Solar Constant and the Earth's Atmosphere, Big Bear Observatory, Big Bear City, CA, pp. 232-263.
- Thomas, J., Alexander, G. and Dubbin, M., 1976: SATTEL - An Army Dedicated Meteorological Telemetry System, EOM-5587, 25 pp.
- Thompson, A. H., 1973: Vertical Temperature Soundings from Satellites as Data for the AMTEX, a paper presented to the Second AMTEX Study Conference, Tokyo, Japan.
- Thompson, A. H., 1972: Environmental Sources and Responses, a paper presented to Summer Institute of Glaciological and Arctic Sciences, Juneau, Icefield, Alaska.
- Twomey, S., 1965: Indirect Measurements of Atmospheric Temperature Profiles from Satellites: II. Mathematical Aspects of Inversion Problem, Mon. Wea. Rev., 94, pp. 363-366.
- Vesely, C. J. and Botzong, W. B., 1974: Defense Meteorological Satellite Program, Preprint, Sixth Conference on Aerospace and Aeronautical Meteorology, pp. 146-149.
- Wachtmann, R. L., Weichell, R. L. and Smith, W. C., 1974: Temperature Soundings from the Defense Meteorological Satellite Program, presented at the Sixth Conference on Aerospace and Aeronautical Meteorology.
- Wang, Wei-Chyung and Comoto, G. A., 1974: The Radiative Effect of Aerosols in the Earth's Atmosphere, J. of Appl. Meteor., Vol. 13, No. 5, pp. 521-534.

- Wark, D. Q. and Fleming, H. E., 1966: Indirect Measurements of Atmospheric Temperature Profiles from Satellite I. Introduction, Mon. Wea. Rev., Vol. 94, No. 6, pp. 351-362.
- Wark, D. Q. and Hilleary, D. T., 1969: Atmospheric Temperature: Successful Test of Remote Probing, Science, Vol. 165, No. 3899, pp. 1256-1258.
- Wark, D. Q., Fleming, H. E., Smith, W. L. and Liensch, J. H., 1969: Atmospheric Temperature Determinations from the SIRS-A on NIMBUS III., Proceedings of the Sixth International Symposium on Remote Sensing of the Environment, Ann Arbor, MI, pp. 451-467.
- Waters, J. W., Kunzi, K. F., Pettyjohn, R. L., Poon, R. K. L., and Staelin, D. H., 1975: "Remote Sensing of Atmospheric Temperature Profiles with the NIMBUS 5 Microwave Spectrometer", Journal of Atmospheric Sciences, October 1975, pp. 1953-1969.
- Weast, R. C. (Ed), 1975: Handbook of Chemistry and Physics, CRC Press, Cleaveland, OH, E229 - E246.
- Webb, W. L., 1975: "Meteorological Satellite Applications", Atmospheric Sciences Laboratory, Monograph Series, #2.
- Webb, W. L., Ward, F., and Nagle, R. E., 1977: "Workshop on Satellite Atmospheric Soundings".
- Weinreb, M. P. and Neurendorffer, A. C., 1973: Method to Apply Homogeneous - Path Transmittance Models to Inhomogeneous Atmospheres, J. of the Atmos. Sci., Vol. 30, No. 4, pp. 662-666.
- Weinreb, M. P. and Fleming, H. E., 1974: Empirical Radiance Corrections: A Technique to Improve Satellite Soundings of Atmospheric Temperature, Geophys. Res. Lett., Vol. 1, No. 7.
- Westwater, E. R. and Strand, O. N., 1968: Statistical Information Content of Radiation Measurements Used in Indirect Sensing, J. Atmos. Sci., Vol. 25, pp. 750-758.
- Westwater, E. R., Snider, J. B. and Carlson, A. V., 1975: Experimental Determination of Temperature Profiles by Ground-Based Microwave Radiometry, J. of Appl. Meteor., Vol. 14, No. 4, pp. 524-539.
- White, O. R. (Ed), 1977: The Solar Output and its Variations, Section by C. Frohlich on "Contemporary Measures of the Solar Constant", Colorado Associated University Press.
- Whitehead, V. S., 1971: A Note on the Effect of Reflected Solar Radiation on Airborne and Ground Measurements in the Thermal Infrared, NASA, Manned Spacecraft Ctr. (JSC), Houston, TX, 16 pp.

- Whitehead, V. S., Kuhn, P. M., Marlatt, W. E. and Williamson, L. E., 1974: The Skylab Concentrated Atmospheric Radiation Project - An Overview, Proc. of the Sixth Conference on Aerospace and Aeronautical Meteorology, Amer. Met. Soc. Boston, MA, pp. 117-119.
- Wijnbergen, J. J. and Kelly, A. A., 1974: Far Infrared Transmission and Reflection of Intran 1 Through Intran 6 at Low Temperatures, Appl. Opt., 13 (11), pp. 2716-2718.
- Williamson, E. J., 1970: The Accuracy of the High Resolution Infrared Radiometer on Nimbus 2, NASA Tech Note D-5551, GSFC, Greenbelt, MD, 14 pp.
- Williamson, L. E., 1976: A United States Facility for the Collection of Satellite Calibration Air and Ground Truth Data, presented at the Symposium on Radiation in the Atmosphere, Garmisch-Partenkirchen, Germany.
- Willson, R. C., 1975: JPL Absolute Radiometry and Solar Constant Measurements, Proc. of the Workshop on the Solar Constant and the Earth's Atmosphere, Big Bear Observatory, Big Bear City, CA, pp. 301-316.
- Wolski, R. J., 1975: Estimation of Tropopause Height and its Importance to the Inference on Vertical Temperature Profiles from Satellite Radiance Measurements, Technical Note BN 814, Institute for Fluid Dynamics and Applied Mathematics, University of Maryland, College Park, MD, 64 pp.
- Yamamoto, G., 1961: Numerical Method for Estimating the Stratospheric Temperature Distribution from Satellite Measurements in the CO₂ Band, J. Meteorology, Vol. 18, No. 5, pp. 581-588.
- Yamamoto, G., Tanaka, M. and Asano, S., 1970: Radiative Transfer in Water Clouds in the Infrared Region, J. Atmos. Sci., 27, pp. 282-292.

AUTHOR - SUBJECT INDEX

- Abbot Silver-disk Pyrheliometer** 52
accuracy 2, 15, 17, 23, 38, 53,
 56, 63
air convection 21
albedo 69, 78
Alexander, G. v
Angstrom Scale of Pyrheliometry 52, 57
angular response 16, 18
 cosine effect 16
 FOV 16, 19
 surface characteristics 19
area aperture 41
atmosphere 68, 111

backscatter 66
Barnett, T. vi
Bede, D. 28, 29
Bedford, R. E. 51
Berdahl, C. M. 39, 52, 53, 55
bias 19
black body 27, 34, 35, 44, 50, 63
blockage 41
Brawer, R. L. 103
Brusa, R. E. 53, 55, 56, 69
Buettner, K. J. K. 36, 65

calibration
 electronic 105
 frequency 23
 in-flight 43, 58, 64, 75, 78, 80,
 81, 83, 88, 89, 93
 infrared 69, 75, 76, 77, 78
 internal 14
 mirror sum 42
 objectives 1
 on-board 58, 60
 pre-flight 33, 58, 68, 77, 79,
 81, 82, 87, 89, 93
 process v, 91, 92, 104
 radiometric 58, 59

random noise 13
satellite sensor v, 1
shutter, infrared 49
thermal 22, 106, 107, 108
TV cameras 34
total system 3, 91, 92
visible 69, 75, 77, 78

Canfield, L. R. 28
capacity 23
cavities 35, 39
 black body 51, 53
Cavity Radiometric Scale 82
chopper 18, 25, 63
Cline, R. W. 25, 63
clouds 67
Cogan, J. vii
contaminant 42
contamination 15, 16, 19, 38, 45,
 61, 93
Coulson, K. v, vi, 64, 66
Crommelynck, V. 55
cylinder, 2π 34

data
 application 111
 processing 22
 quality 1, 2
Davis, L. R. 78, 88, 89
degradation 17, 19, 38, 41, 42,
 45, 61, 62, 93
detectors 52
dew point 4, 5, 8
Dickenson, L. 25, 27, 74
diffraction 39
discharge tube 28
DMSP 26
DRIR 103
Drummond, A. J. v, 27, 29, 38,
 44, 50, 52, 54, 56, 58
Dubbin, M. v
Duncan, L. v

- emission 15,38
emissivity 15,34,35,36,63
EPAC 55
ERB 24,26,35,48,60,62,82,83
EREP 66
errors 13
 computation 23
 causes 13
 geometry 17,20
 instruments 14
 source 14,15
ESMR 79,80
excitation 41

Fastie, W. G. 28
FOV 25,26
Fried, J. 33
Frohlich, C. 53,55,56,69

gain 19,25
Geist, J. 55
geometry 65
geopotential height 4,6
geostrophic wind 4,6,87
Green, A. E. S. 28,29
Gruber, A. 66

Harper, R. 78
Hickey, J. K. 25,26,60,83,85
Hollinger, J. P. 81,82
honeycombs 35
Horan, J. J. 41
Horowitz, R. 78,88,89
House, F. vi
Hulstrom, R. L. 66

imagery 3,4,110
infrared 49,50,58
instrument response 43,44,
 56,64
International Pyrheliometric
 Scale 54,55,56,82
irradiance 41,46,48,50,56

Jacobowitz, H. v,vi,66,95
Jones, G. D. 29,34,78

Kano, M. 36,65
Karoli, A. R. 25,26,34,35,60,
 63,85,87,88
Kelly, A. A. 38
Kendall, J. M. 39,40,52,53,
 55,56
Kern, C. D. 36,65
Kerr, D. E. 28

Labs 33
lamps 29,30,31,32,34,50,56
 arc 13,34,56
 plasma 13,56
 standard 56
Lansing, J. C. 25,63
laser 29,30
Lerner, R. M. 81,82
Lienesch, J. H. 75,76
light emitting diodes 30
linearity of response 58,60,
 75,88
longwave 34,38,65
LRIR 26,87
luminescent (fluorescent)
 materials 28

manmade objects 65
McMillin, L. M. 25,27,60,87
microwave 15,37,58,63
moon 69
MSS 41

NASA 25,26,44,80,82,90
National Physical
 Laboratory 51,52
National Research Council 51
NBS 50,55,56
Neuder, S. M. 33,34
New Initiative v
Nichols, D. A. 27,63,74

- noise 60
noise generators 37,58,81
- OLS 69
optical elements 38
 alignment 30,45
optical system 16
 orientation 17
 temperature changes 18
Ott, W. R. 28
- Paresce, F. 28
photo-multiplier tube 41
Pipkin, F. B. 25
plasma 28,33,34
plates
 diffusion 29,33,62
 grooved 35,63
 quartz 38
PMR/SCR 26,88
polarization 15,16,17,28
precision 15,38,39,56,60
precision voltage stair-
 case 60,75
pressure effects, 20
pressure modulated cell, 26
PACRAD 53,55,57,83
primary standards, 58
Pyrheliometric Scales
 Angstrom Scale of
 Pyrheliometry 52,57
 International Pyrheliometric
 Scale 54,55,56,82
 Smithsonian Scale 52,57
- radiance 50,51,67
radiation
 instruments 21
 solar 29
 sources 27
 Van Allen 41
radiometers
 absolute 55
 active microwave 27,88
- cavity 52,53
comparisons 40
fixed 25
Primary Absolute Cavity
 Radiometer 53,55,57,83
restricted scan 25,26
scanning 24,25,77,103
radiometric references 50-52,
 54,56
radiosonde profiles 8
random noise 13,22
rawinsonde data 4
 comparisons 5-12
Reeves, K. G. v
reflection 15,38
 discontinuities 66
reflectivity 19,65
remote sensing v
Reynolds, J. 66
- Sabatini, R. R. 25,80
Samson, J. A. R. 28
satellites
 environmental 1
 geosynchronous 1,24
 LANDSAT 3,41,44,111
 meteorological 2,3,111
 polar orbiters 2
 SEASAT 27
- satellite data 2,4,68
satellite technology v,3,12
 profiles 8
SATFAL v
SATTEL v
saturation effects 21
SCAMS 63
scanning systems 24
 error sources 41
 mechanical and elec-
 tronic 24
 operations 25
 spin scan 24
SCARP v
scattering 15

- Scoggins, J. 4
sensitivity pattern 16
sensor response 39
shortwave 29,48
Showalter Index 4,8,9
shuttered channel 61
Sissala, J. E. 25,26,27,63,
 85,88,89
site criteria 109
Skliarov, V. 55
Smith, E. 66
Smithsonian Scale 52,57
SMS-2 49
solar 29,33
 constant 54,56,69
 measurements 39
 radiation 52
 simulators 29,33,34,62
Solar Constant Reference
 Scale 54,55
Solar de Uyuni 66
Soule, H. V. 69
soundings 26
SPACELAB 68,93,94
space look 60,61
Spangler, M. J. 72,74
spectral response 17,18,21,
 29,45,64
spectrometer
 (monochromator) 33
stability 60
Stair, R. 31
Steering Committee vi
step wedge 105,106
stray light 18
sunlight 65
Suzuki, M. 36,65
synchrotron radiation 28
system checks 60

target 13,15,61,64,65
temperature 5
 brightness 27,41,66,69,80,81
radiometer 40

Thekaekara, M. P. 45,54,56
thermal effects 18,21
thermal resistance 40
Thomas, J. v
time constant 13,22,40
TMI 55
transmission 15,17,38
transmissivity 15,100

ultraviolet 27,28,42,50,64

ventilation 21
view of space 60
visible 29,58
VISSR 49,61,74
Vonder Haar, T. vii,66
VTPR 60,61,85

water 35,65
Weast, R. C. 38
Webb, W. V.vii
White, O. 54-57
Whitehead, V. V.vii,65
White Sands 66,67,95,96,109,110
Wijnbergen, J. J. 38
Williamson, E. J. 60
Williamson, L. E. 109
Willson, R. C. 53,55
working standards 58

CALIBRATION TECHNOLOGY